April 2009

Modeling of a Catalytic Packed Bed Reactor and Gas Chromatograph Using COMSOL Multiphysics

Daniel J. Szewczyk
Worcester Polytechnic Institute

Gabriella P. Serrati
Worcester Polytechnic Institute

John Tyler Waterman
Worcester Polytechnic Institute

Nicholas Edward Bartal
Worcester Polytechnic Institute

Project Number: WMC 0675

Modeling of a Catalytic Packed Bed Reactor and Gas Chromatograph Using COMSOL Multiphysics

A Major Qualifying Project Report

submitted to the Faculty

of the

WORCESTER POLYTECHNIC INSTITUTE

in partial fulfillment for the requirements for the

Degree of Bachelor of Science

By:

Nicholas Bartal

Gabriella Serrati

Daniel Szewczyk

John Waterman

Date: April 24, 2009

Approved:

Professor William M. Clark, Project Advisor

Abstract

The operation and understanding of catalytic packed bed reactors is an important part of the education of chemical engineers. The unit operations course, ChE4402, at WPI emphasizes this with the use of a differential reactor as one of the laboratory experiments. A major part of this experiment is to understand how the variation of some variables, such as temperature and inlet concentration of each species, affects the reaction rate and conversion that occurs. The experiment also asks students to explore mass transfer limitations that could be present in the reactor and to describe them.

The purpose of this project, then, was to create a model of the reactor and gas chromatograph setup using COMSOL Multiphysics so that students could gain a better understanding of how the experiment will run before running the actual experiment. A visual and interactive aid can more clearly demonstrate the affects of changing variables in the experiment. In addition, while the lab outline asks students to relate mass transfer limitations to the reaction and to design an experiment to test for these limitations, the lab does not provide enough time to test any theories. The COMSOL model, however, allows students to adjust parameters, such as the mass transfer coefficient and the velocity, and see the effect this has on the rate of reaction and the conversion. Finally, the gas chromatograph model produces plots that accurately depict plots generated by the real gas chromatograph so that students may fully complete a simulated test run of the entire experiment and know how they will go about using the data they obtain in the real experiment.

Three working models of a reactor were created in this project. One model uses the same assumptions that students are asked to make in the lab, namely that the reactor is differential and there are no mass transfer limitations. The next two models consider a literature reactor, with a different activation energy, pre-exponential factor, rate constant, and orders with respect to methane and oxygen. This reactor model produced a conversion of 6.2%, as opposed to the 2.4% experienced by the experimental reactor model. The third model applies mass transfer limitations so that this literature reactor achieves 2.4% conversion, mimicking the experimental reactor. A model of the gas chromatograph was also created that can accurately produce results very similar to those produced in reality. However, the model assumes constant temperature while the real gas chromatograph is temperature dependent. Therefore, while the model produces accurate results, it does not accurately depict how the separation of the species is achieved.

Table of Contents

Table of Figures

Table of Tables

Introduction

Worcester Polytechnic Institute strives under a "theory and practice" based curriculum. The information taught in every lecture is reinforced by some application of the learned material. One method of applying classroom material in practice is through laboratory experiments, a vital part of a student's progress in learning. The chemical engineering department offers two classes devoted to the understanding and performance of laboratory experiments that apply the fundamental principles of chemical engineering. There are a variety of experiments intended to demonstrate the versatility of chemical engineering and allow for hands on experience that will teach the necessary skills required by professionals in the field. Topics include thermodynamics, fluid dynamics, and reaction kinetics. The purpose is to solidify the students' fundamental understanding of small scale unit operations so they will have the ability to approach design and operation of macroscopic chemical processing equipment in a professional environment.

Receiving a solid education as an undergraduate student is imperative in any field, especially chemical engineering. The diverse topics encompassed by chemical engineering play an important role in the daily lives of the public and affect the well being of the entire population. An important contemporary topic involving chemical engineering is the control and removal of hydrocarbon emissions, such as methane, from process waste streams. The oxidation of hydrocarbons is a practical solution for controlling hydro carbon emissions, the simplest case being methane. Therefore, it is critical for students to understand the kinetics and applications of a methane oxidation reaction. Accordingly, methane oxidation in a packed bed reactor is one of the experiments performed in the Unit Operations course offered to chemical engineering undergraduates at WPI. The differential reactor gives students a chance to examine the kinetics of this common reaction on a very small scale.

Unfortunately, the students' understanding of reaction kinetics is limited by the laboratory equipment. However, there is an alternative method of representing the material that can help reinforce fundamental concepts. Computer aided modeling allows students to visualize what is physically happening inside the reactor so as to help them grasp more difficult concepts such as mass transfer. The purpose of this Major Qualifying Project is to simulate the oxidation of methane in a packed bed reactor using COMSOL Multiphysics and to incorporate the simulation in the senior-year Unit Operation classes at WPI.

Background

Catalytic reactors are commonplace in industry, and packed bed reactors are a very typical form of catalytic reactor. Because of this, one of the experiments done in the unit operations labs course at WPI involves working with a differential catalytic reactor to oxidize methane. This chapter discusses what packed bed reactors are and how they are used, as well as information on the reaction taking place in the experiment, and background on the software package, COMSOL Multiphysics.

Packed Bed Reactors

Packed bed reactors are the most common reactors in large-scale chemical product manufacture (Rase, 1990). They are primarily used for gas-phase reactions in synthesis, combustion, and effluent treatment (Rase, 1990). A packed bed reactor consists of a vessel containing one or several tubes of packed catalyst particles in a fixed, non-mobile bed (Rase, 1990). Generally, the gaseous reactant stream passes through these packed tubes, react with the catalyst, and the product stream leaves from the opposite side. Packed bed reactors are an economical choice in large scale production. This is due to the fact that they can operate nearly continuously due to the long catalyst life; which leads to savings in annual costs and shutdown costs. Table 1 describes the advantages and disadvantages of operating a packed bed reactor.

Table 1: Adantages and Disadvantages of Packed Bed Reactors

Advantages	**Disadvantages**
Higher conversion per unit mass of catalyst than other catalytic reactors	Undesired heat gradients
Low operating cost	Poor temperature control
Continuous operation	Channeling can occur
No moving parts to wear out	Difficult to clean
Catalyst stays in the reactor	Difficult to replace catalyst
Reaction mixture/catalyst separation is easy	Undesirable side reactions
Design is simple	
Effective at high temperatures and pressures	

The first commercial packed bed reactor was made in 1831 by Peregine Phillips (Rase, 1990). Phillips patented a process for the oxidation of sulfur dioxide over a platinum sponge in order to make sulfur trioxide. The sulfur trioxide was then dissolved in water, making sulfuric acid. Phillips saw the advantage of using a solid catalyst that could be used continuously without replacement, separation, or recycling. During the 1800's many other catalysts were discovered. Packed bed reactors are the dominant type of reactors for reactions requiring solid catalysts (Rase, 1990).

Types of Packed Bed Reactors

There are four major types of packed bed reactors intended for gas phase reactions: single bed adiabatic reactors, radial flow reactors, multiple bed isothermal reactors, and non-adiabatic multi-tubular reactors.

Reactors with a single adiabatic bed are traditionally used in either exothermic or endothermic reactions. However, they are primarily used for exothermic reactions in industrial practice (Satterfield, 1996). This type of adiabatic reactor is the least expensive to produce and is used as often as is practical. Adiabatic reactors almost always give temperature change unless steps are taken to make them relatively isothermal. There are a number of practices that make a reaction process relatively isothermal so that an adiabatic reactor may be used. Maintaining an adiabatic state conserves energy and can result in large savings for a company. One practice that makes a process isothermal incorporates a recycle stream into the process. A product recycle stream can deposit product into the reactant stream, a reactant may be supplied in excess, or an inert gas may be added to the feed (Satterfield, 1996). Adiabatic reactors are commonly used in hydrogenation reactions. A single adiabatic bed reactor is shown in Figure 1.

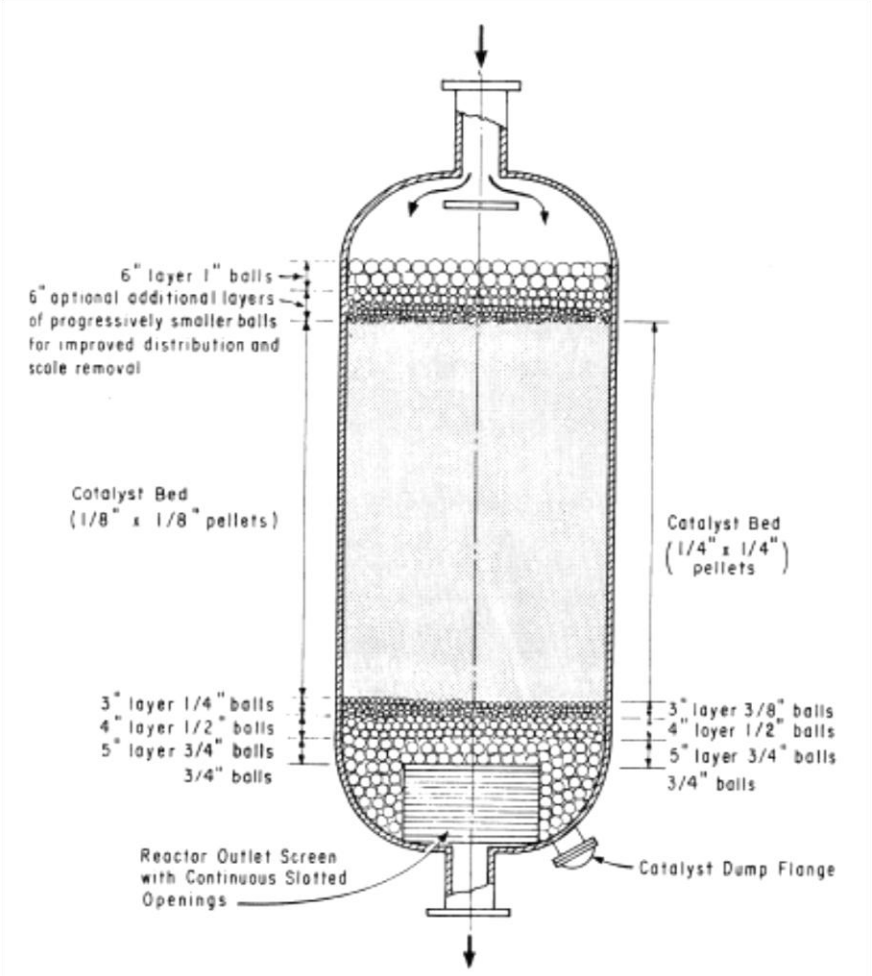

Figure 1: A Single Adiabatic Bed Reactor

A radial flow reactor is used when the pressure drop exhibited by the fluid flow through the reactor must be less than 2 PSI (Figure 2). It is also used for reactions involving a large change in moles. Pressure drop can be a major concern for physical and economical reasons. An acceptable pressure drop is between 3-15% of the total pressure in the bed. Some specific reactions require even less of a pressure drop, in which a radial flow reactor is a good solution (Rase, 1990). An example of this is the production of styrene from ethyl benzene. Dehydrogenation of ethyl benzene is a common reaction that uses radial flow reactors. In a radial flow reactor, gaseous reactants spiral along the outside of the vessel from one end to the other. As the gas particles travel, they pass through columns of catalyst before exiting through the center of the column (Rase, 1977).

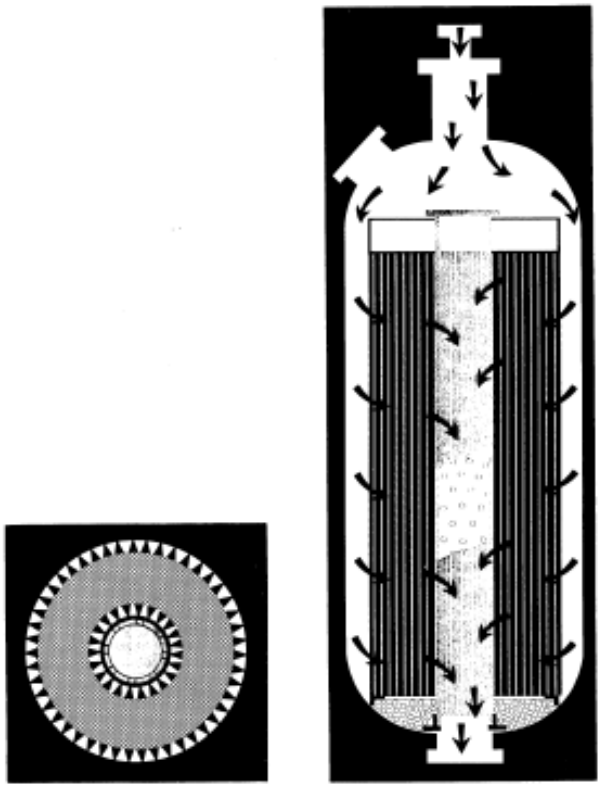

Figure 2: Radial Flow Reactor

A packed bed reactor with adiabatic beds in series is used for high conversion reactions with no heat transfer to the environment (Figure 3). This type of reactor is used with equilibrium-limited exothermic reactions and rapid endothermic reactions; which are arranged in series to optimize heat transfer between the two reactions. These reactors are used less frequently than single-bed reactors because the thermodynamics and flow through the reactors can be irregular (Satterfield, 1996). Applications of this type of reactor include SO_2 oxidation, ammonia synthesis, hydrocracking, and catalytic reforming (Rase, 1977).

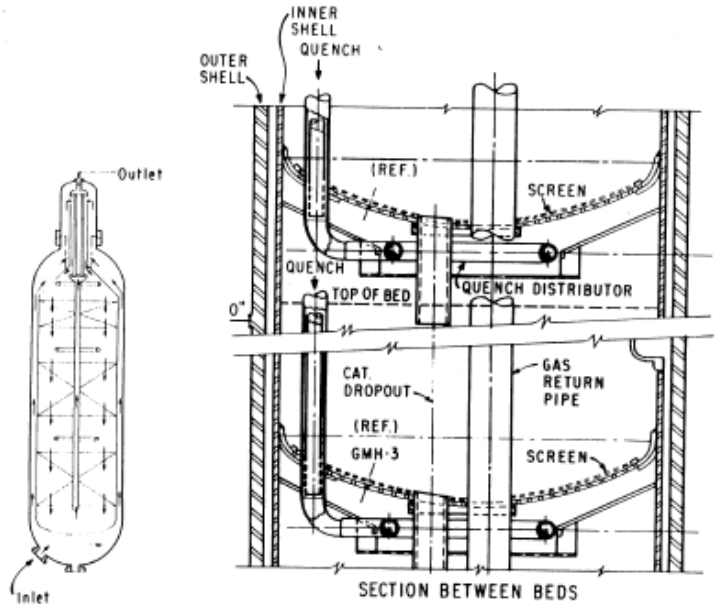

Figure 3: Packed Bed Reactor with Adiabatic Beds in Series

A non-adiabatic multi-tubular reactor is used for highly endothermic or exothermic reactions (Figure 4). A multi-tubular reactor consists of many tubes packed with catalyst in a large vessel. The tubes are present in large quantities in order to optimize surface area available for heat transfer. Fluids that are easily able to conduct heat are usually passed through the vessel in order to balance the highly endothermic/exothermic reaction. This reactor is effective for ethylene oxidation reactions.

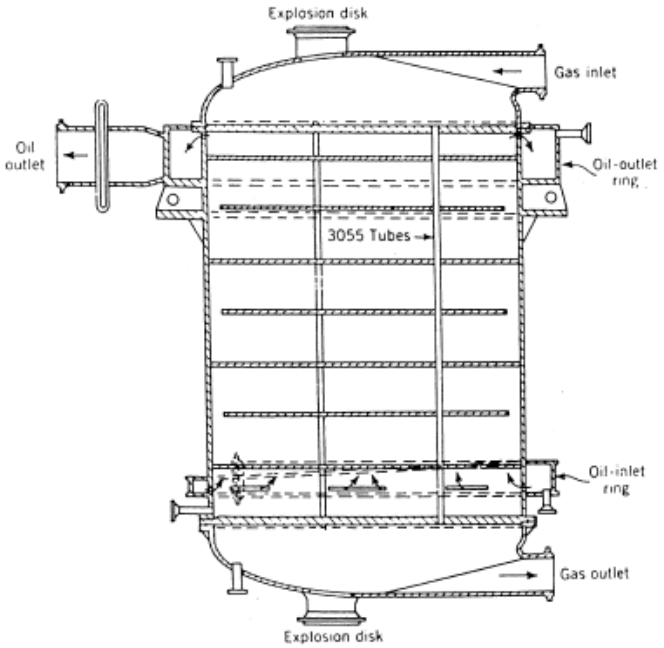

Figure 4: Non-adiabatic Multi-tubular Reactor

Design of Packed Bed Reactors

There are many considerations taken into place when designing a packed bed reactor. Particle shape is of the utmost importance. There are countless particle packing shapes available for use in packed bed reactors, each with a different combination of packing variables. Among these variables are: active surface area per unit volume of material, structural strength, constructability, manufacturing cost, bed voidage, and transport properties (Afandizadeh, 2001). Figure 5: Packing Shapes shows common variations of packing shapes.

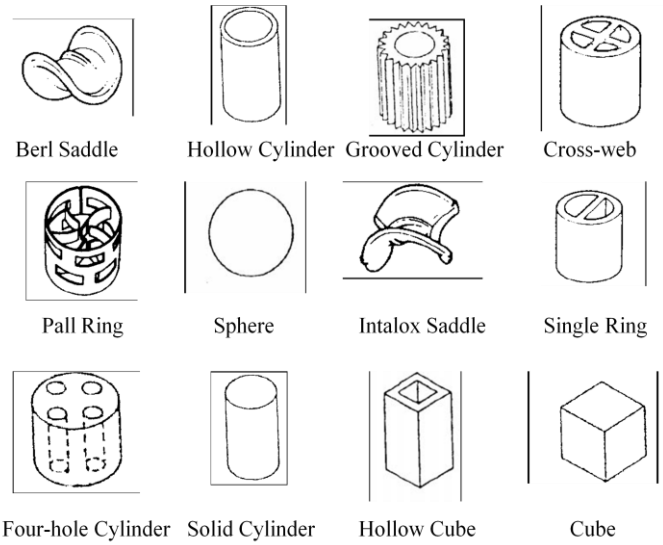

Figure 5: Packing Shapes

Catalyst pellets are traditionally in the shape of spheres or cylinders in order to decrease pressure drop. It is not entirely uncommon to have other shapes, but they require more preparation than spheres and cylinders and the internal and external surface areas need to be greatly considered when preparing the bed (Rase, 1990)

Enhanced surface area per unit volume and reduced pressure drop are of the utmost importance in design. A high surface area leads to less packing needed for the reaction, which influences cost and design. Likewise, the pressure drop influences reactor costs and the design of the reactor as well. One rule regarding pressure drop is to keep the ratio of reactor to catalyst particle diameters less than 10 (Afandizadeh, 2001). It is important that packing material and shape meet the needs of the reactor while minimizing undesirable features (Afandizadeh, 2001).

Most packed bed reactors contain inert balls or pellets preceding the catalyst. The role of this inert material is to catch scale and impurities and to assist in flow distribution of the reactants through the catalyst (Satterfield, 1996).

A packed bed of catalyst in a reactor is targeted so that unstable and inefficient arrangements are avoided (Afandizadeh, 2001). Unlike industrial processes involving packed beds, where packing material of desired shape and size is dumped randomly into a container to form a packed bed, there are two general rules for catalyst loading (Afandizadeh, 2001):

1. “The catalyst particles should have a free fall distance of less than 0.5 meters.”
2. “The pellets must be distributed evenly as the bed is gradually filled.”

These rules prevent undesirable flow distribution and pressure variations in the reactor. Flow obstruction in the tube by the catalyst packing can result in overheating in an exothermic reaction and inefficiency due to voidage. Catalyst pellets in packed beds are typically 1.5 mm to 6 mm in diameter (Satterfield, 1996). Pellets that are smaller than 1.5 mm can cause a major pressure drop through the reactor. Pellets that are 6 mm in diameter may lead to diffusion limitations. Recent developments have led to a hollow shape design for pellets larger than 6 mm in order to meet the needs of reactors with specific applications. These hollow tube pellets are particularly useful for selective exothermic reactions, such as the oxychlorination of ethylene to 1,2-dichloroethane. This shape gives a larger geometric surface for the reaction to occur on, thus increasing the effectiveness of the pellets (Cremaschi, 2006).

Goddard Hall Reactor

The stainless steel reactor located in Goddard Hall Room 116 at Worcester Polytechnic Institute is a single catalytic packed bed reactor. It was designed and built in 1993 by Professor William R. Moser. Jack Ferraro (Ferraro, 2008) in Goddard Hall at Worcester Polytechnic Institute was consulted in order to receive the initial drawings of the reactor. Jack provided the group with a sketch of the reactor, which includes its’ dimensions and structure, as shown in Figure 6. Figure 7 shows a picture of the reactor in Goddard Hall.

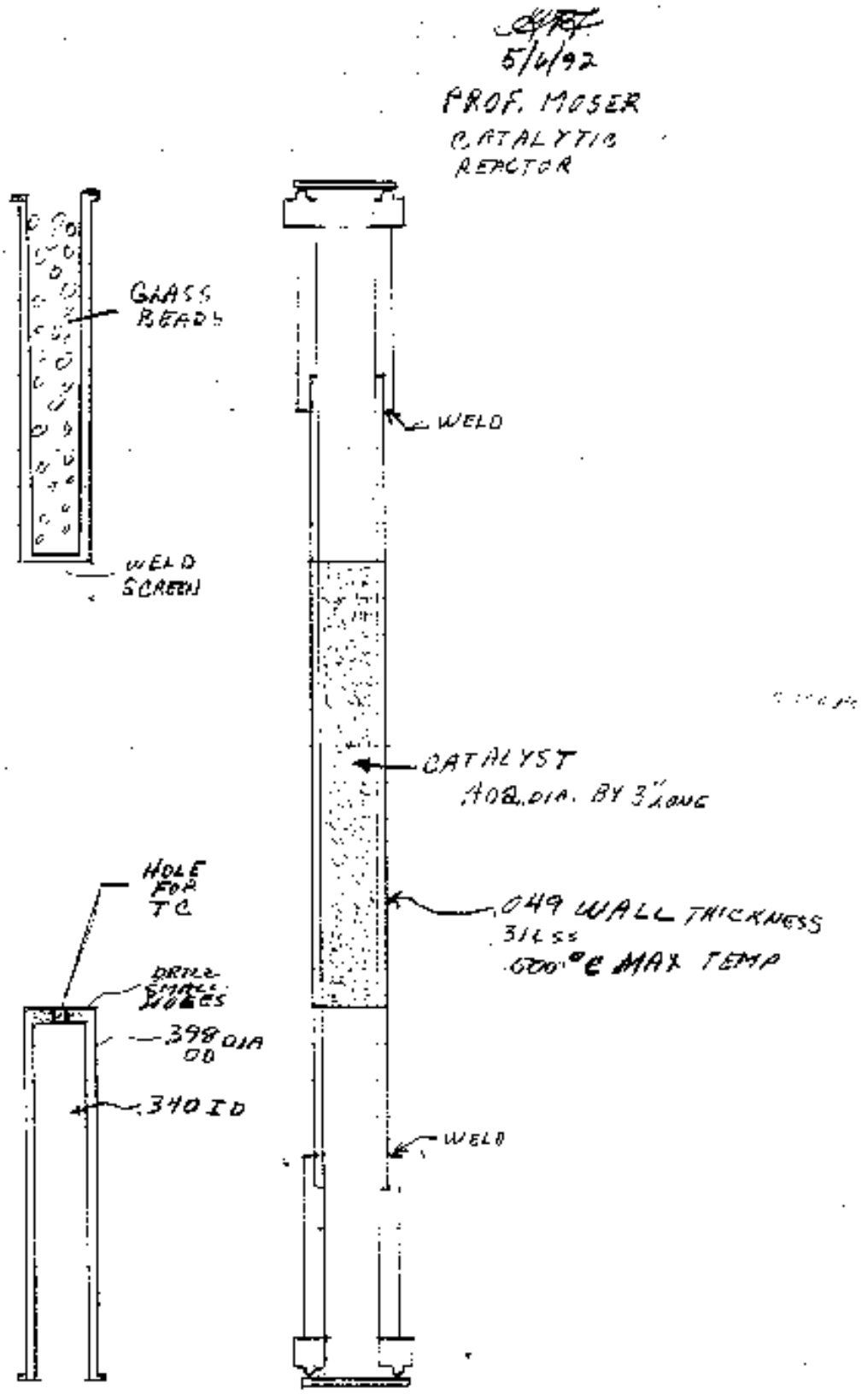

Figure 6: Reactor Tube Blueprint

Figure 7: Catalytic Reactor in Goddard Hall

The reactor is primarily used in the second Unit Operations course to study the oxidation of methane over a 0.5% Pd/alumina catalyst. Methane and air streams are fed through a ¼ inch insulated pipe to a vaporizer before entering the reactor. The reactor consists of a single tube, 3 inches in length and 0.340 inches in diameter (8.636mm) that is packed with cylindrical catalyst of 3.22mm in diameter (0.126 inches). This gives a reactor diameter to particle diameter ratio of 2.68. The wall surrounding the catalyst is 0.049 inches thick. Preceding the catalyst is glass bead packing. The tube following the catalyst has an inside diameter of 0.340 inches. Following the reactor the product stream passes through a gas chromatograph, which analyzes the composition. Figure 8 shows the schematic of the reactor. Figure 9 shows a picture of the reactor set-up in Goddard Hall.

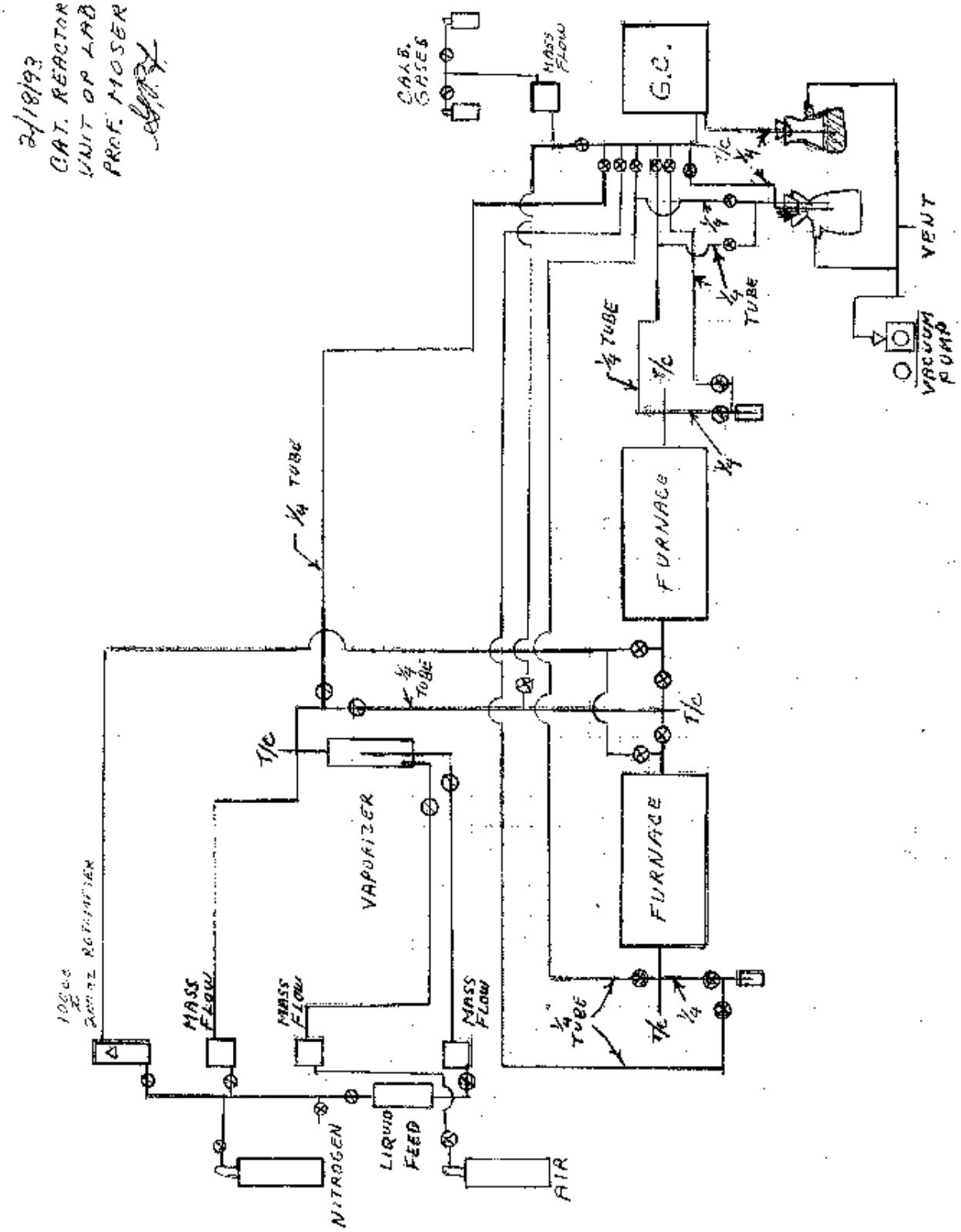

Figure 8: Reactor Schematic

Figure 9: Reactor Set-up in Goddard Hall

Reaction

The emission of hydrocarbons is a critical environmental concern and is being investigated in many laboratories. The reduction of these emissions is used in many practices ranging from biology to chemical engineering. The complete removal of non-reacted hydrocarbons in chemical plants is required to meet the expectations of the U.S. Clean Air Act Title 42.

Reduction of Methane

The oxidation of methane is an example of a reaction that serves to reduce the emission of hydrocarbons. Methane is a good hydrocarbon to use in determining the efficacy of catalysts used in total hydrocarbon oxidation because it is harder to oxidize than higher hydrocarbons. This is because the lack of C-C bonds in methane means that the molecule has a lower tendency to react than hydrocarbons containing multiple carbon atoms (CyberspaceChemistry, 2009).

Attempts to convert methane into more valuable chemicals have used oxidative coupling reactions yielding ethane and ethylene. This has proven to be economically unfavorable at desirable rates of methane oxidation. As a result, a different approach has been taken: the

oxidation of methane to produce synthesis gas (carbon monoxide and hydrogen gas). This can then be used as feedstock for methanol or ammonia synthesis, or converted to higher hydrocarbons, alcohols or aldehydes by Fischer-Tropsch catalysis (Ashcroft, 1990).

Complete Oxidation of Methane

The complete oxidation of methane is a heavily studied alternative to conventional thermal combustion. It is now being studied for a different reason, to remove toxins and odor volatile organic compounds. This process is intended to maintain human amenity, therefore it should occur at lower temperatures versus higher temperature combustions (Muto, Katada, & Niwa, 1996).

This type of reaction completely oxidizes methane and can be represented by the following equation:

$$CH_4 + 2O_2 \rightarrow CO_2 + 2H_2O \quad (1)$$

The complete oxidation of methane specifically is an important process because the thermal energy is produced at a relatively low temperature, therefore making it appropriate for the removal of toxins. It can be done over either noble metals or transition metal oxides. Noble metal catalysts are preferred over metal oxides because they function at lower level combustions of hydrocarbons because of their specific activity. This is especially applicable with methane, since as previously explained, is the hardest hydrocarbon to activate. Of these noble metals, the most common are palladium and platinum. Their increased metal dispersion increases catalytic activity (Gélin & Primet, 2002).

Other advantages of the complete oxidation of methane include: (1) rates can be significantly increased with the use of catalytic materials, as in this case (2) the ability to perform the reaction at a lower temperature yields lower levels of NOx and other emissions. This means that the energy release of the reaction (usually considered waste) could further be used. The catalytic combustors have two uses, to carry out a stable reaction for low concentrations and to attain lower levels of emissions. Gas turbines, furnaces and boilers have used these mechanisms (Shahamiria & Wierzba, 2008).

Reaction Rates

The reaction rate is the rate at which a species loses its chemical identity per unit volume. The rate of a reaction can be expressed as the rate of consumption of a reactant or as the rate of formation of a product (Fogler, 2006). When considering the reaction:

$$A \Rightarrow B \quad (2)$$

r_A is the rate of formation of species A per unit volume
$-r_A$ is the rate of consumption of species A per unit volume
r_B is the rate of formation of species B per unit volume
The rate equation for the theoretical chemical reaction:

$$A + B \rightarrow C \quad (3)$$

Would be written as:

$$\text{Rate (moles/L*s)} = k [A]^a [B]^b \quad (4)$$

The reaction rate is equal to the rate constant (k) times the concentration of species A ([A]) times the concentration of species B ([B]); raised to the power a and b, respectively. The exponents (a and b) refer to the order of the reaction with respect to species A and B. The reaction order describes the proportionality of the species to the rate of reaction. The overall order of the reaction is the sum of the individual orders of reaction for each species which would be (a + b) in this case. The reaction rate is determined using volumetric flow, concentration and the weight of the catalyst or molar flow, conversion and the weight of the catalyst for a differential reactor as shown (Fogler, 2006):

$$-r_A = \frac{v_0 C_c}{\Delta W} = \frac{F_0 X}{\Delta W} \quad (5)$$

The rate constant is dependent on temperature and activation energy as stated by the Arrhenius Equation:

$$k = Ae^{\frac{-E_A}{RT}} \quad (6)$$

A is the frequency factor, E_A is the activation energy, R is the gas constant, and T is the temperature (Fogler, 2006).

When observing multi-step reactions, it is necessary to note the rate determining step in order to determine the overall reaction rate of the process. Though the reaction rates may differ considerably from one step of the overall reaction to the next, the step with the slowest reaction rate is the most important. For example, reaction 1 has a lower rate of reaction than reaction 2 and reaction 2 uses the product (C) from reaction 1 to produce another product (E). Therefore, reaction 1 is the rate determining step because reaction 2 cannot create the final product (E) until enough reactant (C) has been produced by reaction 1. Additionally, increasing the concentration of reactants (A) and (B) would greatly increase the overall reaction rate while increasing the concentration of reactant (D) would not (Fogler, 2006).

A + B -> C Reaction 1 (slow)

C + D -> E Reaction 2 (fast)

The reaction rate can be increased or decreased when certain experimental parameters are varied. These parameters include reactant concentration, temperature, and catalyst. When considering the reactant concentration, adjustments to the reaction rate can be made using methods other than simply adding more moles of reactant. In the case of solid reactants, breaking down a large, single mass into many small particles allows a higher surface area on which aqueous or gaseous reactants can bond, thus increasing the rate of reaction. In the case of gaseous reactants, an increase in pressure will result in an increase in concentration based on the ideal gas law and temperature remaining constant. The temperature of a reaction can be varied in order to change the collision frequency of the particles and to change the number of particles with energy greater than or equal to the activation energy. Lastly, adding a catalyst to a given reaction can provide a reaction process with lower activation energy than the straightforward reaction, thus increasing the rate of reaction. In reactions where catalysts are present, there are cases where increasing the concentration of reactants does not result in an increase in the reaction rate because the catalysts are completely covered by molecules and do not have enough

room to fit additional ones. Therefore, increasing the amount of catalyst would be necessary before increasing concentrations of reactants (Fogler, 2006).

For a catalytic reaction, $-r_A'$ is the rate of consumption of species A per mass of catalyst since the rate of reaction depends on the amount of catalyst, W, available. The amount of available catalyst can be affected by the turn over number (TON) of the catalyst. This number measures the moles of substrate that one mole of catalyst can affect before becoming inactive.

Reaction Rate in a Packed Bed Reactor

In a packed bed reactor the reaction rate is based on mass of solid catalyst because the reaction takes place on the surface of the catalyst. The rate of reaction is equal to the amount of moles of species A per second that have reacted per unit mass (grams) of the catalyst as shown (Fogler, 2006):

$$-r_A' = \frac{moles\ \ A\ reacted}{s{*}grams\ \ catalyst} \tag{7}$$

Assuming the packed bed reactor is differential (it has no radial gradients in concentration, temperature, or reaction rate) the mole balance for species A reacting on a catalyst with weight, W at steady state is (Fogler, 2006):

$$F_{A|W} - F_{A|(W+\Delta W)} + r_A'\Delta W = 0 \tag{8}$$

Where the first term represents the amount of moles flowing into the reactor, the second term represents the amount of moles flowing out, the third term represents the amount of moles being generated, and the last term represents the amount of moles that have accumulated. The differential form of this mole balance is

$$\frac{dF_A}{dW} = r_A' \tag{9}$$

The integral form can only be used when catalyst decay and pressure drop over the reactor are negligible (Fogler, 2006).

Reported Oxidation of Methane Experiments

There have been many experiments considering the full oxidation of methane over a 0.5% Pd/Alumina catalyst. (Hurtado, 2004) (Monteiro & al., 2001) (Ribeiro & al., 1994) The expected activation energy of this reaction under these conditions can range anywhere from 70-150 kJ/mol for an order with respect to methane being 1 and an order with respect to oxygen being 0. (Hurtado, 2004) Due to experimental conditions, it is possible for the order with respect to methane to be 0.9 and the order with respect to oxygen to be 0.08 (Hurtado, 2004). The turnover rate for this reaction on palladium foil has been reported to be 0.59 1/s for a reaction with an order with respect to methane, oxygen and water being 0.7, 0.2, and -0.9 respectively. (Monteiro & al., 2001) The rate of reaction with respect to water is sometimes reported to be negative due to the fact that water has a pronounced inhibiting effect on the rate (Monteiro & al., 2001). Wetting of the catalyst has an effect of the conversion and limits the surface reaction that takes place.

Activation energy

Reactant particles collide at varying energies during a chemical reaction. In order to react and form products, the particles must collide with enough energy to initiate the reaction by breaking chemical bonds. This minimum amount of collision energy is known as the activation energy. The number of particles that are capable of reacting can be observed using a Maxwell-Boltzmann distribution, which plots numbers of particles against a range of energies at a specific temperature. Catalysts facilitate chemical reactions by providing a separate reaction route with lower activation energy, consequently increasing the reaction rate.

Catalysts

"A catalyst is a material which initiates and enhances the rate of a chemical reaction without being consumed by the reaction" (Tarhan, 1983). A catalyst may also be defined as a substance which lowers the activation energy of a thermodynamically permitted reaction (Satterfield, 1996). In Figure 10, E_a represents the activation energy of the reaction required. It can be seen that in a catalytic reaction, the activation energy of the reaction is lowered while still providing the desired products.

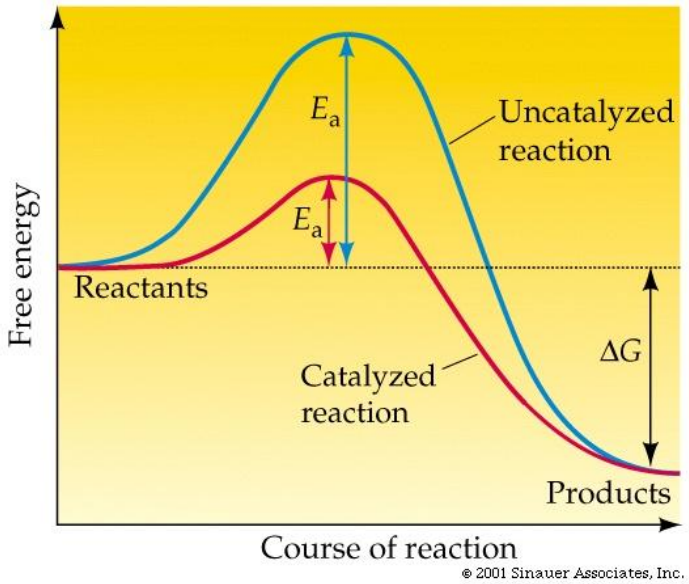

Figure 10: Effect of Catalyst on Activation Energy

Heterogeneous vs. Homogeneous

The two major types of catalysts are homogeneous and heterogeneous catalysts. Homogeneous catalysts exist in the same phase as the reactants and are used less frequently than heterogeneous catalysts in industrial practice. Heterogeneous catalysts exist in a different phase than the reactants. Usually heterogeneous catalysts are solid substances catalyzing gas and/or liquid phase reactions. In a packed bed reactor, the heterogeneous catalyst exists in a fixed or packed bed in which reactants pass through and react (Tarhan, 1983).

There are two types of gas adsorption on catalyst surfaces: physical adsorption and chemical adsorption, also known as chemisorption (Tarhan, 1983). Physical adsorption is when a

gas is adsorbed on a solid and covers it entirely; similarly to liquefaction. It generally happens at low temperatures and is highly reversible. In chemisorptions the bond is strictly chemical, where the gas reacts with the surface of the catalyst.

Sometimes when species are chemisorbed on a catalyst's surface, they can stay there. This leads to poisoning of the catalyst. Poisoning of a catalyst is when a catalyst loses part of its activity (Tarhan, 1983). Where $\alpha = fraction\ of\ pore\ surface\ poisoned$, and $F = \frac{reaction\ \ rate\ \ poisoned}{reaction\ \ rate\ \ unpoisoned}$:

$$F = 1 - \alpha \tag{10}$$

$$F = (1 - \alpha)^{0.5} \tag{11}$$

Equation (10) can be used for selective and non-selective poisoning. Equation (11) can be used for anti-selective poisoning. Selectivity is defined as the rate of generation of desired products divided by the rate of generation of undesired products. Figure 11 shows graphical representation of the difference types of poisoning on a catalyst.

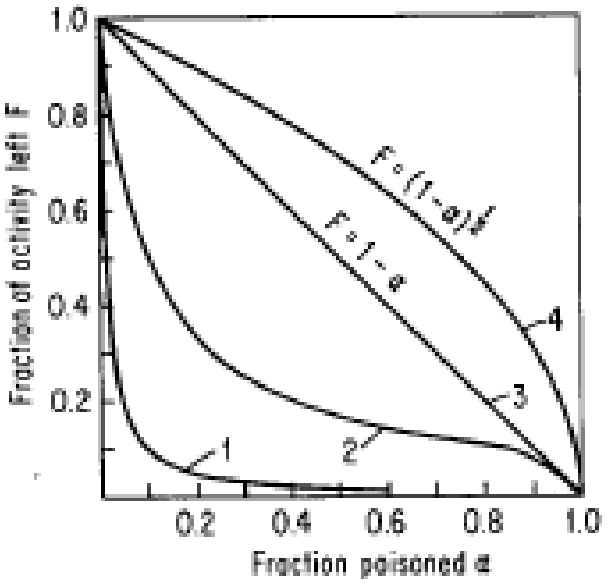

Figure 11: Effect of Poisoning on a Catalyst (Tarhan, 1983)

In the instance of chemisorptions, it is due to the fact that these species are blocking and interfering with the active sites on the catalyst. Carbonaceous (coke) deposits on the catalytic sites on zeolites can deactivate the catalyst (Satterfield, 1996). A traditional method for removing this coke is through oxidation by heating or burning the catalyst (Tarhan, 1983). With increased temperature and over long periods of time the hydrogen-carbon ratio of coke decreases and the coke becomes resistant to removal by oxidation. The shape of the catalyst plays a large role in the formation of coke on a catalyst, with fewer deposits on medium-pored catalysts. The majority of coke formation takes place on acidic sites on a catalyst and is influenced by reaction acidity (Satterfield, 1996).

Mass Transfer Limitations due to Catalysts

Arguably the most important property of a heterogeneous catalyst is its porosity (Tarhan, 1983). The porosity can affect the diffusion phenomena and the kinetics of the reaction. A good catalyst can have several hundred square meters of inner pore surface per gram of catalyst, with the majority having over $300m^2$ of internal surface area/gram of catalyst. The porosity of a catalyst influences mass transfer limitations because of the surface that takes place in a catalytic reaction (Tarhan, 1983).

$$R = kC_s^{\alpha} = k_g a(C_0 - C_s) \quad (12)$$

$$k_g = \frac{D}{\delta} \quad (13)$$

Where:

k=reaction rate constant (1/s)

α=reaction order

k_g=mass-transfer coefficient (m/s)

a=the ratio of surface available per unit volume of reactor space (m^2/m^3)

D=diffusivity of the reactant (m^2/s)

δ=fictitious 'film' of thickness (m)

Equation (12) equates the mass transfer limitation to the rate of the reaction. The right side of the equation represents the mass transfer limitation. The diffusivity of the reactant and the 'film' of the thickness around a catalyst particle are related to the mass transfer coefficient. The diffusion of the reactant through this 'film' controls the reaction. A reactant must pass through a fictitious 'film' around the catalyst particle caused from other flowing reactants in order to react the surface of the catalyst. As the concentration from the bulk, $C_{o,}$ is decreased, the concentration on the surface, $C_{s,}$ is increased. The left side of the equation represents the rate of the reaction taking place on the surface of the catalyst. This reaction is related to the mass transfer coefficient due to the fact that it cannot happen until the reactants have diffused through the 'film' and reached the surface of the catalyst. With increasing velocity/increasing Reynolds number, δ goes to zero and k_g goes to infinity. Increasing the velocity will usually increase k_g and reduce mass transfer limitations.

Often mass transfer limitations are considered to be of two types: external, representing the need to diffuse from the bulk to the surface of the catalyst particle and internal, representing the need to diffuse into the pores of the catalyst particle (Fogler, 2006).

Chromatography

Chromatography encompasses a group of techniques for separating mixtures based on their equilibrium properties, resulting in a partitioning of each species. A gas, a liquid, or a solid mixture may be separated into zones or bands for each component in the sample. All types of chromatography involve a mobile phase which contains the sample to be analyzed and a stationary phase over which the mobile phase flows. Some methods of chromatography include displacement chromatography and column chromatography (Ettre, 1993).

Displacement development is a method of chromatography in which a band of the mixture to be analyzed is injected into the column. Components of the mobile phase have varying magnitudes of attraction to the stationary phase. The component with the strongest attraction occupies the sites near the entrance of the column and the component with the weakest attraction occupies sites near the bottom of the column. After all the components have separated in the column, a displacer substance is injected that interacts more strongly with the stationary phase than any of the components. The most strongly attracted component is displaced and in turn replaces the next most attracted component. This process continues down the column for each component. Eventually the least attracted component of the original sample is forced out of the column first, followed by the remaining components in order. The nature of the process does not allow for discrete elution, however, and each component is somewhat contaminated by its neighbors (Scott, 2005).

Column chromatography is a method of chromatography in which the mixture to be analyzed is fed into a column as the mobile phase. Each component is retained by the stationary phase in varying degrees, resulting in a separation of the components within the column. The component least attracted to the stationary phase flows out of the column more quickly than the other components, which take more time to move through the column (EncyclopediaBritannica, 2009).

Gas chromatography is a type of column chromatography in which the mobile phase is a gas comprised of the sample feed and an inert carrier gas and the stationary phase is a liquid. In addition, gas chromatography is carried out in an oven where the temperature of the gases can be regulated in order to achieve better separation. The column in a gas chromatograph may be a packed column or a capillary column. Packed columns are comprised of inert, solid support material that has been finely divided and coated with the liquid stationary phase so that the mobile phase may flow among the particles. Capillary columns are very small in diameter and either have the stationary phase coated on the walls or have a thin supporting material lining the wall into which the stationary phase has been adsorbed. In general, capillary columns are more efficient than packed columns for achieving separation (SheffieldHellamUniversity, 2006).

COMSOL Multiphysics

COMSOL Multiphysics is a software package developed by graduate students of Germund Dahlquist at the Royal Institute of Technology in Stockholm, Sweden in 1997. The program was originally known as FEMLAB because it uses the finite element method to analyze and solve complex problems. The software comes with several modules in its library for specific applications. These applications include: AC/DC Module, Acoustics Module, CAD Import Module, Chemical Engineering Module, Earth Science Module, Heat Transfer Module, Material Library, MEMS Module, RF Module, and Structural Mechanics Module. Each module contains modeling tools and equations for the application described. Modeling tools from multiple modules can be coupled together to accurately depict complicated systems and processes (COMSOL Group, 2008).

Modules

The AC/DC Module is used for simulating electrical equipment, the CAD Import Module allows geometries created with CAD programs to be imported to COMSOL, and the Earth Science Module simulates geological and environmental systems. The Heat Transfer Module simulates conduction, convection, and radiation phenomena. The Material Library contains properties for thousands of materials. The MEMS Module simulates microfluidic devices, the RF Module simulates electromagnetic fields and high frequency devices, and the Structural Mechanical Module performs stress-strain analyses (COMSOL Group, 2008).

The Chemical Engineering Module contains tools for modeling fluid, heat, and mass transfer, as well as for chemical reactions. These tools can be used for both steady-state and transient analysis. The module can be used to simulate a variety of systems, including batch reactors, separators and scrubbers, filtration, heat exchangers, and packed bed reactors (COMSOL Group, 2008).

Models may be created in 1, 2, or 3 dimensions, and use partial differential equations to relate the physics of each aspect of a model. In order to simulate all the aspects of a system, multiple models are often necessary. For example, modeling a reactor might require fluid flow and heat transfer to be coupled (COMSOL Group, 2008).

Importance

COMSOL is particularly useful for modeling processes involving transport phenomena. The models created can be used as visual aids in instruction and learning. As a research tool, COMSOL has been used in applications ranging from nanotechnology to semiconductors and acoustics since it can accurately model various phenomena in order to optimize and design engineering systems better (COMSOL Group, 2008). Presentations at the 2008 COMSOL conference in Boston included modeling nanoscale heat flow, modeling of musculoskeletal biomechanics, and simulation of chromatographic band transport (COMSOL Group, 2008).

As an academic tool, COMSOL can be used to allow students to obtain a better understanding of practical systems. By creating and manipulating a model of an experiment to be later run in a lab, students can gain a better understanding of the system before entering the lab. This is particularly useful for students who learn best kinesthetically or visually. COMSOL can also help to pull together separate concepts and demonstrate how they are used together. Often topics such as heat and mass transfer are taught separately, but both take place in a chemical reactor, and using COMSOL to model this phenomena can make it easier to understand and visualize (COMSOL Group, 2008).

Using COMSOL

The first step to creating a model using COMSOL is to create the desired geometry to be evaluated. This can be a 1, 2, or 3 dimensional geometry. Irregular geometries are also possible to make using the various drawing tools available to COMSOL. The next step is to mesh the model. This involves breaking the geometry into subsections that will be evaluated individually and then displayed together to give an overview of the phenomena taking place. It is generally

most effective to specify a small mesh size at and near boundaries as this is where the most irregularities will occur. After meshing, the physics of the model may be defined both throughout the subdomain of the model and at each of the boundaries. The model can then be solved and post-processing can occur. Post-processing involves manipulating the solution to obtain plots for relevant data and fluxes. Parametric studies can then be performed in order to optimize the model (COMSOL Group, 2008).

Finite Element Method

The finite element method is a numerical technique that is used to approximate solutions to partial differential equations (PDEs). This is accomplished in simple cases by eliminating the differential part of the equation, and in more complex cases by approximating the PDE by a series of ordinary differential equations that are solvable by other numerical methods. The finite element method is especially useful when evaluating complex and irregular geometries, when the domain is changing, and when varying degrees of accuracy are desired over the domain (Weck & Kim, 2004).

The finite element method was developed by Alexander Hrennikoff and Richard Courant in the 1940's and 1950's for use in civil and structural engineering applications. The methods employed by both men, while not exactly the same, both relied on meshing a large continuous domain into smaller sub-domains, called elements. This method has found applications in many disciplines, from structural simulations depicting stresses and strains on a structure, to fluid flow through a pipe (Widas, 2008).

Since an equation describing an entire geometry at once can be difficult to obtain and solve, the finite element method operates by first dividing a geometry into elements which are connected by nodes. This process results in a set of simultaneous equations that describe the geometry. By describing a simple equation at one element, usually at a boundary, the entire mesh can be solved by working out from the starting point since adjacent elements share a boundary. The resulting equations can then be combined to obtain an overall description of the geometry. This overall description is not an exact equation, but rather an approximation of the geometry (Weck & Kim, 2004).

Methodology

The purpose of this Major Qualifying Project was to simulate the oxidation of methane in a packed bed reactor using COMSOL Multiphysics and to facilitate future incorporation of the simulation in the senior-year Unit Operation classes at WPI. The reactor operated under various temperatures and feed flow rates to provide comparison data for the model. Using this data, simulations of both the reactor and the gas chromatograph were created using COMSOL.

Reactor Data Collection

The reactor was first run as it is in the ChE4402 Unit Operations class in order to obtain data from which the models could be built.

Equipment

The packed bed catalytic reactor and gas chromatograph are shown schematically in Figure 12. Air, nitrogen, and methane can all flow through the system. During the actual experiment, only the air and methane were flowing. Once the gases passed through the evaporator, they could either continue through a bypass line or through the reactor by adjusting valves. The gas flowed through the bypass line without reacting in order to calibrate the gas chromatograph. The inlet species flow rates were set manually by flow meters. The exiting gases from both the reactor and the bypass passed through the gas chromatograph, where the levels of methane, oxygen, carbon dioxide, and nitrogen were indicated.

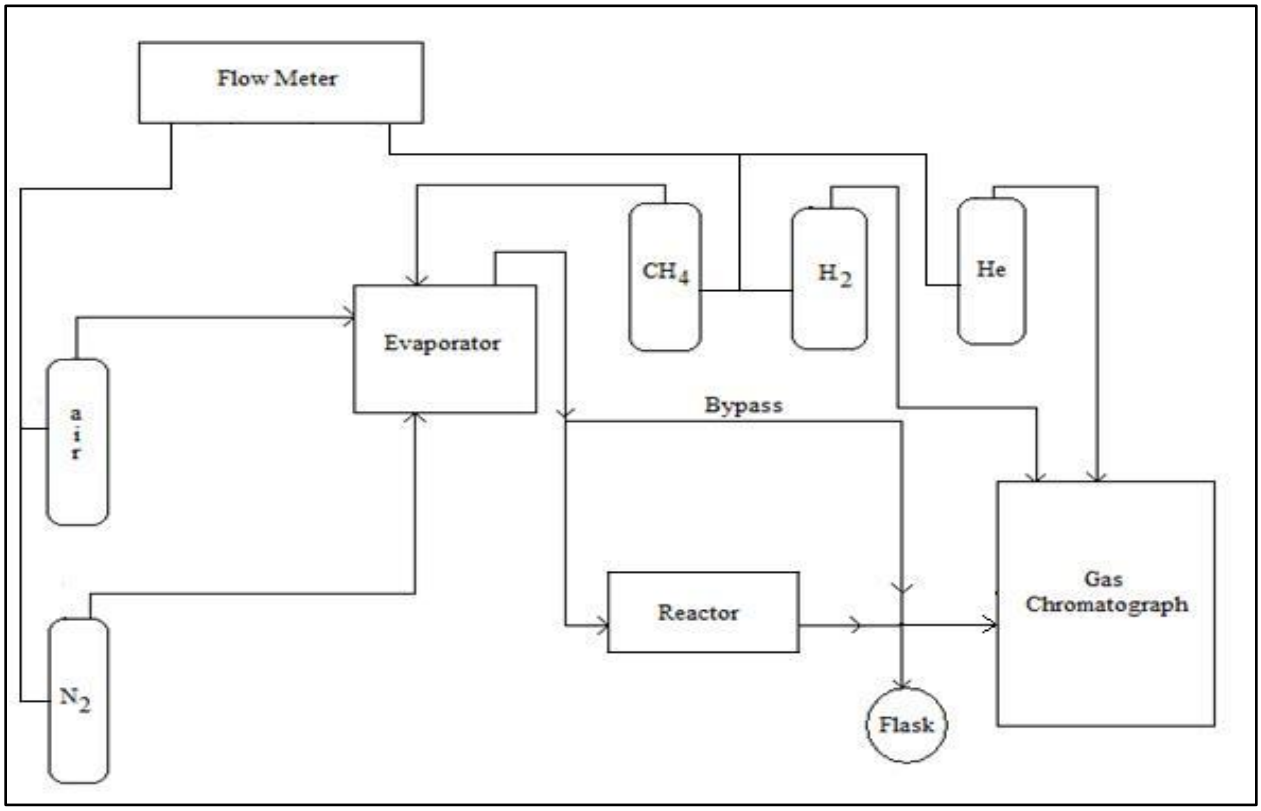

Figure 12: Catalytic Reactor Block Diagram

The reactor itself is a tube of 0.340 inch diameter with a 3 inch section of 0.5% Pd/alumina catalyst with a total mass of 5.26 g. The catalyst pellets are cylindrical shaped and 3.2mm in diameter. The catalyst section is preceded by a section of glass packing beads that serve to disperse the inlet flow evenly over the cross-section of the catalyst. A cross sectional diagram of the reactor tube is shown in Figure 13.

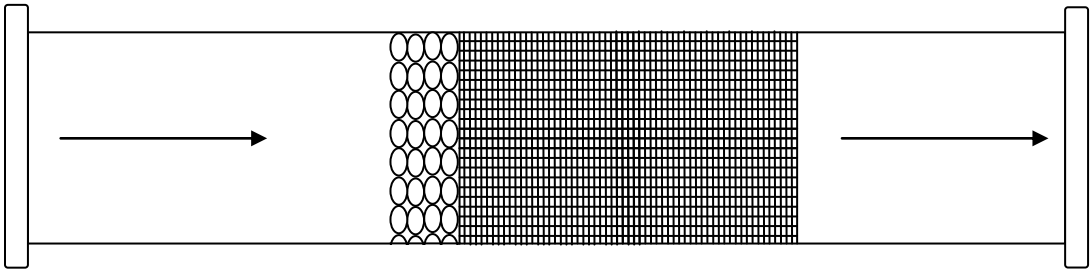

Figure 13: Reactor Cross Section

The catalytic reactor was first run to determine the reaction order in methane and the rate of the reaction of methane in air. The reaction order in methane was determined by examining the conversion of methane to carbon dioxide by varying the flow rate of methane while the total flow rate of gas into the reactor remained constant. The total flow rate was maintained at 300 mL/min (STP) at a temperature of 227°C. The ratio of oxygen to methane was varied between 5:1 and 13:1, as shown in Table 2. The velocity of the gases at this total flow rate was 0.1563 m/s through the reactor tube.

Table 2: Inlet Flow Rates

Ratio (O_2/methane)	Air Flow (mL/min)	Methane Flow (mL/min)
5/1	288.3	12.08
7/1	290.58	8.46
9/1	292.86	6.64
11/1	294.01	5.44
13/1	295.15	4.63

Experimental

Data from five experimental runs were used to calculate the reaction order with respect to methane. The units of measurement from all experimental runs had to be compatible with COMSOL in order to correctly simulate the reaction. Consequently, all volumes were converted to cubic meters from milliliters and all flow rates to seconds from minutes. Temperature was given in units of Kelvin and pressure was assumed to be 101,325 Pascals. This assumption is not 100 percent accurate but it is close enough to give accurate approximations and was necessary to make because there are no pressure gauges in the reactor system.

The inlet volumetric flow rates were set for air and methane first by adjusting the flow meter to the channel that corresponded to the desired flow rate. The calibration curves for the flow meters are located in Appendix A.

The total concentration was determined by rearranging the ideal gas law as such:

$$C_{Total} = \frac{n}{V} = \frac{P}{RT} \quad (14)$$

The gases were assumed to be ideal, allowing the ratio of the initial volumetric flow rate of methane to the initial total volumetric flow rate to be equal to the initial mole fraction of methane:

$$\frac{\dot{V}_{CH4}}{\dot{V}_{Total}} = y_{CH4} \quad (15)$$

The initial mole fraction of methane multiplied by the total concentration gives the initial concentration of methane:

$$C_{Total} * y_{CH_4} = C_{CH_{4;initial}} \quad (16)$$

This inlet concentration of oxygen was determined using the same method except the mole fraction of oxygen was used instead of methane. Since the flow rate of the air includes both oxygen and nitrogen, 21 percent of the air flow rate was used as the volumetric flow rate of oxygen.

After passing through the reactor, the outlet stream was fed into a gas chromatograph, which analyzed the effluent stream. Using the area peaks from the gas chromatograph data and the calibration curves that related area ratios to partial pressure ratios, the partial pressures of each species relative to nitrogen were determined. The calibration curves for the gas chromatograph can be found in Appendix B

The partial pressure of the effluent nitrogen was determined from the ideal gas law:

$$p_{N2} = (C_{Total})(y_{N_2})RT \quad (17)$$

The partial pressure of each species was the product of the species to nitrogen partial pressure ratio (determined from the gas chromatography and associated calibration curve) multiplied by the partial pressure of nitrogen:

$$p_A = \frac{p_A}{p_{N2}} * p_{N2} \quad (18)$$

In order to find the moles of methane that reacted, the ratio of the carbon dioxide to nitrogen partial pressures was divided by the ratio of the methane to nitrogen partial pressures from the bypass run. The moles of CO_2 in the GC equal the moles of CH_4 that were consumed in the reaction. Therefore, the ratio of moles of methane reacted to moles of methane fed into the reactor is known, giving the conversion of methane (X_{CH_4}):

$$\frac{\frac{p_{CO2}}{p_{N2}}}{\frac{p_{CH4}}{p_{N2}}} = \frac{p_{CO2}}{p_{CH4}} = \frac{y_{CO2}}{y_{CH4}} = \frac{n_{CH4;initial} - n_{CH4;final}}{n_{CH4;initial}} = X_{CH4} \quad (19)$$

The molar flow rate of methane was then determined from the ideal gas law:

$$F_{CH4} = \frac{p_{CH4}\dot{V}_{CH4}}{RT} \quad (20)$$

The rate of reaction is equal to the molar flow rate of methane times the conversion of methane divided by the weight of the catalyst (0.5% Pd/alumina in 5.26 grams of catalyst):

$$-r_{CH_4} = \frac{F_{CH_4}X_{CH_4}}{\Delta W} \quad (21)$$

In order to obtain the rate of reaction in units compatible with COMSOL, the flow rate of methane was multiplied by the conversion divided by the reactor volume.

$$-r_{CH_4} = \frac{F_{CH_4} X_{CH_4}}{V_{reactor}} \tag{22}$$

The outlet concentration of methane is equal to the outlet volumetric flow rate of methane divided by the total volumetric flow rate of the gases:

$$C_{CH4;final} = \frac{F_{CH4}}{\dot{V}_{CH4} + \dot{V}_{Air}} \tag{23}$$

The reaction order with respect to methane can be found by manipulating the rate equation into a plot of the natural log of the reaction rate versus the natural log of the methane concentration:

$$-r_{CH_4} = kC_{CH4}^{\alpha} \tag{24}$$

$$\ln(-r_{CH_4}) = \alpha * \ln(C_{CH4}) + \ln(k) \tag{25}$$

By taking the natural log of the rate equation, the subsequent equation is of the form:

$$y = m * x + b \tag{26}$$

The slope of the graph, m, is equal to the reaction rate with respect to methane, α, and the intercept, b, is equal to the natural log of the reaction constant, k.

Once the reaction order with respect to methane was known, the activation energy could be determined. The rate of reaction was calculated again for the five different temperatures using:

$$-r_{CH_4} = \frac{F_{CH_4} X_{CH_4}}{\Delta W} \tag{27}$$

The methane molar flow rate and conversion were calculated the same way as before using the ideal gas law and gas chromatograph analysis. The rate of reaction was then used in the rate law equation with the methane outlet concentration and reaction order found earlier to give the value of the reaction constant at each temperature:

$$k = \frac{C_{CH4}^{\alpha}}{-r_{CH_4}} \tag{28}$$

The concentration of methane exiting the reactor was also found using the methods discussed previously.

The activation energy was determined by manipulating the Arrhenius equation into another natural log plot and solving for the slope:

$$k = A * exp(\frac{-E_A}{RT}) \tag{29}$$

$$\ln(k) = \frac{1}{T}\left(\frac{-E_A}{R}\right) + \ln(A) \tag{30}$$

This form of the equation plots the natural log of the reaction constant against the inverse of the temperature to give activation energy divided by the gas constant as the slope.

Modeling the Reactor

Using the data gathered from the actual reactor, models of the reactor were created using Polymath and COMSOL Multiphysics.

Determining Model Inputs

In order to model the reactor effectively in COMSOL, several properties of the reaction had to be known first. As previously described, the order, activation energy, pre-exponential factor, and inlet/outlet concentrations of species were obtained experimentally. The velocity of the inlet gas was determined from the volumetric flow rate and the cross-sectional area of the reactor. The inlet gas velocity was determined to be 0.1563 m/s. In this experiment, nitrogen acts as a carrier for the gases and has a constant, predominant concentration compared to the other reactants and products. Also, every mole of gas reacted resulted in a mole gas produced. Due to these two conditions, the velocity was assumed to be constant. The gases were assumed to be ideal.

Three differential rate equations were created in order to simulate the reaction throughout the reactor (Finlayson, 2006). For the reaction:

$$CH_4 + 2O_2 \rightarrow CO_2 + 2H_2O \tag{31}$$

The four differential equations are as follows:

$$\frac{dC_{CH4}}{dz} = rch4 = -\frac{k}{v*w} * [CH_4]^{\alpha} \tag{32}$$

$$\frac{dC_{CO2}}{dz} = rco2 = \frac{k}{v*w} * [CH_4]^{\alpha} \tag{33}$$

$$\frac{dC_{H2O}}{dz} = rh2o = 2 * \frac{k}{v*w} * [CH_4]^{\alpha} \tag{34}$$

$$\frac{dC_{O2}}{dz} = ro2 = -2 * \frac{k}{v*w} * [CH_4]^{\alpha} \tag{35}$$

Where:

C_{CH4} = Concentration of CH_4 (mol/gram catalyst*m^3)

C_{O2} = Concentration of O_2 (mol/gram catalyst*m^3)

C_{H2O} = Concentration of H_2O (mol/gram catalyst*m^3)

C_{CO2} = Concentration of CO_2 (mol/gram catalyst*m^3)

w =Weight of Palladium in Catalyst (grams)

v = Velocity of gas (m/s)

z = Length of reactor (m)

k = Rate constant (m^3/mol*2)

α = Reaction order of methane

In COMSOL, the rate of reaction is in units of mol/m^3s, where m^3 is the volume of the reactor. In order to have our equations match COMSOL's units, our rate equation were re-arranged as follows:

$$\frac{dC_{CH4}}{dz} = rch4 = -k[CH_4]^{\alpha} \tag{36}$$

$$\frac{dC_{CO2}}{dz} = rco2 = k[CH_4]^{\alpha} \tag{37}$$

$$\frac{dC_{H2O}}{dz} = rh2o = 2 * k[CH_4]^{\alpha} \tag{38}$$

$$\frac{dC_{O2}}{dz} = ro2 = -2 * k[CH_4]^{\alpha} \quad (39)$$

Where

V=volume of reactor (m^3)

The rate constant, k, was set as a variable dependent on the temperature of the reaction, T, as in equation (29).

The other constants that were set in COMSOL were the: inlet concentration of CH_4 (oCch4), inlet concentration of O_2 (oCo2), the velocity of the gas (v), the activation energy (A), the pre-exponential facto (Phi), the gas constant (R), the temperature of the reaction (T), and the rate constant (k), determined from equation (29) .The activation energy and pre-exponential were found experimentally, as previously described. The activation energy was found to be 68287.09 J/mol and the pre-exponential factor was found to be 678744.5 1/s.

The inlet concentration of methane was determined to be 0.9750 mol/m^3 and the inlet concentration of oxygen was determined to be 4.914 mol/m^3 (from equation 16).

As previously mentioned, the velocity was determined from the cross-sectional area of the reactor and the volumetric flow rate of the gas.

$$q = \dot{v}_{total} * A \quad (40)$$

Where:

A=cross-sectional area of the reactor (m^2)

The cross-sectional area of the reactor was determined from the definition of $A = \pi r^2$; where r is equal to the radius of the reactor.

Modeling Using Polymath

The reaction was first modeled using POLYMATH 6.10 in order to gain a fundamental understanding of the reaction. The following was input into POLYMATH in order to simulate the reactor:

```
d(Cch4) / d(z) = -r1
Cch4(0) = 0.974982

d(Co2) / d(z) = -2*r1
Co2(0) = 4.91391

d(Cco2) / d(z) =r1
Cco2(0) = 0

d(Ch2o) / d(z) = 2*r1
Ch2o(0) = 0

z(0) = 0
z(f) = .0762

alpha = 0.6525
beta = 0
```

r1=k/(v)*(Cch4^alpha)*(Cco2^beta)
k=0.049837
v=0.1563

Modeling Using COMSOL Multiphysics

After a preliminary model using POLYMATH was made, the group was ready to make the model using COMSOL Multiphysics. The group used a 2-D model with axial symmetry. This provided a model of the reactor cut down the center length-wise.

A chemical Engineering Module for convection and diffusion with steady state was used with four dependent variables, cCH4, cO2, cCO2, and cH2O, the concentration of methane, oxygen, carbon dioxide, and water, respectively. The incompressible Navier-Stokes domain was eliminated from the model due to the fact that plug flow with constant velocity in the cross section was assumed because it is a packed column. Ideal constraints were used and the quadratic element was used in the model. A mesh of 640 elements was used for the model.

The reactor was drawn vertically with a height of 0.0762m and a radius of 0.004318m. The subdomain settings for the reactor are shown in Table 3, with the diffusion coefficients being neglected due to the fact that the reactor is gradient-less.

Table 3: Reactor Model Subdomain Settings

Variable	Diffusion Coefficient (isotropic) (m^2/s)	Reaction Rate ($mol/(m^3*s)$	r-velocity (m/s)	z-velocity (m/s)	Initial Value (mol/m^3)
cCH4	0	rch4	0	v	oCch4
cO2	0	ro2	0	v	oCo2
cCO2	0	rco2	0	v	0
cH2O	0	rh2o	0	v	0

Figure 14: Reactor Model Boundary Settings shows the drawing of the reactor. Boundary 1 (red) was given the conditions of axial symmetry, because there is symmetrical flux across this boundary condition. This model shows the reactor sliced down the middle length-wise. Boundary 2 (green) is the inlet of the reactor. The inlet concentrations of methane, oxygen, carbon dioxide and water were set to oCch4, oCo2, 0, and 0 respectively. Boundary 3 (blue) was given the condition of convective flux. This allows the finite element method to solve for the concentration of the species at this point; in order to treat this boundary as the outlet of the reactor. Boundary 4 (black) was given the conditions of Insulation/Symmetry so that there is no flux through this boundary. This is in order to simulate this boundary as a wall of the reactor.

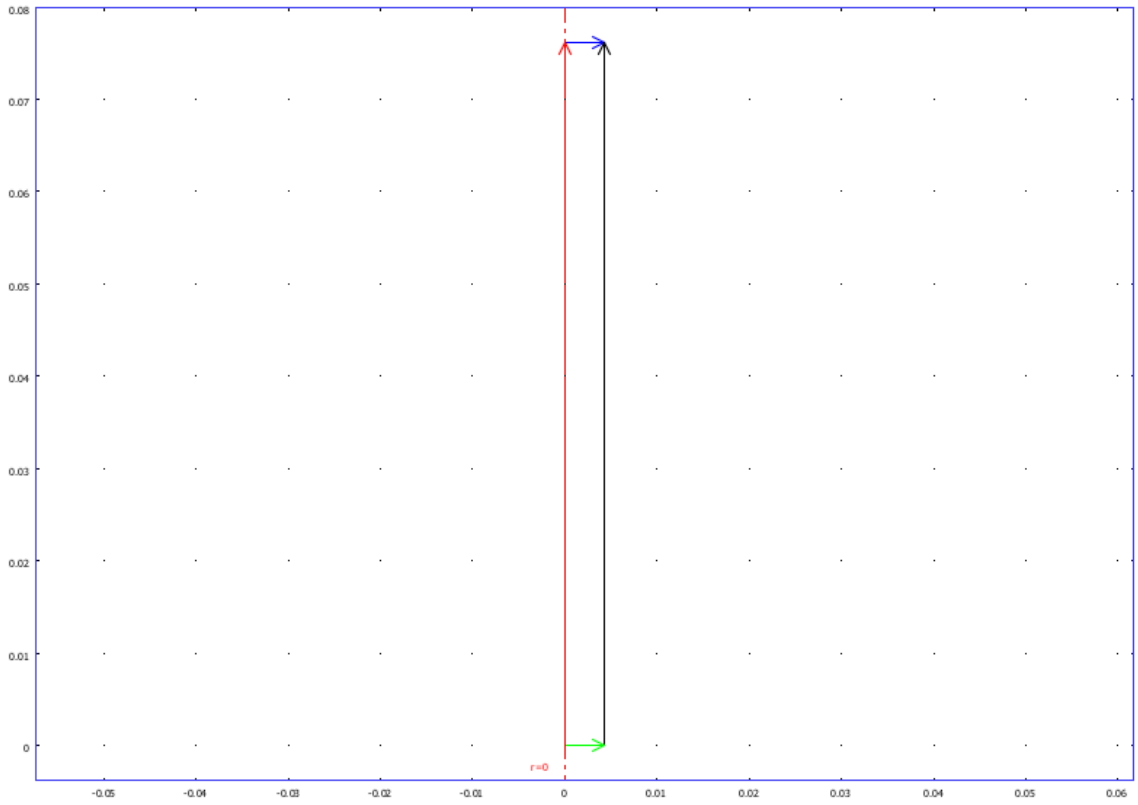

Figure 14: Reactor Model Boundary Settings

Applying Mass Transfer Limitations in COMSOL Multiphysics

Rate equations for the surface reaction between methane and oxygen were included in the COMSOL model to account for mass transfer limitations. After consulting several journal articles, values of activation energy, pre-exponential factor, rate constant, and orders with respect to methane and oxygen were determined to be: 56500 (J/mol), 100000(1/s), 0.1251 (1/s), 0.90, and 0.08. Due to the fact that no two reactions, reactors, or catalysts are alike, these values had to be generalized to the group's findings in literature. These values were approximated using a combination of literature findings.

A reactor was modeled using these values. The group has reason to believe that the reactor in Goddard Hall has mass transfer limitations due to the size of the catalyst pellets. The group used these new values of constants from literature in order to create a new "ideal" reactor, without mass transfer limitations.

Mass transfer limitations were then included in this model in order to try to replicate the Goddard Hall model. A new rate equation was given to methane.

$$r_{CH_{4_s}} = -k[CH_4]_s^{\alpha}[O_2]_s^{\beta} \quad (41)$$

Where:
k=rate constant

α=order with respect to methane
β=order with respect to oxygen

This equation represents the reaction between methane and oxygen on the catalyst surface. Equation (41) was used in order to find the rate constant. A mass transfer flux equation was used as a "reaction" equation in COMSOL to account for methane disappearing from the bulk and arriving at the surface of the catalyst. Equation (42) is identical to the right side of equation (12). Both external and internal mass transfer limitations, if present, have been lumped into one mass transfer coefficient in this equation.

$$r_{CH_4} = -km(C_{CH_4} - C_{CH_{4_s}}) \quad (42)$$

Where:
r_{CH4}=mass transfer "reaction"
km=mass transfer coefficient (1/s)
C_{CH4}=Concentration of methane (mol/m^3)
C_{CH4s}=Concentration of methane at the surface of the catalyst

The overall rate of disappearance of methane is given by:

$$r_{s_{CH_4}} = r_{CH_{4_s}} - r_{CH_4} \quad (43)$$

Where:
r_{sCH4}=Overall rate of disappearance of methane
r_{CH4s}=Disappearance of methane due to reaction at the surface of the catalyst
r_{CH4}=Appearance of surface species due to mass transfer limitations

After determining the mass transfer coefficient which provides a model similar to the reactor model a constant can be used to relate the mass transfer coefficient with the velocity of the gas flowing through the reactor.

$$k_m = k_o v^{0.7} \quad (44)$$

Where the velocity dependence was assumed to be to the 0.7 power. This relationship between the mass transfer coefficient and velocity was estimated using relations from literature (Cussler, 2008).

Modeling the Gas Chromatograph

An approximate model of the gas chromatograph used for analyzing the reactor output was made using COMSOL. Because the actual gas chromatograph uses a varying temperature profile with time in order to achieve separation of the components, a more sophisticated model would need to be created in order to model it exactly. Since this was outside the scope of this project, the temperature within the model was assumed constant while other variables were adjusted to approximate the actual results.

The template for the model was the "Liquid Chromatography 1" model under the Chemical Engineering Module in COMSOL. The chromatograph was modeled as a straight tube of length 0.12 using time dependent convection and diffusion equations with four species. The necessary constants were defined, including the phase ratio (Φ), the linear velocity of the mobile

phase (v_l), the effective diffusion constant for each species(D_{eff_j}), the adsorption constant for each species(K_j), the monolayer capacity for each species (n_{j_0}), a time scaling constant (Ac), the normal distribution parameter (a), and the starting point (x_0). Because the purpose of this model was only to obtain results similar to those produced by the real GC, the values used for these constants were rough approximations. The initial concentrations (c_{j_0}) of each species were also specified, and were obtained from the output of the reactor model. A scalar expression was defined for each species relating the change in monolayer capacity to the change in concentration of that species as follows:

$$\frac{dn_j}{dc_j} = \frac{(n_{j0} * K_j)}{(1 + K_j * c_j)^2} \tag{45}$$

The subdomain settings were defined as follows for each species:

$$\delta_{ts} = Ac * (1 + \Phi * \frac{d_{n_j}}{d_{c_j}}) \tag{46}$$

$$D = D_{eff_j} * Ac \tag{47}$$

$$R = 0 \qquad u = V$$

In addition, artificial diffusion was added for each species to improve the smoothing of the results. Artificial streamline anisotropic diffusion was used at a tuning parameter of 0.05 for each species. The initial conditions for each species were then defined as follows, with x being the position in the tube:

$$c_j(t_0) = c_{j_0} * \exp(-a * (x - x_0)^2) \tag{48}$$

The boundary at the inlet of the chromatograph was set to a concentration of 0 for each of the species (because it is an injection system), and the boundary at the outlet was set to convective flux for each of the species.

In order to solve the model, a standard mesh of 400 elements was used. A domain point plot was created at the outlet boundary for each of the concentrations on the same plot. This results in a plot of the output of the gas chromatograph with each species displaying a peak at the time it left the system.

To make the plot more accurately depict the results from the actual gas chromatograph, the adsorption constant for each species was then altered through trial and error so that the peak for each species occurred at the proper time.

After being set up, the model was then used to generate chromatography data on each reactor output simply by changing the inlet concentrations to match the reactor outputs.

Results and Discussion

This chapter discusses the findings of each step of the project and how they relate to each other.

Experimental Results

Figure 15 shows the plot of the natural log of the reaction rate against the natural log of the methane concentration. The equation for the trend line is also included.

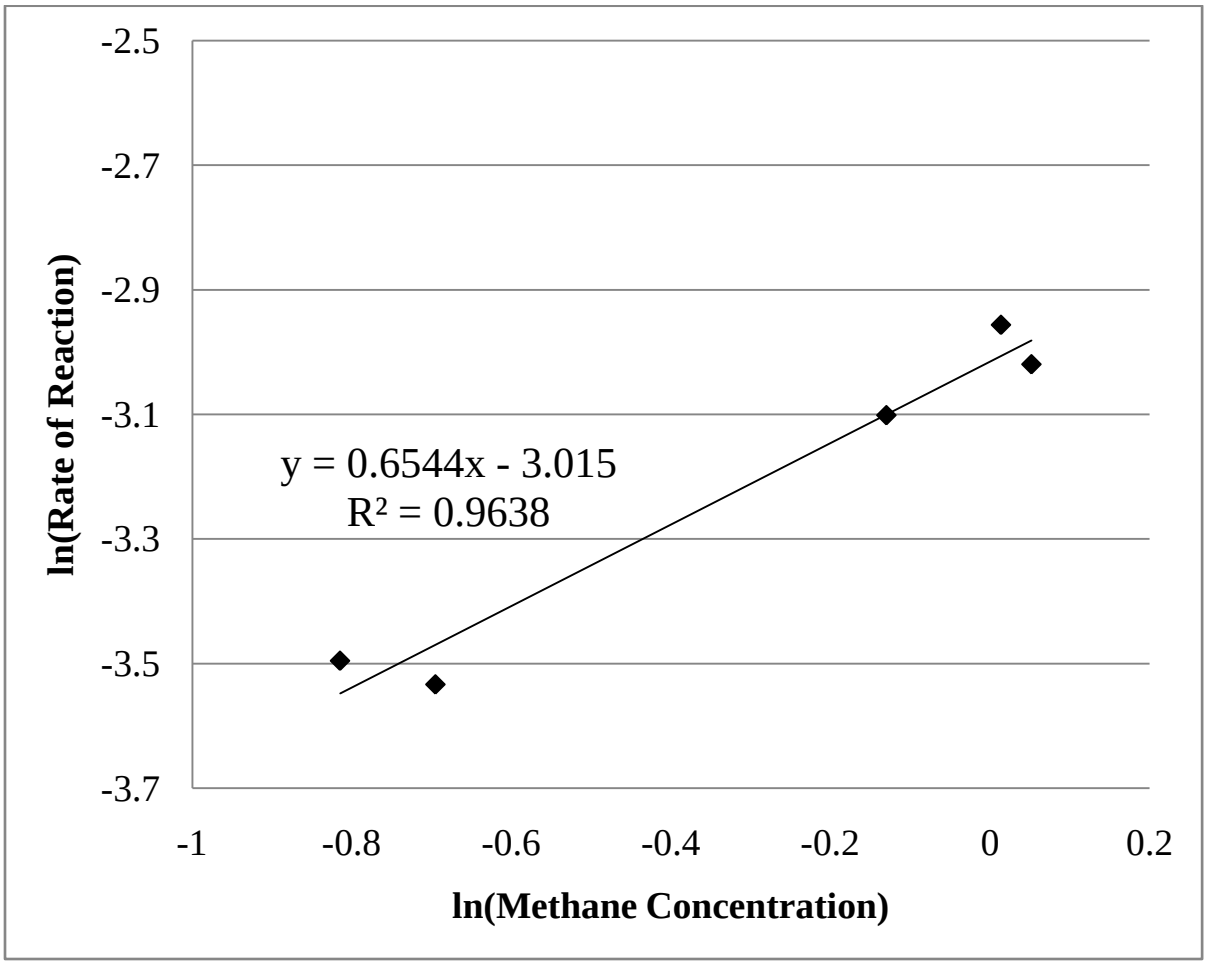

Figure 15: Natural Log Plot of Reaction Rate versus Methane Concentration

The graph indicates that the reaction order with respect to methane is 0.65 and the natural log of the reaction constant is -3.02. Therefore the reaction constant is equal to 0.049 1/s after the exponential is taken.

The plot of the activation energy versus 1/T, as well as the trend line, is shown in Figure 16.

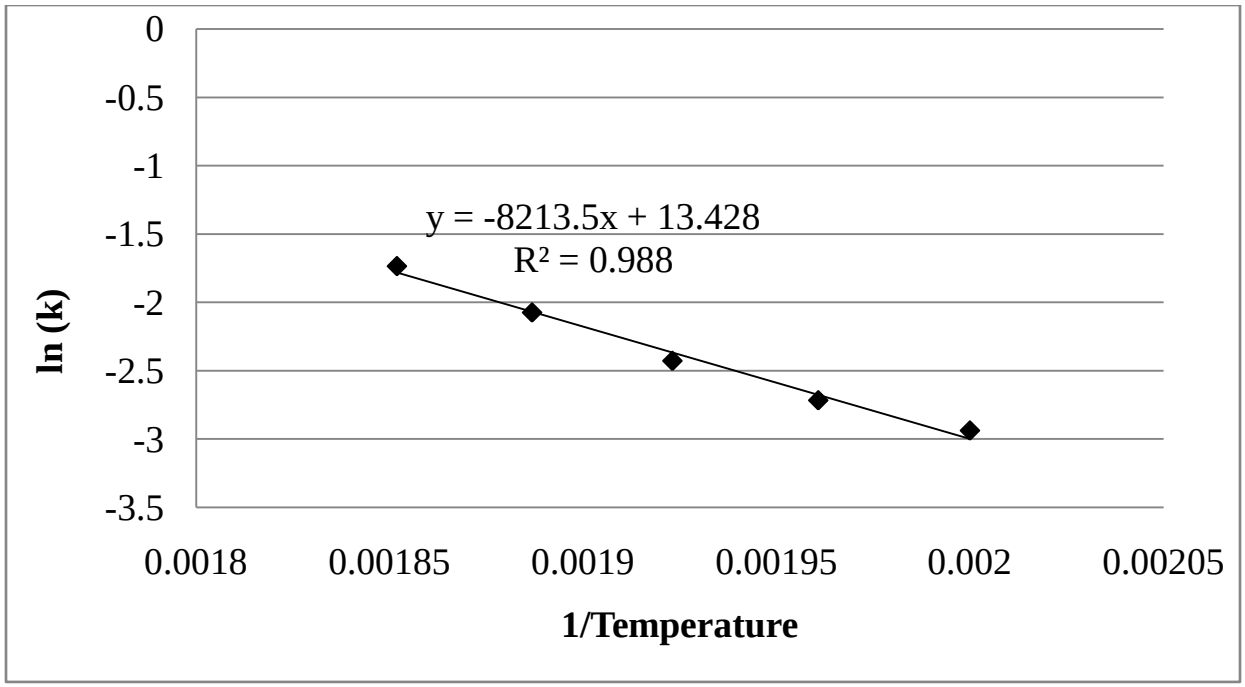

Figure 16: Plot of Natural Log of Reaction Constant versus 1/Temperature

The slope of the line is -8213.5. This number multiplied by -8.314 (Pa*m^3)/ (gmol*K) gives an activation energy of 68,287 joules. The intercept of the graph, 13.43, gave the natural log of the pre-exponential factor from the Arrhenius equation. Therefore, the pre-exponential factor is equal to 678,744 1/s.

The reaction order with respect to methane, activation energy, and pre-exponential factor were then used in COMSOL to simulate the concentration profile for each species for this particular reaction. The tabulated results for the experimental work are located in Appendix C.

Polymath Results

The output results of the polymath equations can be seen in Appendix D. The outlet concentration of methane was determined to be 0.9513 mol/m^3; giving a conversion of 2.4% of methane. Experimentally, for the 5:1 ratio of oxygen to methane a conversion of 2.2% and an outlet concentration of 0.9530 mol/m^3 were obtained. This provides a model close to the experiment, but it does not show the concentration visually and as effectively as COMSOL Multiphysics does.

Figure 17 shows the concentration of each species vs. the length of the reactor. There is not much change in concentrations, due to low conversion and then length of the reactor. Figure 18 shows the concentration of methane against the length of the reactor.

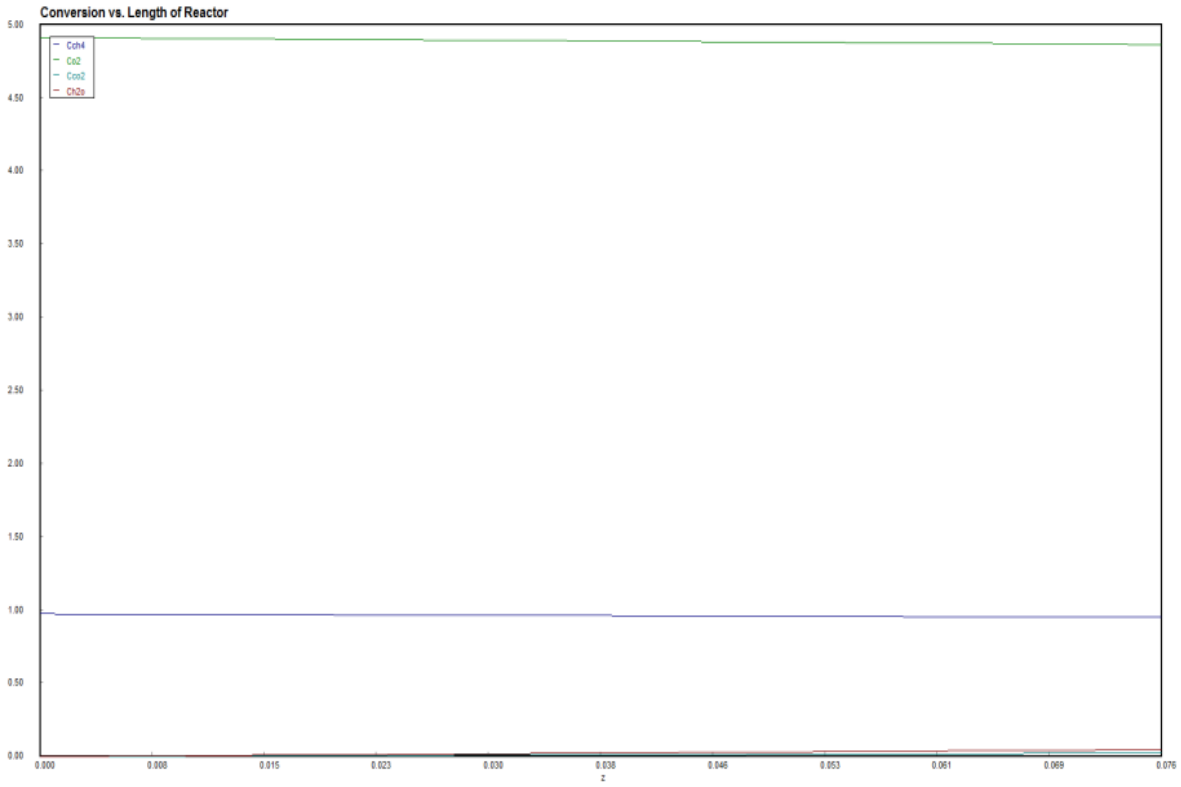

Figure 17: Species Concentrations versus Reactor Length

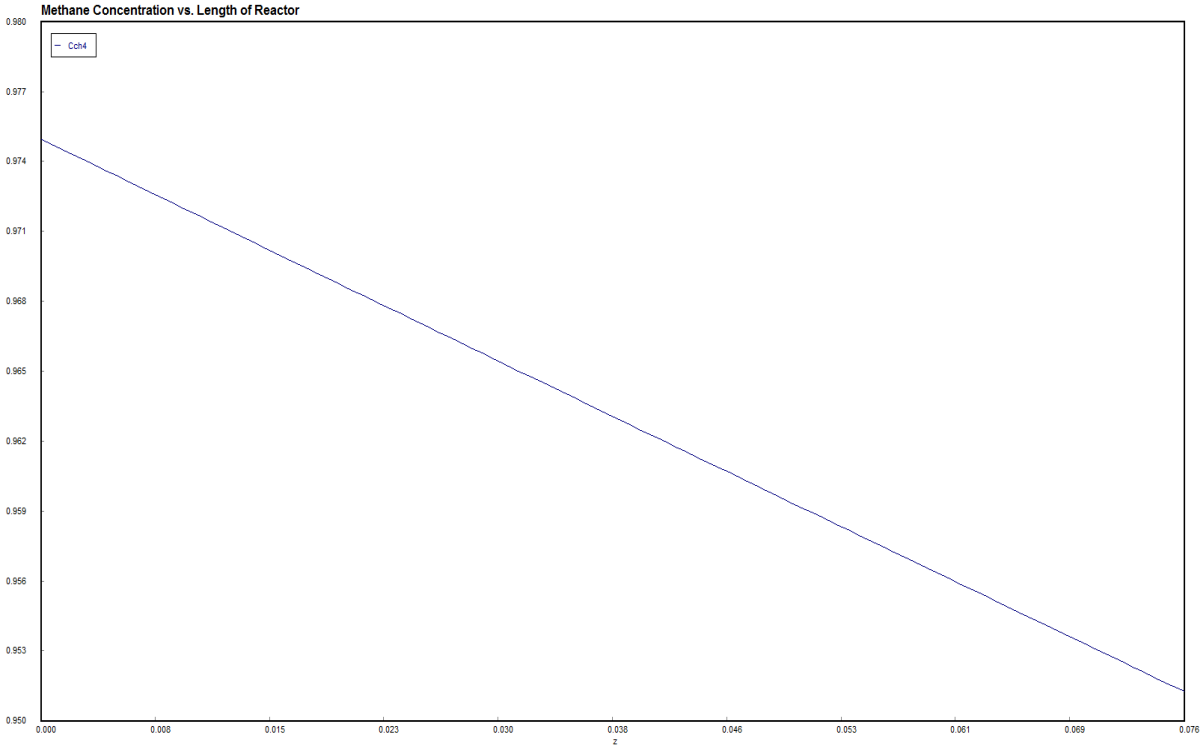

Figure 18: Concentration of Methane versus Reactor Length

COMSOL Results

A model of the differential reactor was simulated through the COMSOL program as previously discussed in the methodology. For these results and discussion, the reaction run with a ratio of 5:1 oxygen to methane was used. The reactor was simulated using the constants obtained from the experimental results. The outlet concentration of the methane was 0.9513mol/m^3; with an inlet concentration of 0.9750 mol/m^3. The surface concentration for methane can be seen in Figure 19. A plot of the concentration of methane against the length of the reactor, z, can be seen in Figure 20.

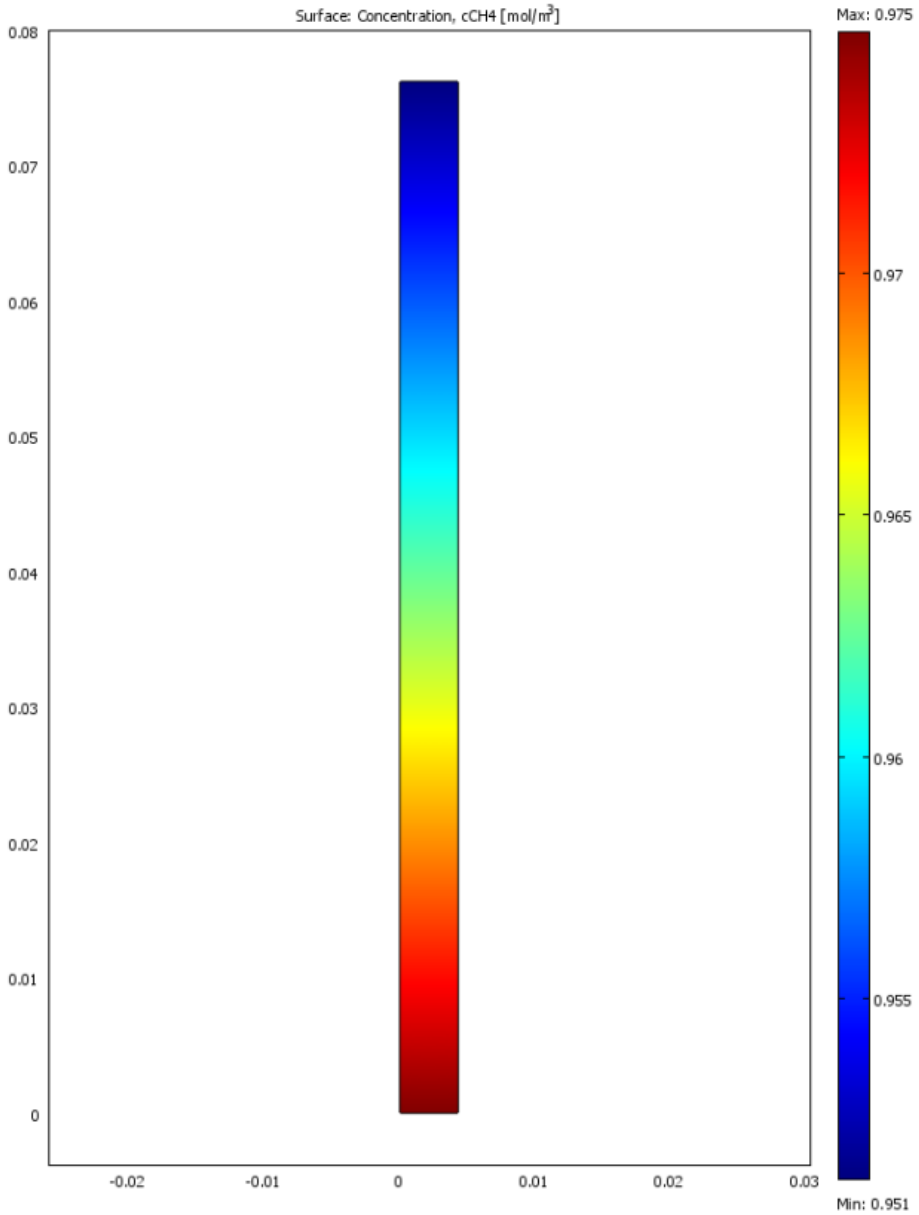

Figure 19: Surface Concentration of Methane

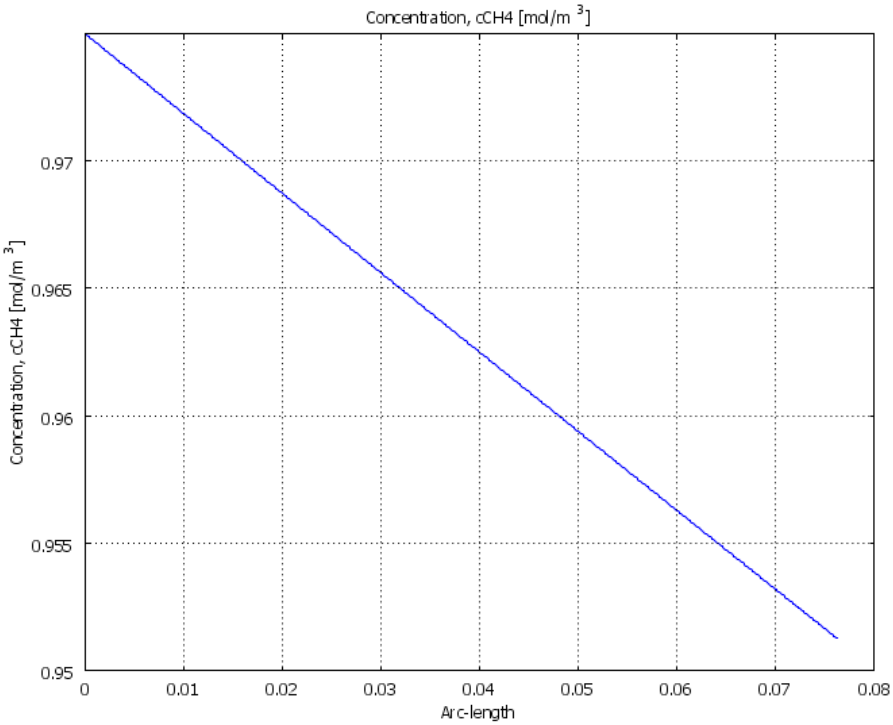

Figure 20: Methane Concentration versus Reactor Length

Surface plots of O_2, CO_2, and H_2O may be seen in Appendix E. Line plots of O_2, CO_2 and H_2O of concentration against the length of the reactor can be seen in Appendix F.

A linear trend can be seen for the concentration of each species in this reactor. This has been attributed to the fact that this is a differential reactor, and length of the reactor is incredibly small relative to an average reactor.

Table 4 shows the inlet and outlet concentrations of each species.

Table 4: Species Inlet and Outlet Concentrations

Species	Inlet Concentration (mol/m^3)	Outlet Concentration (mol/m^3)
Methane, CH_4	0.9750	0.9530
Oxygen, O_2	4.914	4.803
Carbon Dioxide, CO_2	0	0.02204
Water, H_2O	0	0.04408

This model shows a conversion of 2.4% of the methane to carbon dioxide. Experimental problems can explain the discrepancy for this conversion compared to the experimental conversion of 2.26%. This reactor assumes ideal conditions. Mass transfer limitations have not been included, and diffusion and porosity of the catalyst were neglected. Dispersion affects (and the assumption of plug flow) should not have been neglected due to the fact that the reactor has a reactor diameter/particle diameter ratio is less than 10 and the catalytic bed length/particle diameter is less than 50 (Hurtado, 2004). For this reactor, the reactor diameter/particle diameter is 8.636/3.22; a ratio of 2.68. The ratio of catalytic bed length to particle diameter is 76.2/3.22; a

ratio of 23.7. These ratios are not close enough to ideal conditions to be considered plug flow. (Hurtado, 2004).

It has also been reported in this reaction that the production of H_2O can lead to mass transfer limitations. As water is produced, the steam in the reactor blocks the catalyst's sites and prevents surface reactions (Ribeiro & al., 1994). This may have been experienced in the reaction, but it is hard to tell without examining the catalyst or measuring the steam out of the reactor.

The Diffusion Coefficient Dependence on Mass Transfer

The goal of the model with typical literature values is to try to show the possibilities of mass transfer limitations. If the literature model can be altered so that it is close to the experimental model, it might provide reason to believe that there are mass transfer limitations.

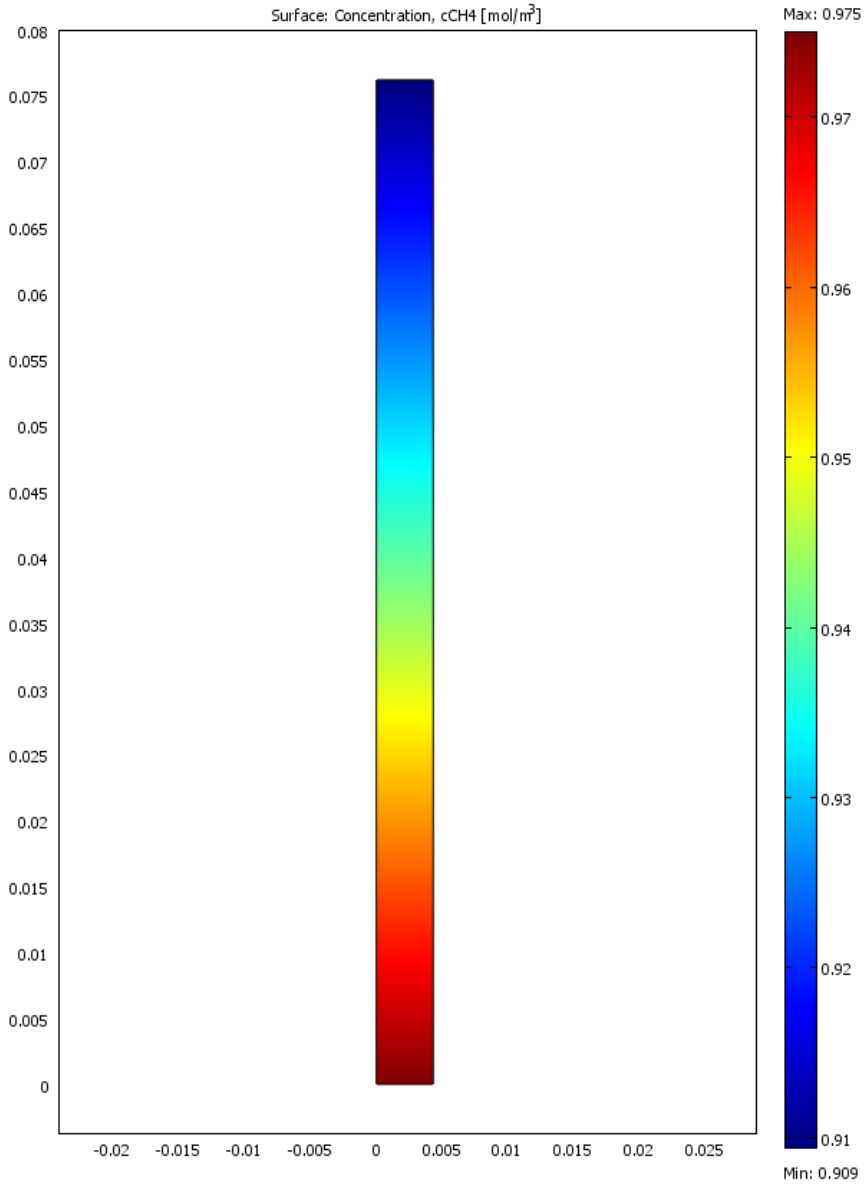

Figure 21: Surface Concentration of Methane (Literature Reactor)

The model with literature values can be seen in Figure 21Figure 21: Surface Concentration of Methane (Literature Reactor). The conversion of this reaction is 6.2%, as opposed to 2.4%which is the conversion of the experimental model. After adding the surface reaction rate equations and the mass transfer equations, the lower conversion of 2.4% was obtained by using a mass transfer coefficient of 0.074 at a velocity of 0.1563m/s. The model with literature values may be seen in Appendix G, and the model with mass transfer limitations can be seen in Appendix H. The tabulated results from the mass transfer limitations model are located in Appendix I.

In the relationship between velocity and the mass transfer coefficient (given by equation 52), k_o, was determined to be 0.2713.

Figure 22 shows the dependence of the outlet concentration of methane on velocity with and without mass transfer limitations. As the velocity is increased, the outlet concentration of methane is increased and the conversion is decreased. From the plot of methane without mass transfer limitations in Figure 22 it can be seen that as velocity is increased, the reactants spend less time in the reactor and have less time to react with each other. Therefore, a higher outlet concentration of methane will occur with increasing velocities.

The dependence of mass transfer limitations on the outlet concentration can be seen in Figure 22 as well. With mass transfer limitations, there is less conversion of methane than without mass transfer limitations; which can be seen by comparing the blue plot to the red plot in Figure 22. It is obvious that the dependence of velocity is not as drastic on the outlet concentration of methane with mass transfer limitations as it is without the limitations. This is because as the velocity increases, the boundary layer, or "film" around the catalyst particles, decreases and the mass transfer limitations are less evident. Figure 22 shows that the two plots seem to approach each other because as velocity is increased the outlet concentration is less dependent on the mass transfer limitations.

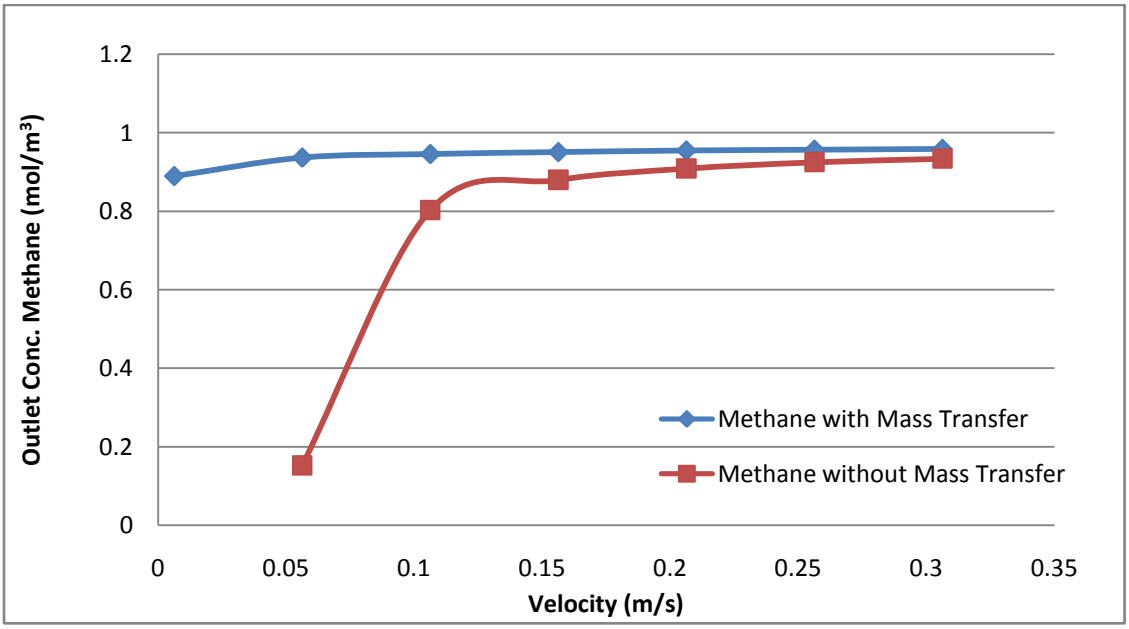

Figure 22: Outlet Methane Concentration versus Velocity

Figure 23 shows the dependence of the outlet concentration of methane on the mass transfer coefficient for a velocity of 0.1563 m/s. As the mass transfer coefficient is increased, the outlet concentration of methane decreases. This is due to the fact that more methane from the bulk concentration is reaching the surface of the catalyst and reacting. From equations (12) and (42) it can be seen that as the mass transfer coefficient is increased, the concentration moves from the bulk to the surface and is the driving force for the reaction.

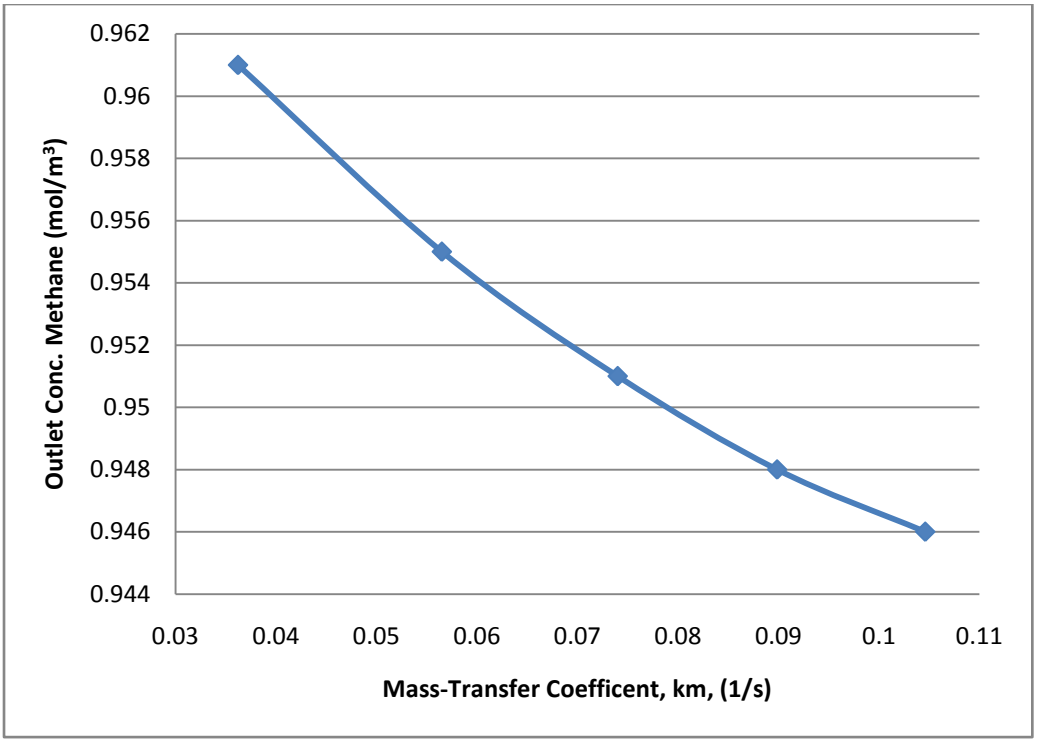

Figure 23: Outlet Methane Concentration versus Mass Transfer Coefficient

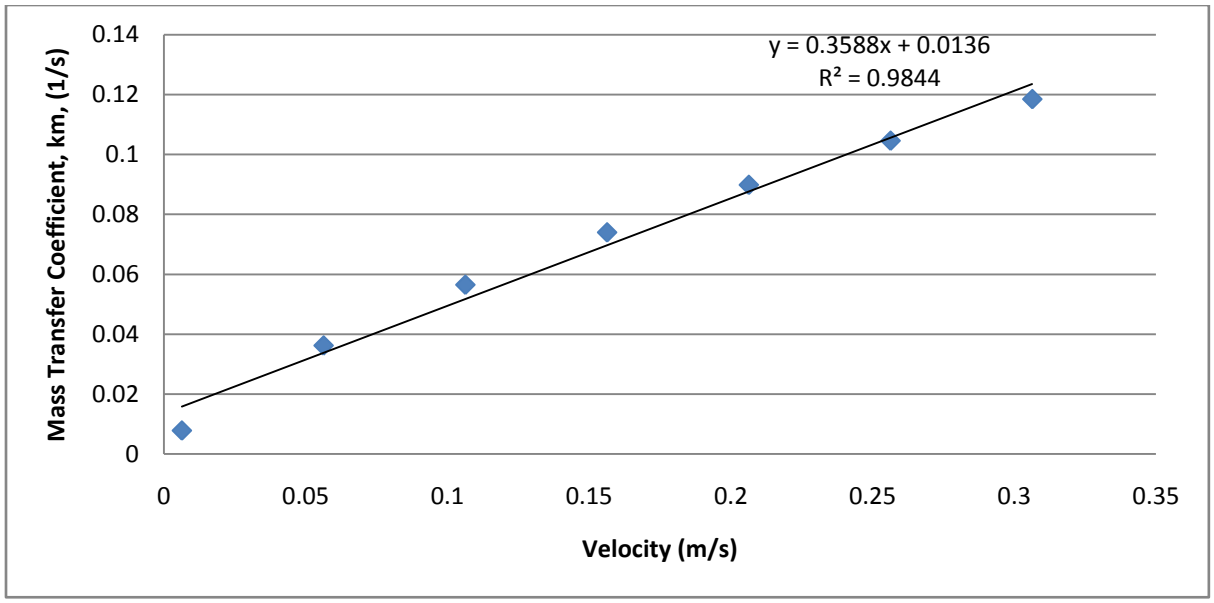

Figure 24: Relationship Between Mass Transfer Coefficient and Velocity

Figure 24 shows the relationship between the mass transfer coefficient and the velocity. This figure simply shows the relationship of equation (44) visually. As the velocity of reactants is increases, the mass transfer coefficient increases.

From equation (42), it can be seen that as the mass transfer coefficient is increased, the rate at which the concentration on the surface of the catalyst appears is increased. This provides more reaction on the surface of the catalyst. When the mass transfer coefficient is decreased, less methane is moving from the bulk to the surface, and therefore less of it is available to react. This leads to a decrease in conversion and an increase in the outlet concentration of methane.

The use of mass transfer limitations in this model can explain why the conversion is not the same in the literature reactor model as it is in the experimental model. Comparing Figure 19 to Figure 21 shows how the conversion of methane in the experiment is different from literature values. With the addition of mass transfer limitations, the literature model can replicate the experimental model. Mass transfer limitations can also provide reasoning for different rate constants and reaction orders with respect to methane observed in the Unit Operations experiment. These models can also effectively show students the influence of mass transfer in a catalytic packed bed reaction.

Gas Chromatography Model Results

A model of the gas chromatograph used to analyze the reactor output was made in order to show how the results from the actual reactor would be displayed since the reactor model simply gives the outlet concentrations of each species. As mentioned in the methodology, the chromatography model is an approximate model that gives properly sized and spaced species peaks but does not accurately model how the actual chromatograph achieves separation. A more complex model could take into account the varying temperature profile with time as well as changes in properties as the species separate.

Overall, the chromatography model is relatively easy to manipulate for those who are inexperienced with COMSOL as only the inlet concentrations need to be changed for each simulation. Generating the domain plot with the peaks for each species can be tedious as each peak must be plotted individually on the same graph, and the graph must be manually updated with each simulation. Figure 25 shows an example of the output generated by the GC model. Appendix J contains model outputs for each run.

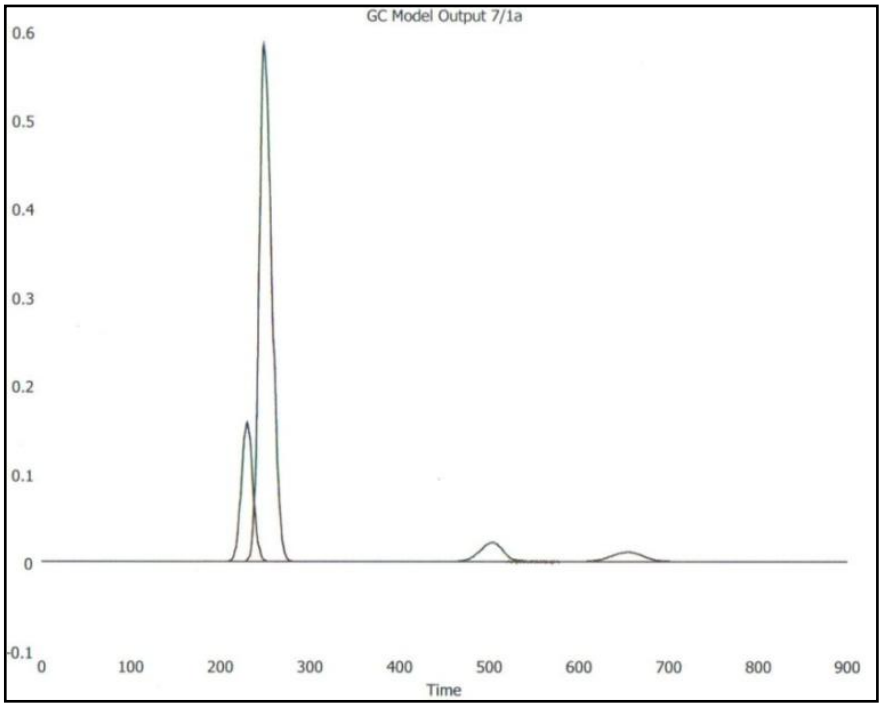

Figure 25: Gas Chromatograph Model Output

The plots provided by the model do give an accurate picture of the actual gas chromatograph output, as shown in Figure 25, which is the model generated for the second experimental run at a 7/1 inlet ratio of O_2 to CH_4. The peaks represent O_2, N_2, CH_4, and CO_2, respectively, and the times at which they appear are consistent with the exit times from the real chromatograph. Because the peak heights in the model are based directly on the concentrations of the species, they have much lower values than those from the actual chromatograph, which generates peak heights in the thousands. However, the heights of the peaks relative to each other are the same in the model as they are in reality, and therefore may still be used.

Conclusions and Recommendations

The COMSOL model can help provide students in the Unit Operations course with a visual learning tool. Conversion in a differential reactor can be a hard concept for students to grasp without visually seeing the concentration gradient. This model can provide students with an accurate representation of what is happening inside the reactor. All of the models in this report consider a reaction of 5:1 oxygen to methane. It is recommended that students in the Unit Operations course alter the model for other ratios in order to observe expected results from the experiment.

The comparison of a literature reactor model with the experimental model can show students the effect of mass transfer limitations on a catalytic reaction. The two models visually show the concentration gradient through the reactor and show the difference between literature outlet concentration of methane and the Goddard Hall reactor's outlet concentration of methane. The mass transfer model can provide students with an explanation of low conversions and can help students grasp mass transfer concepts visually.

The following recommendations apply to the catalytic experiment. Better insulation of the reactor feed and effluent lines would support better comprehension of the mass transfer limitations present in the reaction. This insulation as well as more frequent calibration of the gas chromatograph and more accurate flow meters to measure the flow-rates of the feed gases would account for the small discrepancy between the experimental calculations of the reaction order and activation energy from the literature values. Some additional suggestions include using an improved method of flushing residual gases out of the system lines in order to have only the feed gases in the lines, as well as weighing the catalyst before every experimental run.

It would be recommended to simulate the reactor models again and including pressure drop, temperature changes due to heat of reaction, diffusion, and porosity of the catalyst. These were aspects of the reaction that are difficult to estimate in this project and would require much more insight on the packing of the catalyst. It would also be very beneficial to run the reactor at different velocities to test the mass transfer limitations on velocity. The reaction could be run at different velocities in order to witness the dependence that velocity has on the outlet concentration of methane. Using Figure 22 in this report, the relationship could provide justification of mass transfer limitations in the reactor. If possible, the reaction could be run with different sized catalyst particles in order increase or decrease mass transfer limitations and see if it agrees with the model. It would also be beneficial to look into the dependence of the production of water on the reaction order with respect to methane and the rate of reaction and it affects the Goddard Hall reactor.

The model of the gas chromatograph is effective at showing what the results given by an actual GC would give, but it does not accurately depict how these results are achieved. The model is adequate for showing students what to expect from the GC in the Unit Operations course, but it should not be used as an accurate representation of how the GC achieves its separation. Future work with this model should consider modeling the changing temperature

profile along the column. Experimentation should also be done to obtain the proper phase ratio, the effective diffusion constant for each species, the adsorption constant for each species, and the monolayer capacity for each species. If possible, the GC model could be attached to the reactor model in order to consolidate these tools into one for easier use by students.

References

Afandizadeh, S. a. (2001). Design of Packed Bed Reactors: Guides to Catalyst Shape, Size, and Loading Selection. In *Applied Thermal Engineering 21* (pp. 669-682).

Ashcroft, A. T. (1990). *Partial Oxidation of Methane to Synthesis Gas*. Retrieved April 12, 2009, from http://www.springerlink.com/content/g451052045335l1n/fulltext.pdf

Chiticar, M. (1999). Carbon and Hydrogen Isotope Systematics of Bacterial Formation and Oxidation of Methane. *Chemical Geology* , 291-314.

COMSOL AB. (1997). *Mass Transport*. Retrieved from http://www.polysep.ucla.edu/c210/Femlab/Packed%20Bed%20Reactor.htm

COMSOL Group. (2008). *COMSOL Conference*. Retrieved October 2008, from COMSOL: http://www.comsol.com/conference2008/usa/presentation/

COMSOL Group. (2008). *COMSOL Multiphysics*. Retrieved October 2008, from COMSOL: http://www.comsol.com/products/multiphysics/

COMSOL Group. (2008). *Using COMSOL in the Classroom*. Retrieved October 2008, from COMSOL: http://www.comsol.com/products/multiphysics/education

COMSOL Group. (2008). *Working and Researching with COMSOL Multiphysics*. Retrieved October 2008, from COMSOL: http://www.comsol.com/products/multiphysics/research

Cremaschi, B. M. (2006). *US Patent 7141708 - Hollow pellet suitable as carrier of catalysts for selective exothermic reactions*. Retrieved April 11, 2009, from Patentstorm: http://www.patentstorm.us/patents/7141708/description.html

Cussler, E. L. (2008). *Diffusion mass transfer in fluid systems.* New York: Cambridge University Press.

Cyberspace Chemistry. (2009). *Bond Lengths and Energies*. Retrieved April 12, 2009, from http://www.science.uwaterloo.ca/~cchieh/cact/c120/bondel.html

Deng, B., Kong, S., & Kim, C. N. (2007). Modeling of photocatalytic oxidation of VOCs in a packed bed reactor under continuous and discontinuous illuminations. *Korean Journal of Chemical Engineering* , 577-582.

EncyclopediaBritannica. (2009). *Column Chromatography*. Retrieved February 19, 2009, from Encyclopedia Britannica Online: http://www.britannica.com/EBchecked/topic/127156/column-chromatography

Ettre, L. (1993). *Nomenclature for Chromatography (IUPAC Recommendations 1993)*. Retrieved February 2009, from IUPAC.org: http://www.iupac.org/publications/pac/1993/pdf/6504x0819.pdf

Ferraro, J. (2008, October 5). Goddard Hall Reactor. (D. Szewczyk, Interviewer)

Finlayson, B. A. (2006). *Introduction to Chemical Engineering Computing.* Hoboken, N.J: Wiley.

Fogler, S. H. (2006). *Elements of Chemical Reaction Engineering, Fourth Edition.* Upper Saddle River, NJ: Pearson Education.

Gélin, P., & Primet, M. (2002). Complete oxidation of methane at low temperature over noble metal based catalysts: a review . *Science Direct* .

Grob, R. L., & Barry, E. F. (2004). *Modern Practice of Gas Chromatography.* Malvern: Pennsylvania.

Gurmen, H. S. (2008). Packed Bed Reactors (PBRs). Michigan.

Hurtado, P. e. (2004). Development of a kinetic model for the oxidation of methane over Pd/Al2O3 at dry and wet conditions. *Applied Catalysys B: Environmental* , 229-238.

Li, J., Fu, H., Fu, L., & Hao, J. (2006). Complete combustion of methane over indium tin oxides catalysts. *Environmental Science & Technology, 40(20)* , 6455-6459.

Monteiro, R., & al., e. (2001). Turnover Rate and Reaction Orders for the Complete Oxidation of Methane on a Palladium Foil in Excess Dioxygen. *Journal of Catalysis* , 291-301.

Muto, K.-i., Katada, N., & Niwa, M. (1996). Complete oxidation of methane on supported palladium Catalysts. *Applied Catalysis* .

Rase, H. F. (1977). *Chemical Reactor Design for Processing Plants Vol.1.* John Wiley & Sons, Inc.

Rase, H. F. (1990). Gas-Phase Reactions. *Fix-Bed Reactor Design and Diagnostics* .

Ribeiro, F., & al., e. (1994). Kinetics of the Complete Oxidation of Methane over Supported Palladium Catalysts. *Journal of Catalysis* , 537-544.

Satterfield, C. N. (1996). *Heterogeneous Catalysis in Industrial Practice.* Boston, MA: Krieger Company.

Scott, R. (2005). *Principles and Practices of Chromatography*. Retrieved February 2009, from http://www.chromatography-online.org/topics/displacement.html

Shahamiria, S., & Wierzba, I. (2008). Modeling catalytic oxidation of lean mixtures of methane–air in a packed-bed reactor. *ScienceDirect* .

Sheffield Hellam University. (2006). *Gas Chromatography*. Retrieved February 2009, from http://teaching.shu.ac.uk/hwb/chemistry/tutorials/chrom/gaschrm.htm

Tarhan, O. M. (1983). *Catalytic Reactor Design.* New York: McGraw-Hill Education.

Weck, O. d., & Kim, I. Y. (2004, January 12). Finite Element Method. Boston, MA, USA.

Widas, P. (2008). *Introduction to Finite Element Analysis.* Retrieved October 2008, from http://www.sv.vt.edu/classes/MSE2094_NoteBook/97ClassProj/num/widas/history.html

Appendix A: Flow Meter Calibration Curves

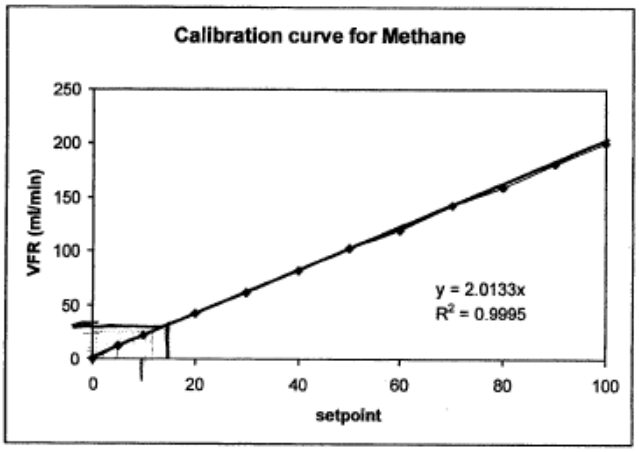

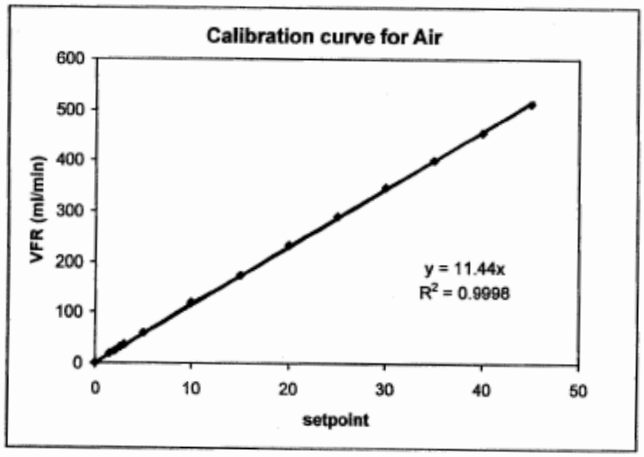

Assume that the response is linear up to a setpoint of 100%

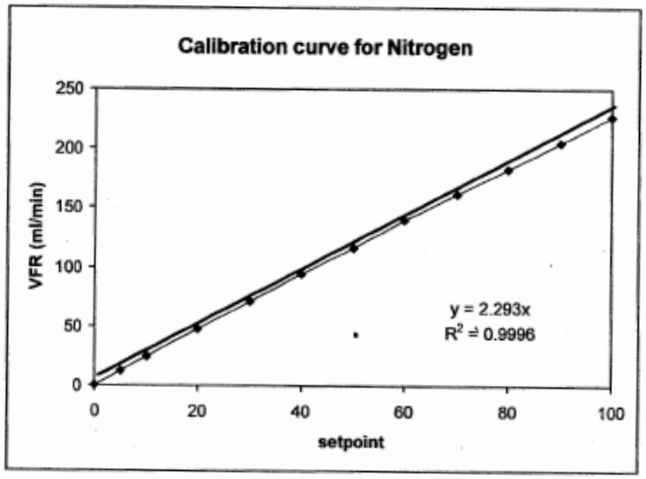

Appendix B: Gas Chromatograph Calibration Curves

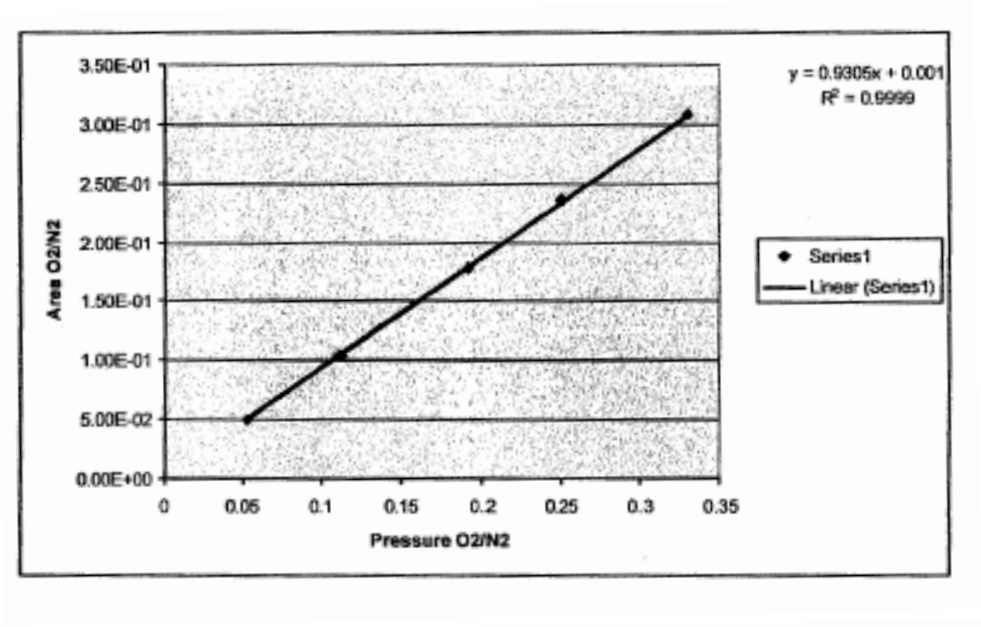

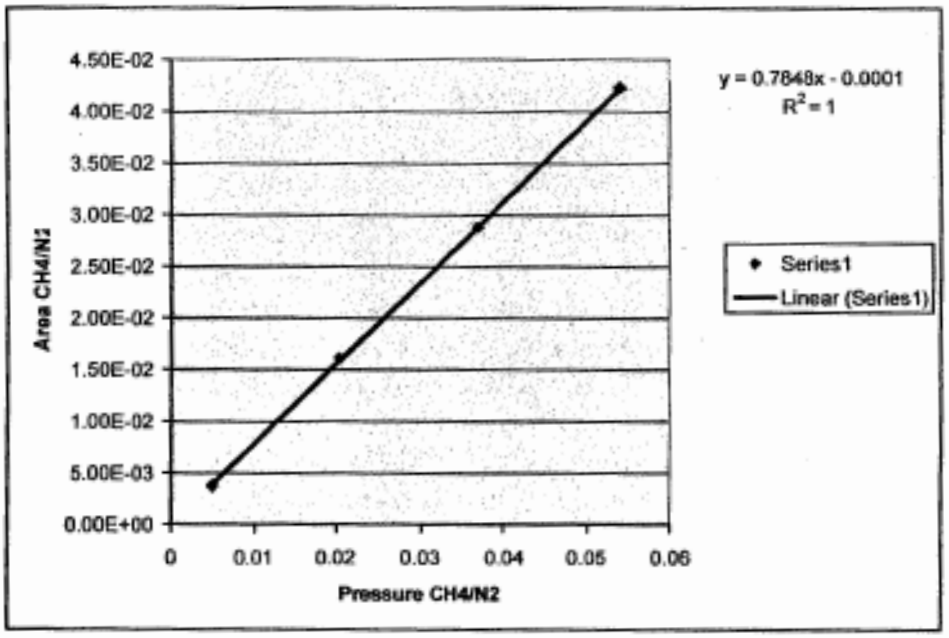

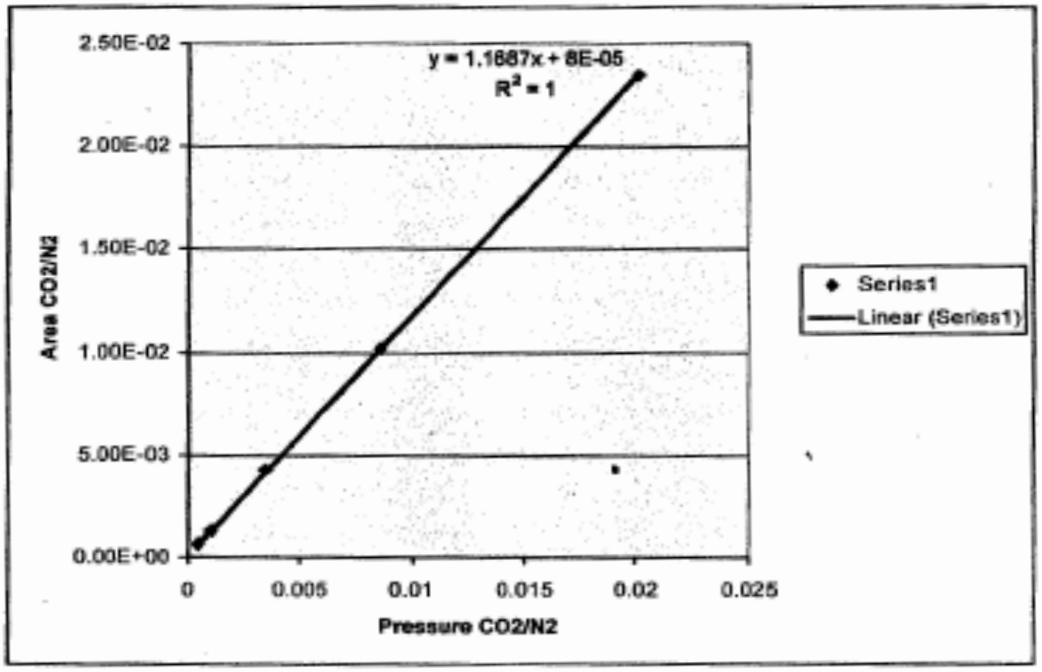
y = 1.1687x + 8E-05
R² = 1
2.50E-02
2.00E-02
1.50E-02
1.00E-02
5.00E-03
0.00E+00
Area CO2/N2
0
0.005
0.01
0.015
0.02
0.025
Pressure CO2/N2
Series1
Linear (Series1)

Appendix C: Experimental Results

Ratio of O_2 to CH_4	Inlet flow rate of air (mL/sec)	Inlet flow rate of CH_4 (mL/sec)	Partial pressure ratio CO_2:N_2	Partial pressure ratio CH_4:N_2 (bypass)
5:1	4.80	0.20	0.00190	0.057
5:1 (a)	4.80	0.20	0.00194	0.056
6:1	4.83	0.17	0.00183	0.048
11:1	4.91	0.09	0.00147	0.027
13:1	4.92	0.08	0.00147	0.026

Experimental data for reactor runs at 500 K (determining reaction order with respect to methane)

Ratio of O_2 to CH_4	Conversion	Outlet flow rate CH_4 (mol/sec)	Reaction rate (mol/s*g)	Concentration of CH_4 (mol/m^3)
5:1	0.0226	9.64E-6	8.29E-6	1.93
5:1 (a)	0.0250	9.28E-6	8.83E-6	1.86
6:1	0.0250	8.04E-6	7.64E-6	1.61
11:1	0.0285	4.57E-6	4.96E-6	0.91
13:1	0.0334	4.05E-6	5.15E-6	0.81

Result for reactor runs at 500 K

Temperature (K)	Partial pressure ratio CO_2:N_2	Partial pressure ratio CH_4:N_2	Partial pressure N_2 (Pa)	Partial pressure CH_4 (Pa)
500	0.00190	0.0574	140742	6277.7
510	0.00238	0.0574	140742	6241.6
520	0.00316	0.0574	140742	6138.2
530	0.00438	0.0574	140742	5840.5
540	0.00615	0.0574	140742	5781.8

Experimental data for reactor runs at 5:1 oxygen to methane flow rate ratio (determining activation energy)

Temperature (K)	Conversion	Outlet flow rate CH_4 (mol/sec)	Reaction rate (mol/s*g)	Reaction constant (1/s)
500	0.0330	5.84E-4	1.93E-5	6.33E-8
510	0.0414	5.72E-4	2.37E-5	7.80E-8
520	0.0550	5.61E-4	3.08E-5	1.03E-7
530	0.0763	5.51E-4	4.20E-5	1.45E-7
540	0.1071	5.41E-4	5.79E-5	2.01E-7

Result for reactor runs at 5:1 oxygen to methane flow rate ratio

Appendix D: Polymath Results

Calculated values of DEQ variables

	Variable	Initial value	Minimal value	Maximal value	Final value
1	alpha	0.6525	0.6525	0.6525	0.6525
2	beta	0	0	0	0
3	Cch4	0.974982	0.9512743	0.974982	0.9512743
4	Cco2	0	0	0.0237077	0.0237077
5	Ch2o	0	0	0.0474155	0.0474155
6	Co2	4.91391	4.866495	4.91391	4.866495
7	k	0.049837	0.049837	0.049837	0.049837
8	r1	0.3136268	0.3086295	0.3136268	0.3086295
9	v	0.1563	0.1563	0.1563	0.1563
10	z	0	0	0.0762	0.0762

Differential equations

1 d(Cch4)/d(z) = -r1

2 d(Co2)/d(z) = -2*r1

3 d(Cco2)/d(z) = r1

4 d(Ch2o)/d(z) = 2*r1

Explicit equations

1 alpha = 0.6525

2 beta = 0

3 v = 0.1563

4 k = 0.049837

5 r1 = k/(v)*(Cch4^alpha)*(Cco2^beta)

General

Total number of equations	9
Number of differential equations	4
Number of explicit equations	5
Elapsed time	0.000 sec
Solution method	RKF_45
Step size guess. h	0.000001
Truncation error tolerance. eps	0.000001

Appendix E: Surface Plots of O_2, CO_2, & H_2O

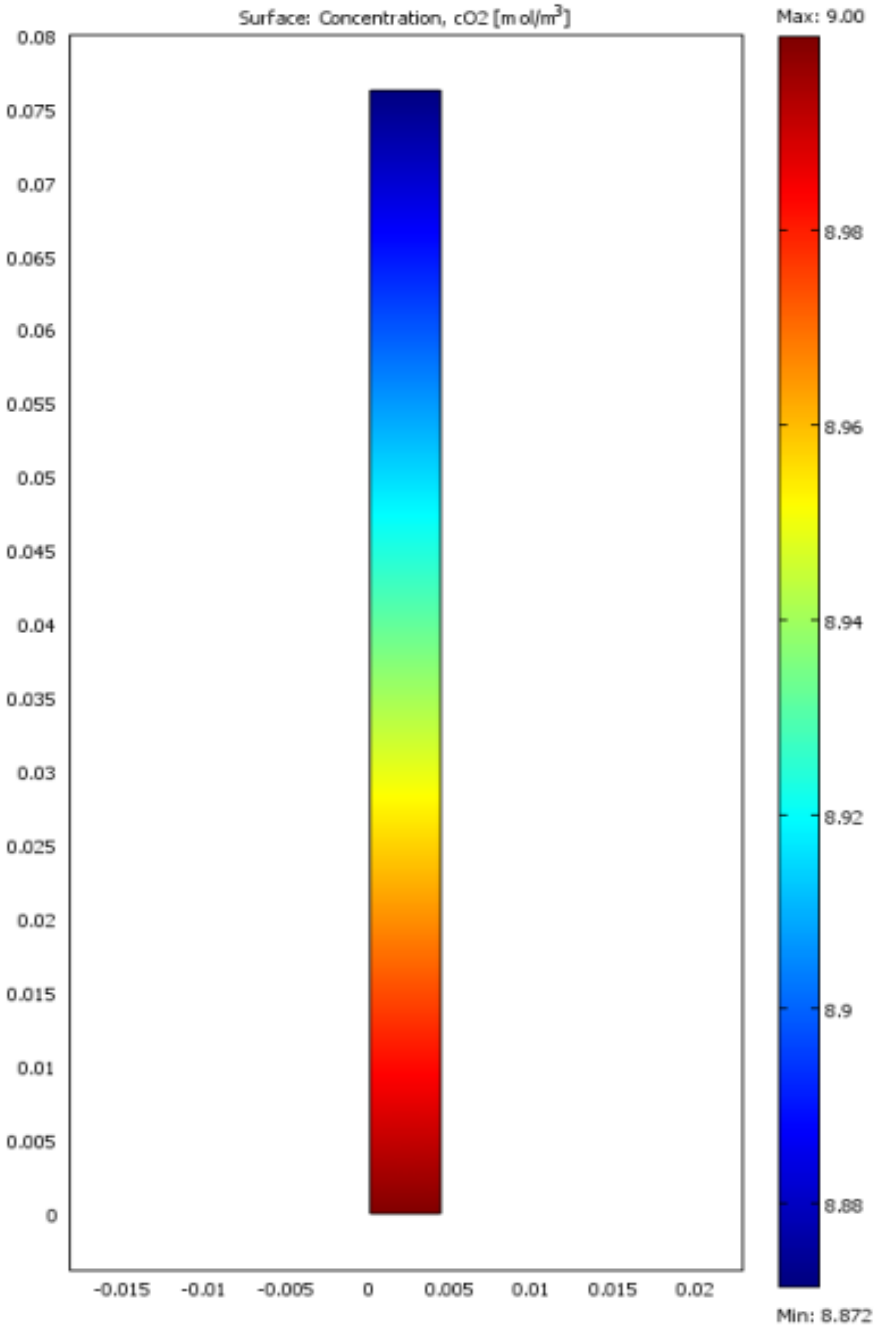

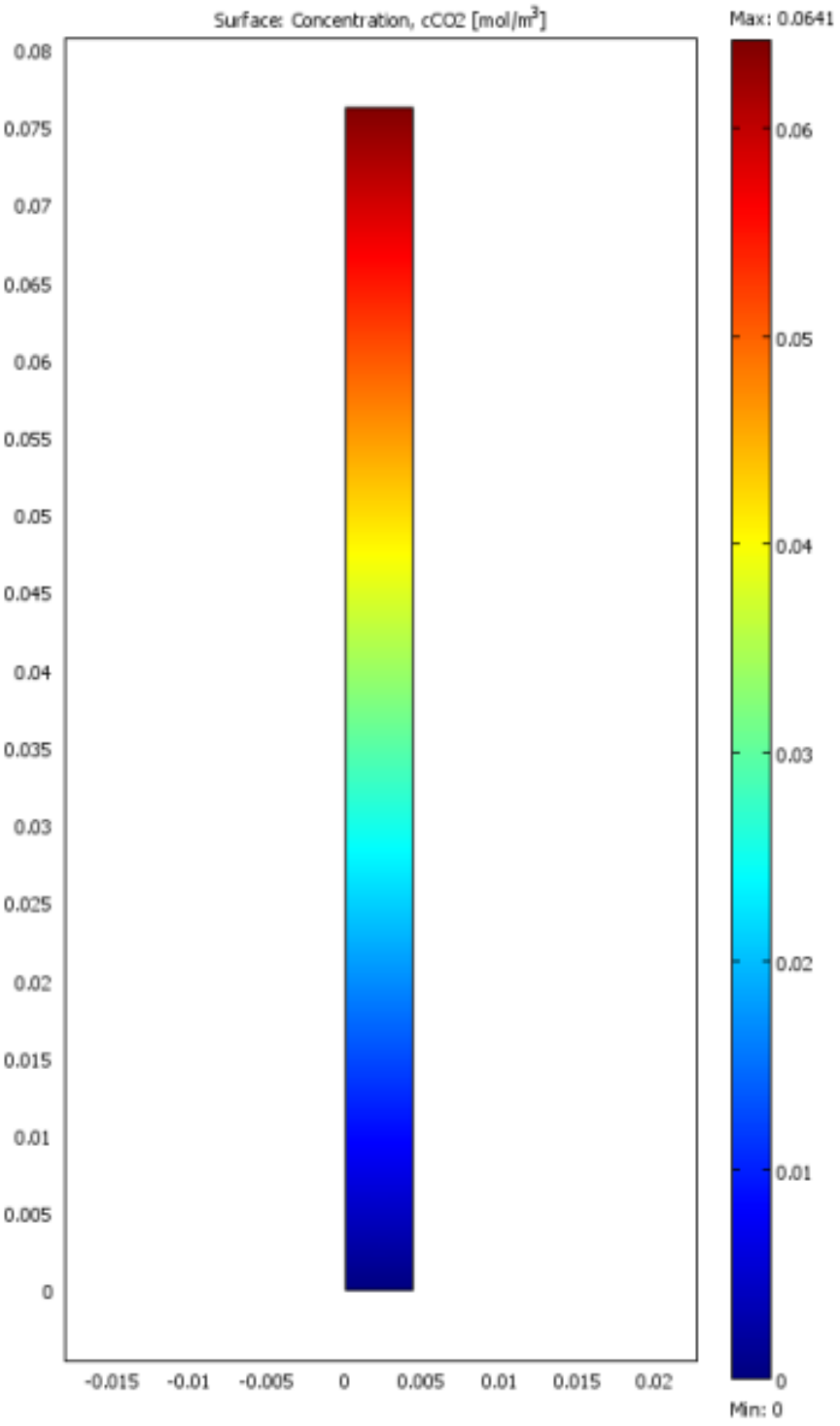
Surface: Concentration, cCO2 [mol/m3]
Max: 0.0641
Min: 0
0.08
0.075
0.07
0.065
0.06
0.055
0.05
0.045
0.04
0.035
0.03
0.025
0.02
0.015
0.01
0.005
0
-0.015
-0.01
-0.005
0
0.005
0.01
0.015
0.02
0.06
0.05
0.04
0.03
0.02
0.01
0

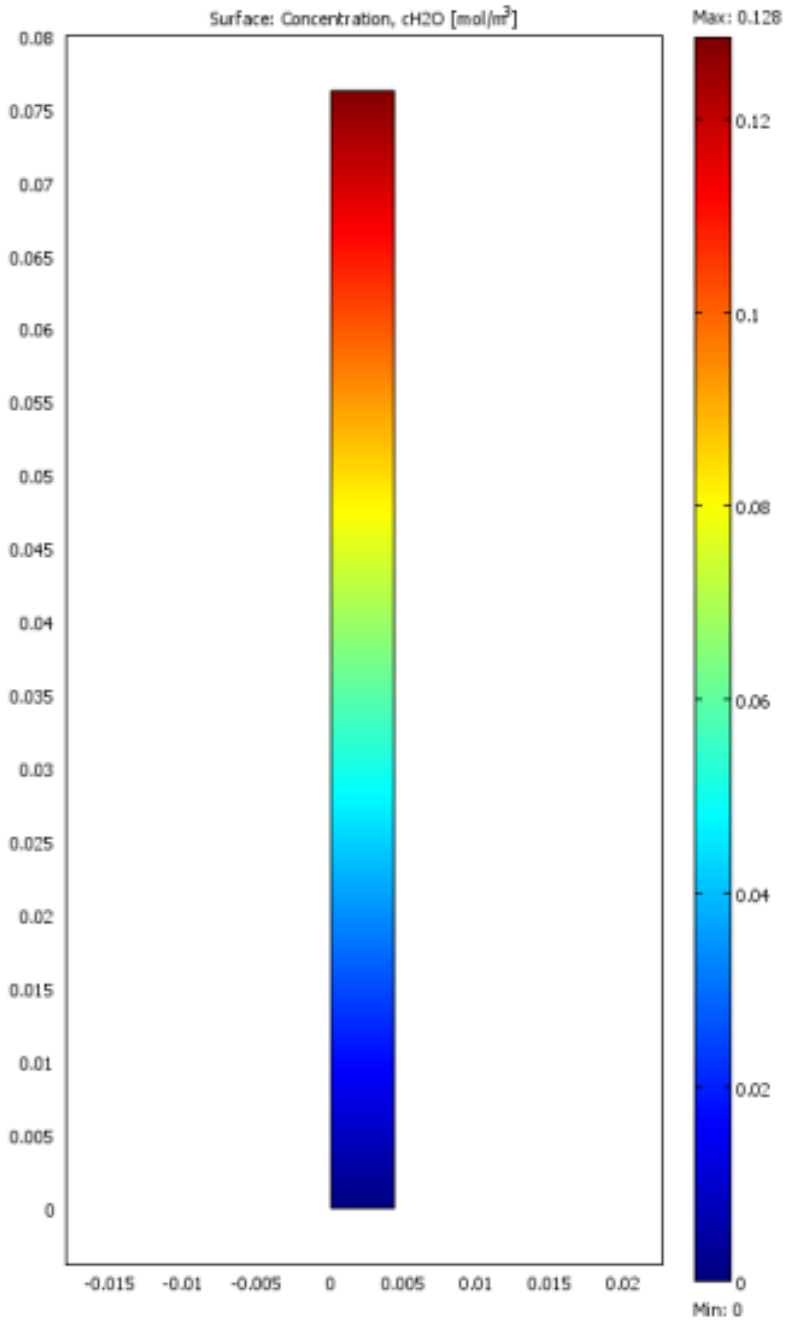
Surface: Concentration, cH2O [mol/m³]
Max: 0.128
0.12
0.1
0.08
0.06
0.04
0.02
0
Min: 0
0.08
0.075
0.07
0.065
0.06
0.055
0.05
0.045
0.04
0.035
0.03
0.025
0.02
0.015
0.01
0.005
0
-0.015
-0.01
-0.005
0
0.005
0.01
0.015
0.02

Appendix F: Plots of $[O_2]$, $[CO_2]$, & $[H_2O]$ versus Length of Reactor

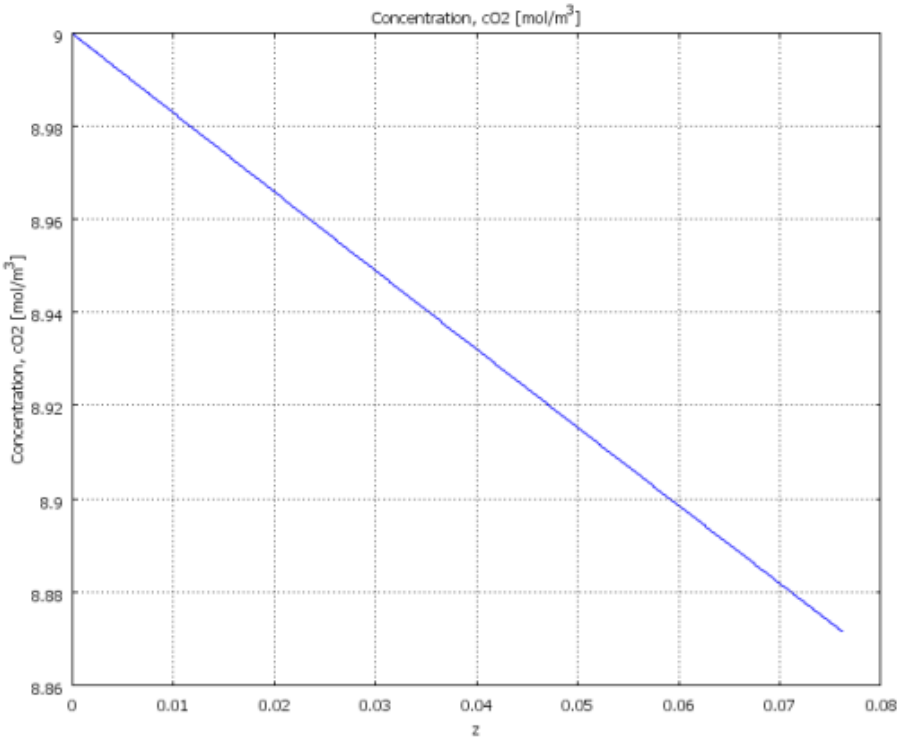

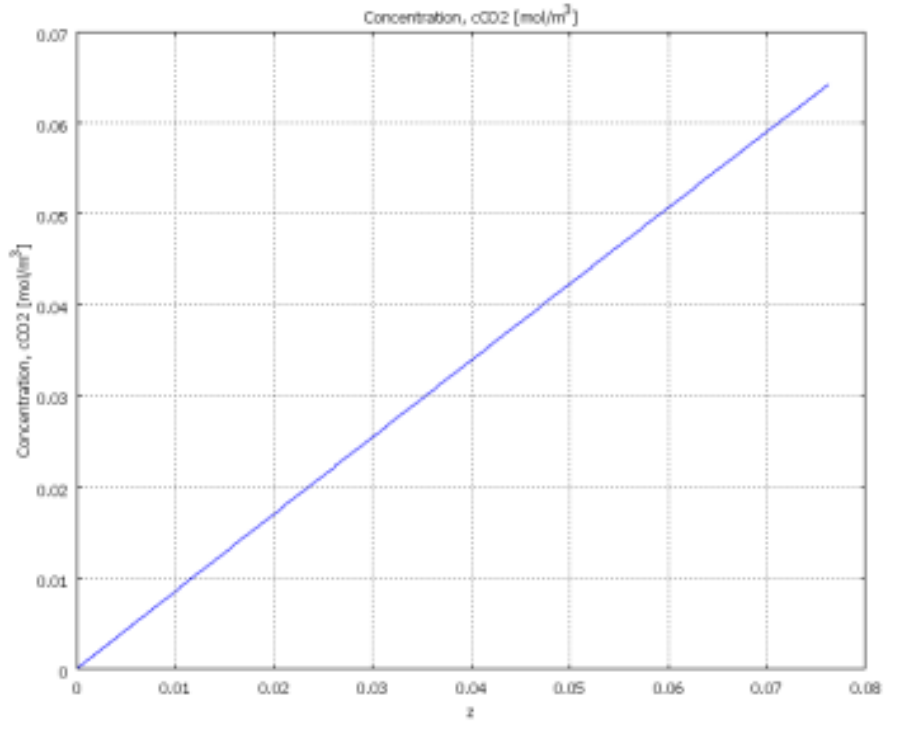

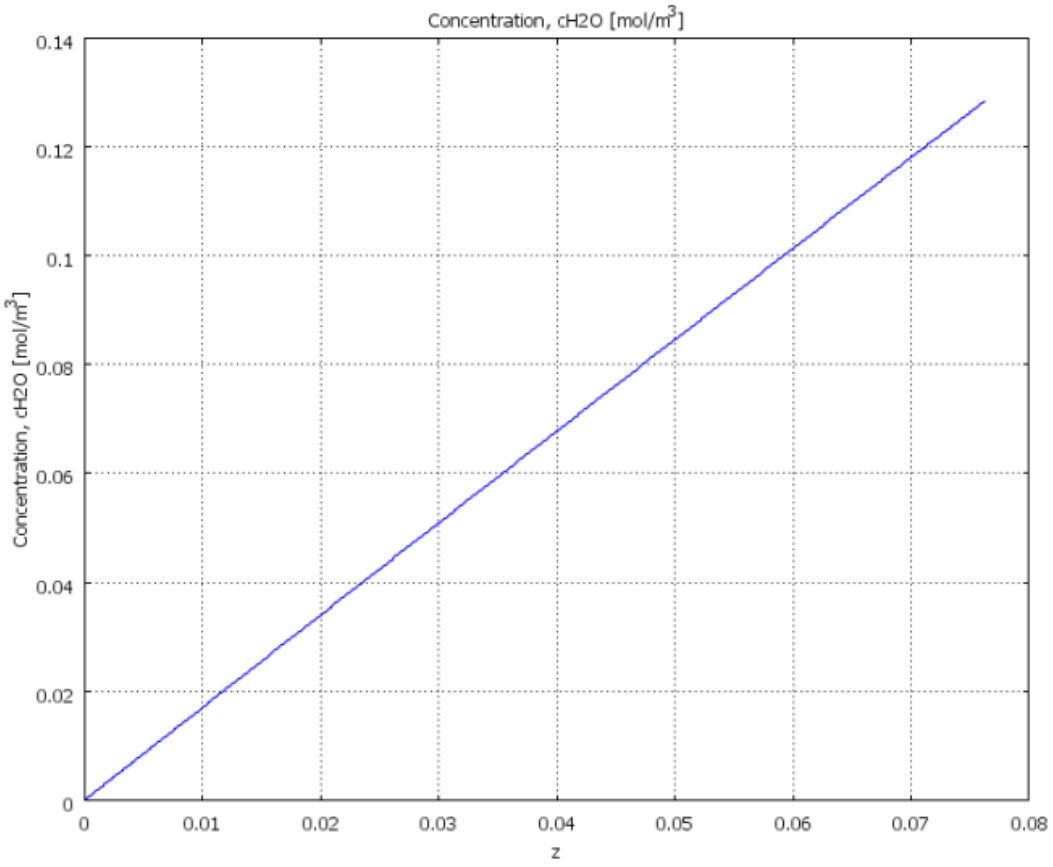
Concentration, cH2O [mol/m3]
Concentration, cH2O [mol/m3]
0.14
0.12
0.1
0.08
0.06
0.04
0.02
0
0
0.01
0.02
0.03
0.04
0.05
0.06
0.07
0.08
z

Appendix G: Literature Reactor Model

The following are surface plots of each species through the literature reactor model.

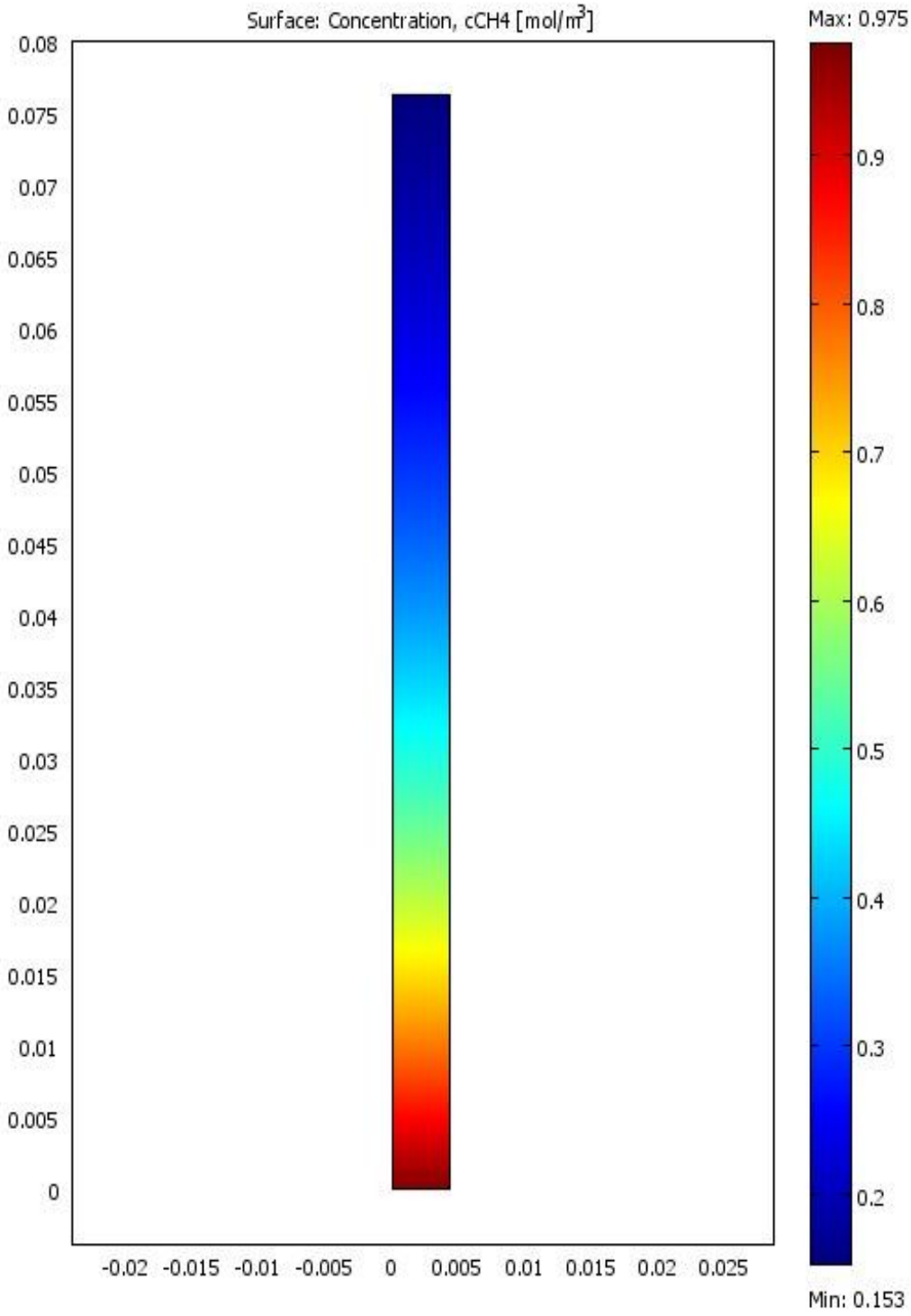

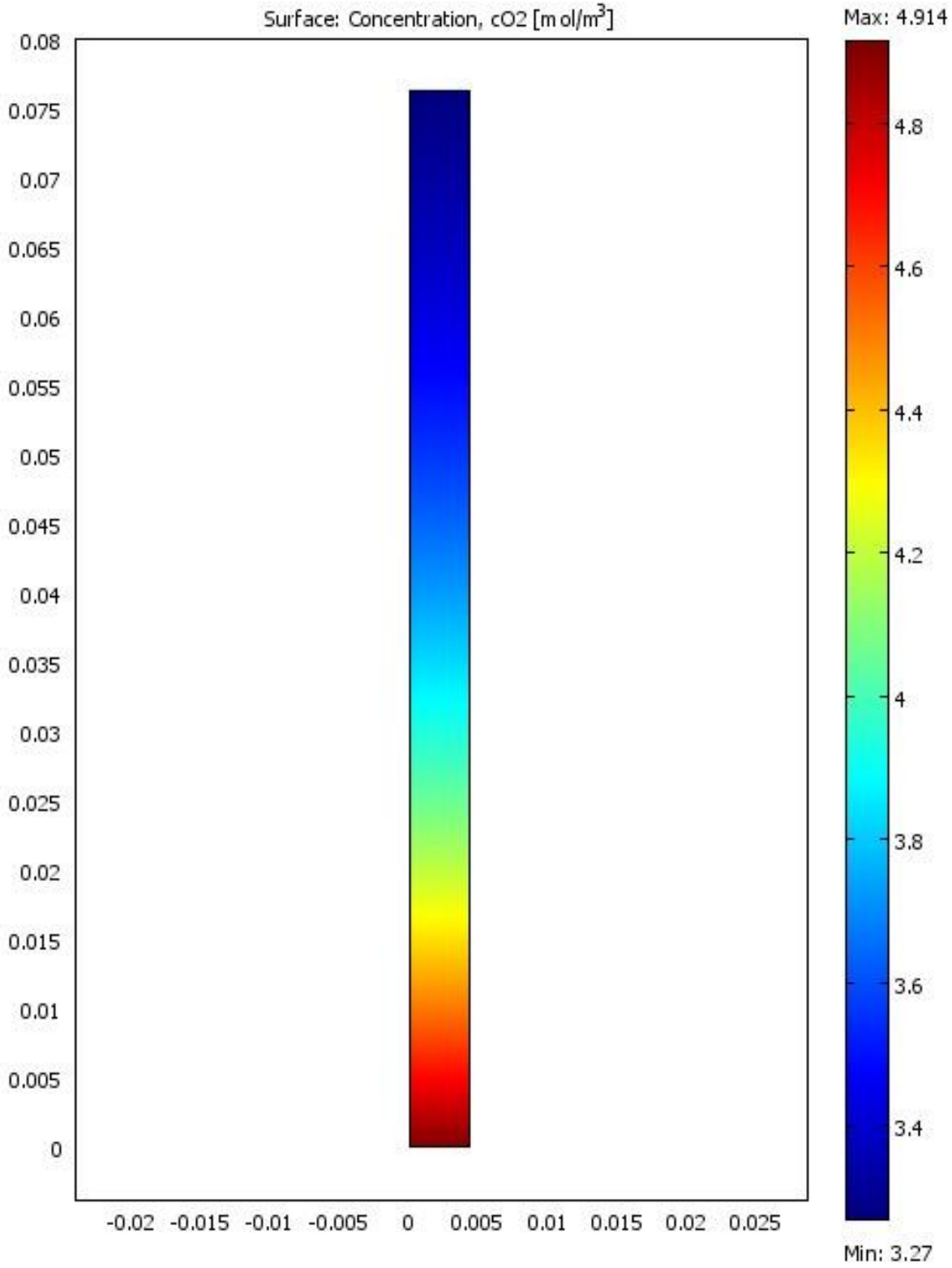
Surface: Concentration, cO2 [mol/m3]
Max: 4.914
Min: 3.27
0.08
0.075
0.07
0.065
0.06
0.055
0.05
0.045
0.04
0.035
0.03
0.025
0.02
0.015
0.01
0.005
0
-0.02
-0.015
-0.01
-0.005
0
0.005
0.01
0.015
0.02
0.025
4.8
4.6
4.4
4.2
4
3.8
3.6
3.4

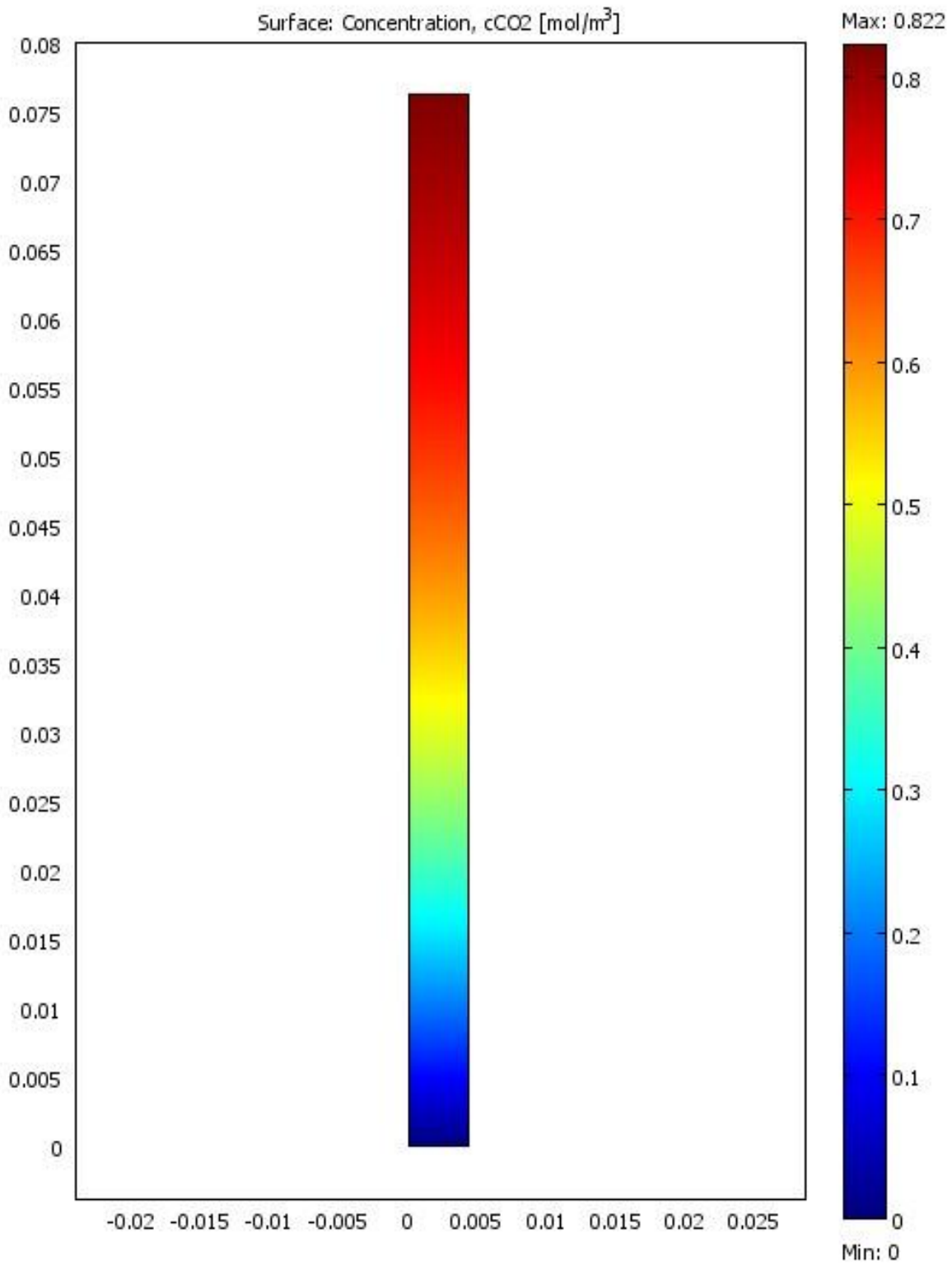
Surface: Concentration, cCO2 [mol/m3]
Max: 0.822
0.8
0.7
0.6
0.5
0.4
0.3
0.2
0.1
0
Min: 0
0.08
0.075
0.07
0.065
0.06
0.055
0.05
0.045
0.04
0.035
0.03
0.025
0.02
0.015
0.01
0.005
0
-0.02
-0.015
-0.01
-0.005
0
0.005
0.01
0.015
0.02
0.025

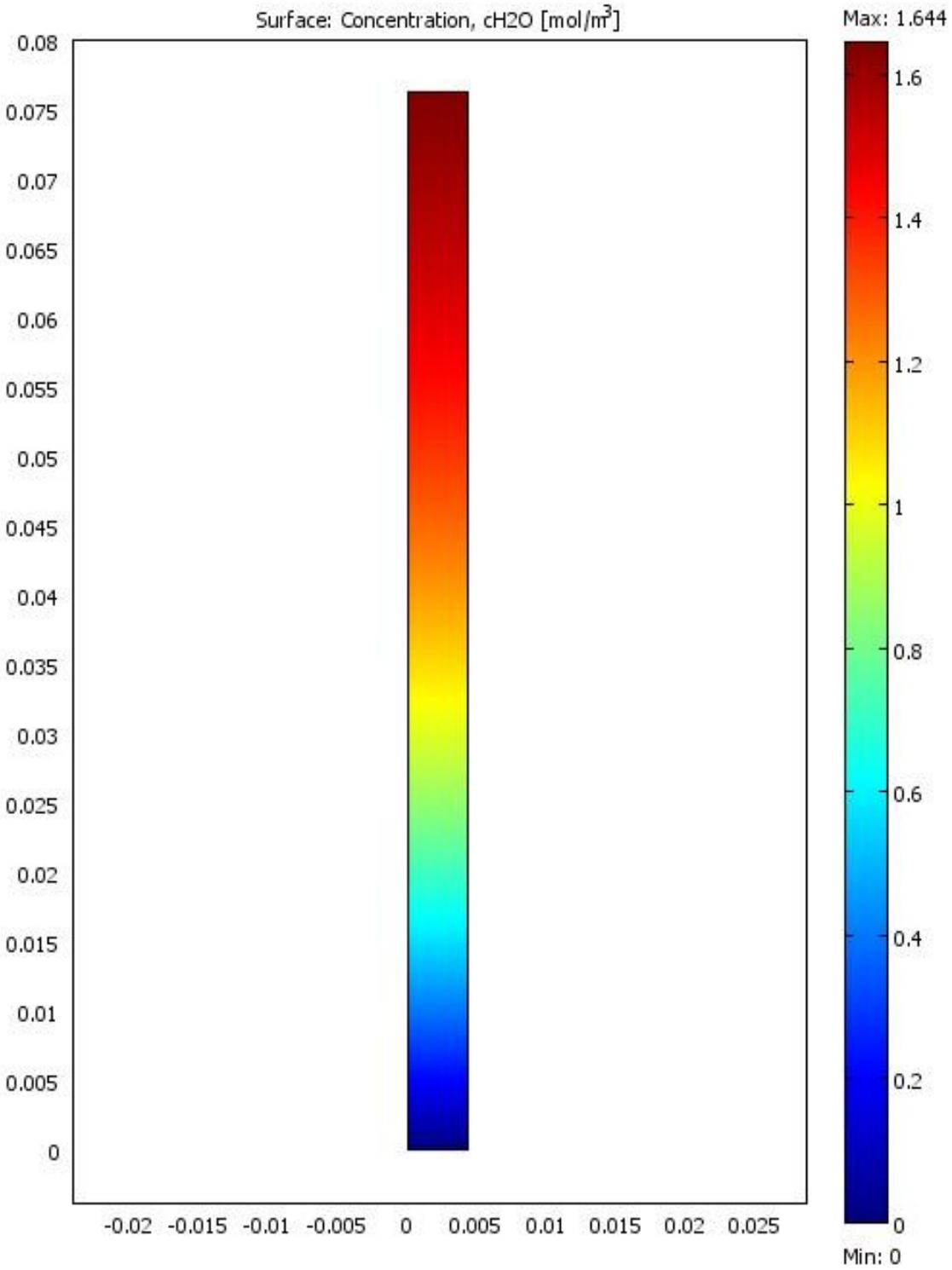
Surface: Concentration, cH2O [mol/m3]
Max: 1.644
Min: 0
0.08
0.075
0.07
0.065
0.06
0.055
0.05
0.045
0.04
0.035
0.03
0.025
0.02
0.015
0.01
0.005
0
-0.02
-0.015
-0.01
-0.005
0
0.005
0.01
0.015
0.02
0.025
1.6
1.4
1.2
1
0.8
0.6
0.4
0.2
0

Appendix H: Mass Transfer Limitations Model

The following are the surface plots from COMSOL Multiphysics for the literature reactor with mass transfer limitations. These are identical to Figure 20 and Appendix C, but show how mass transfer might account for the discrepancy between the literature reactor surface plots and the experimental reactor surface plots.

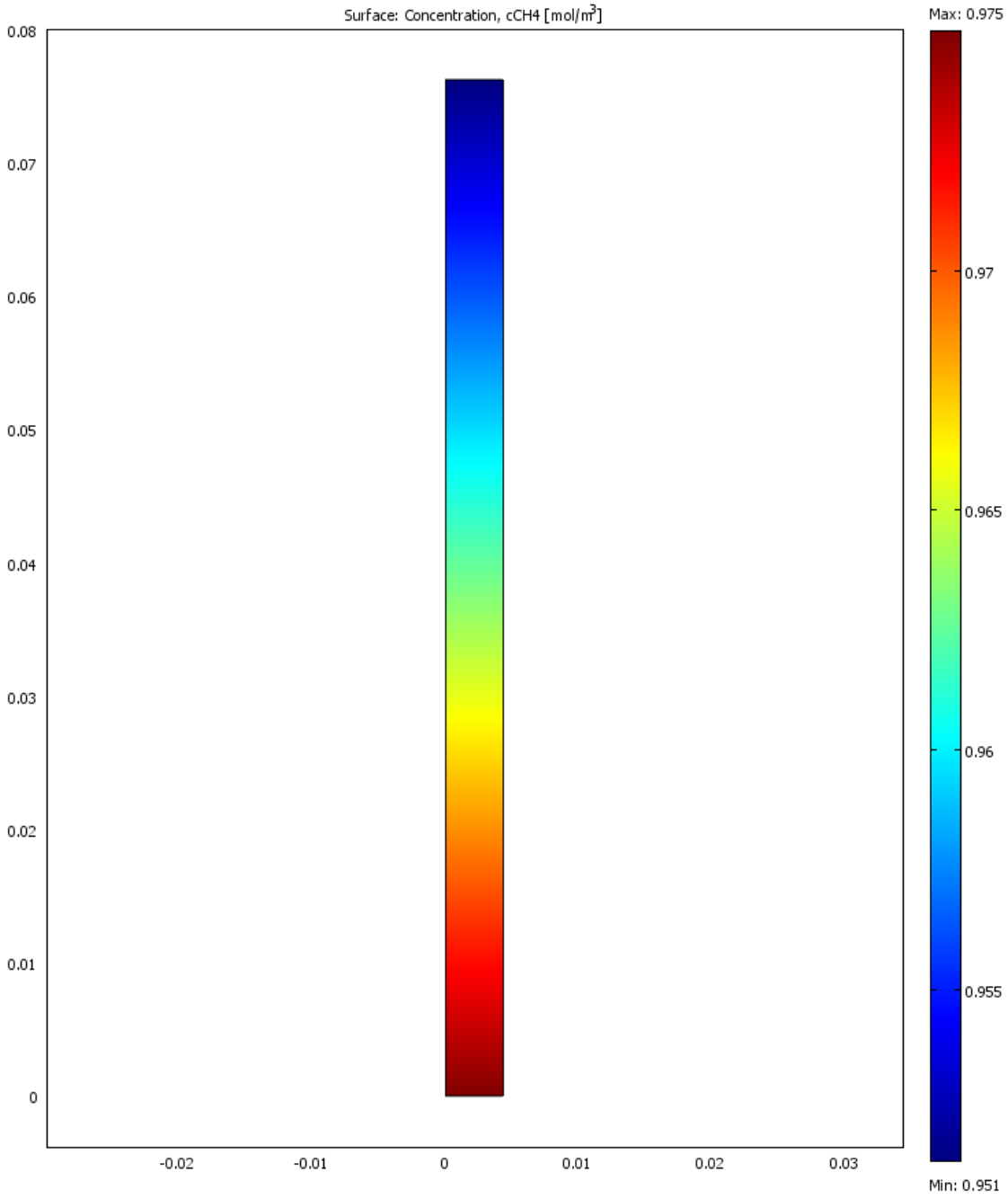

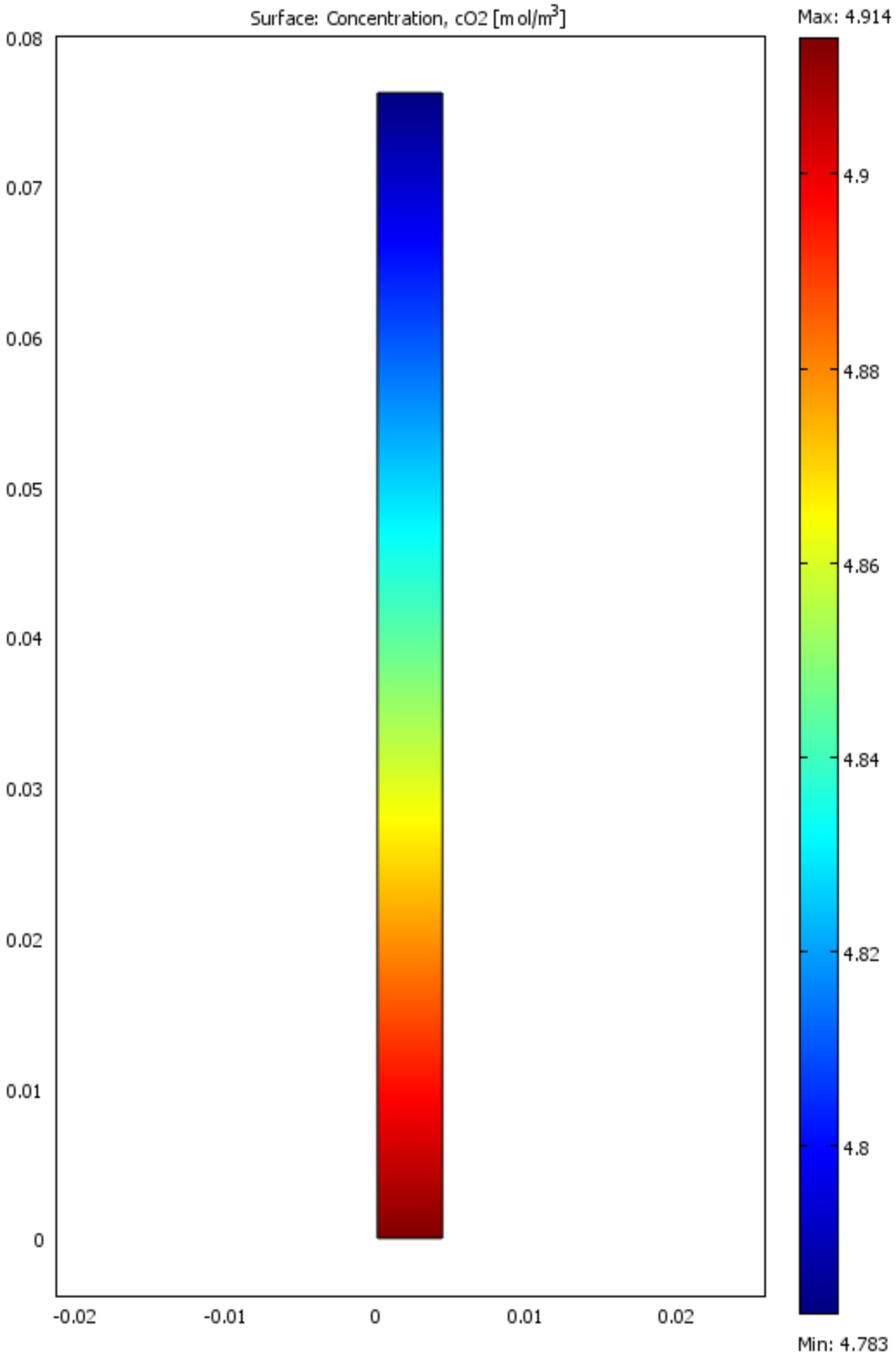
Surface: Concentration, cO2 [mol/m3]
Max: 4.914
0.08
0.07
0.06
0.05
0.04
0.03
0.02
0.01
0
-0.02
-0.01
0
0.01
0.02
4.9
4.88
4.86
4.84
4.82
4.8
Min: 4.783

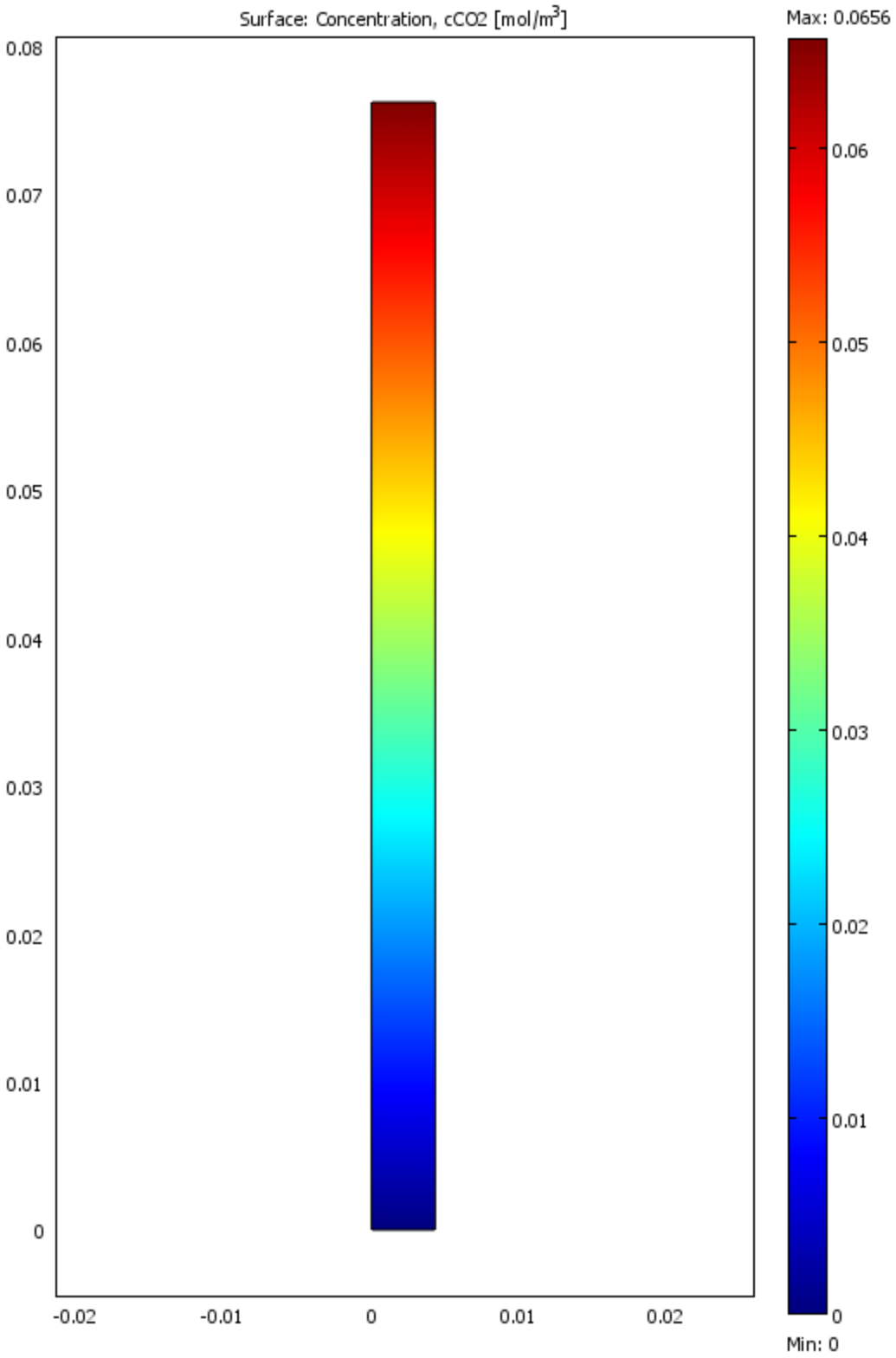
Surface: Concentration, cCO2 [mol/m3]
Max: 0.0656
0.08
0.07
0.06
0.05
0.04
0.03
0.02
0.01
0
-0.02
-0.01
0
0.01
0.02
0.06
0.05
0.04
0.03
0.02
0.01
0
Min: 0

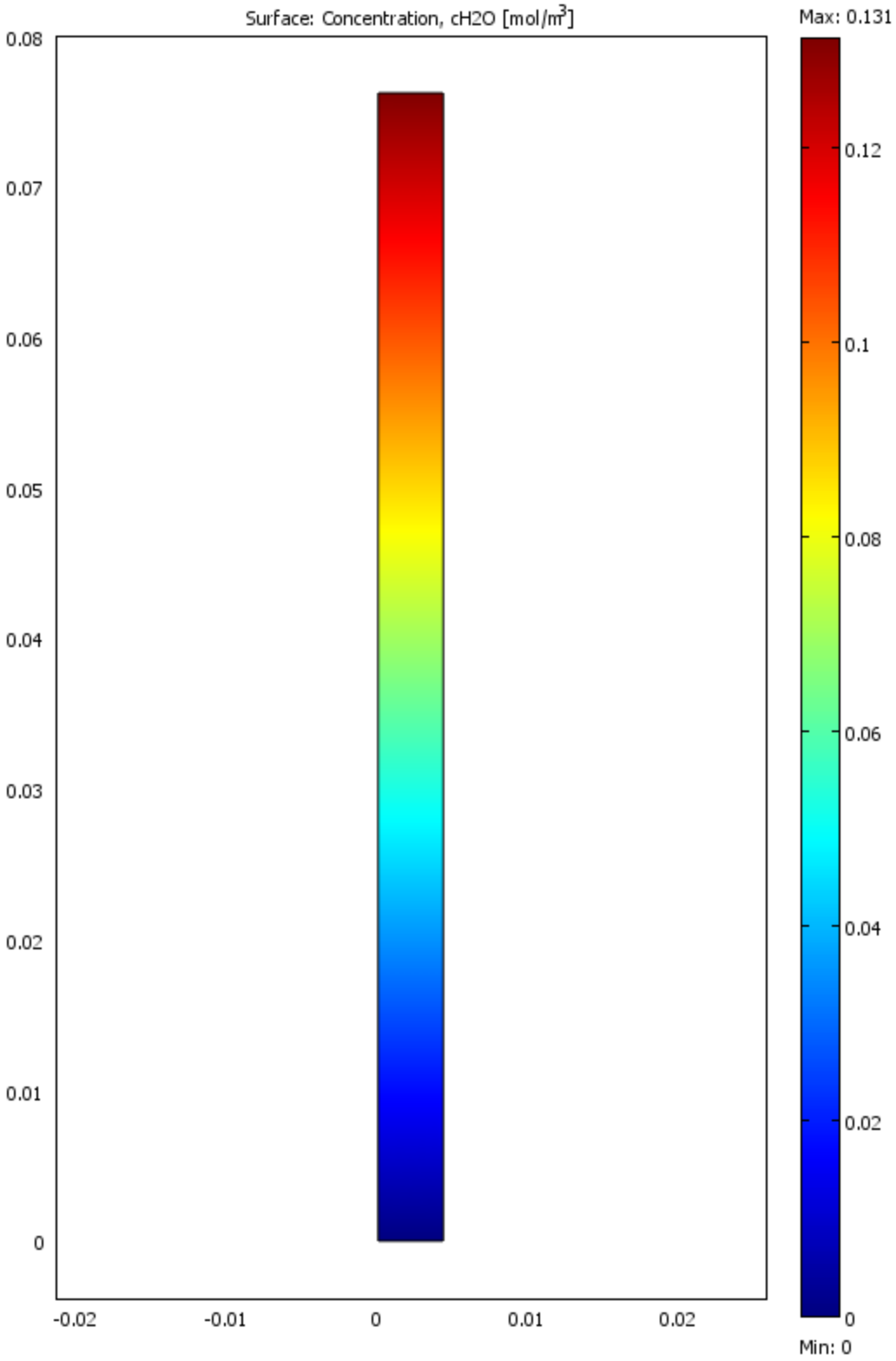
Surface: Concentration, cH2O [mol/m3]
Max: 0.131
0.08
0.07
0.06
0.05
0.04
0.03
0.02
0.01
0
-0.02
-0.01
0
0.01
0.02
0.12
0.1
0.08
0.06
0.04
0.02
0
Min: 0

Appendix I: Mass Transfer Table Results

Velocity (m/s)	km (1/s)	k_o (1/s)	CH_4 Outlet Concentration with Mass Transfer Limitations (mol/m^3)	CH_4 Outlet Concentration without Mass Transfer Limitations (mol/m^3)
0.0063	0.00782	0.27131	0.890	0.153
0.0563	0.03621	0.27131	0.937	0.803
0.1063	0.0565	0.27131	0.946	0.880
0.1563	0.074	0.27131	0.951	0.909
0.2063	0.08987	0.27131	0.955	0.925
0.2563	0.10461	0.27131	0.957	0.934
0.3063	0.11851	0.27131	0.959	0.941

Appendix J: GC Model Outputs

The following plots were generated by the GC model using data obtained in the experimental runs. The units were converted into units that COMSOL uses, so the peak heights do not match those generated by the real gas chromatograph (which are in the thousands). The peaks, in order from left to right, represent O_2, N_2, CH_4, and CO_2.

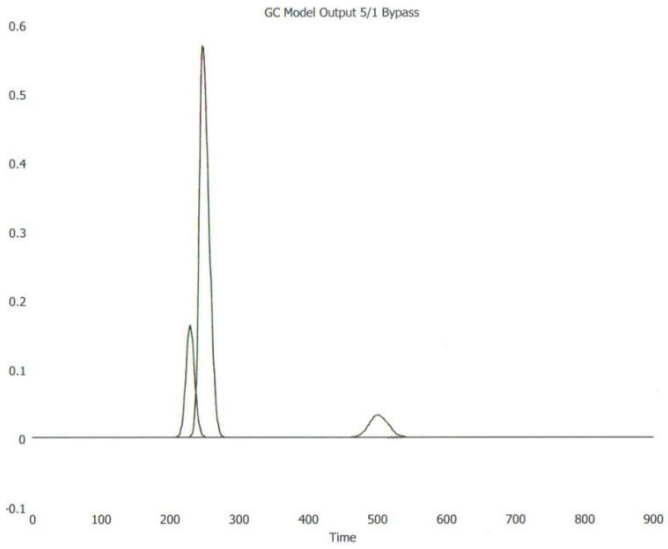

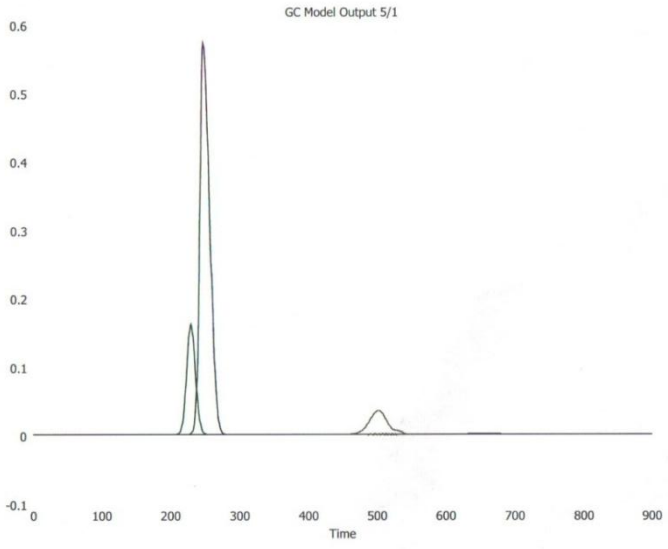

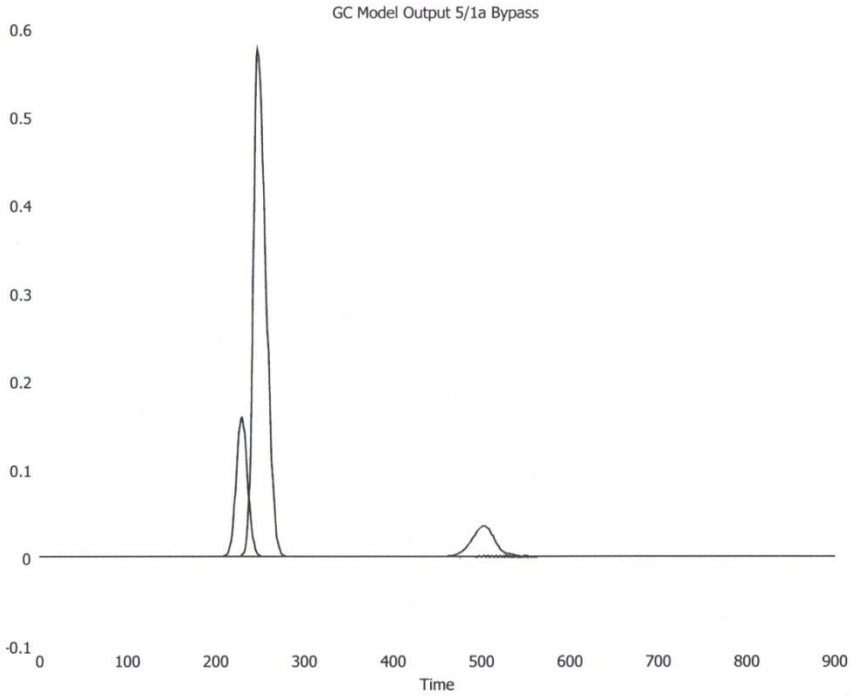
GC Model Output 5/1a Bypass
0.6
0.5
0.4
0.3
0.2
0.1
0
-0.1
0
100
200
300
400
500
600
700
800
900
Time

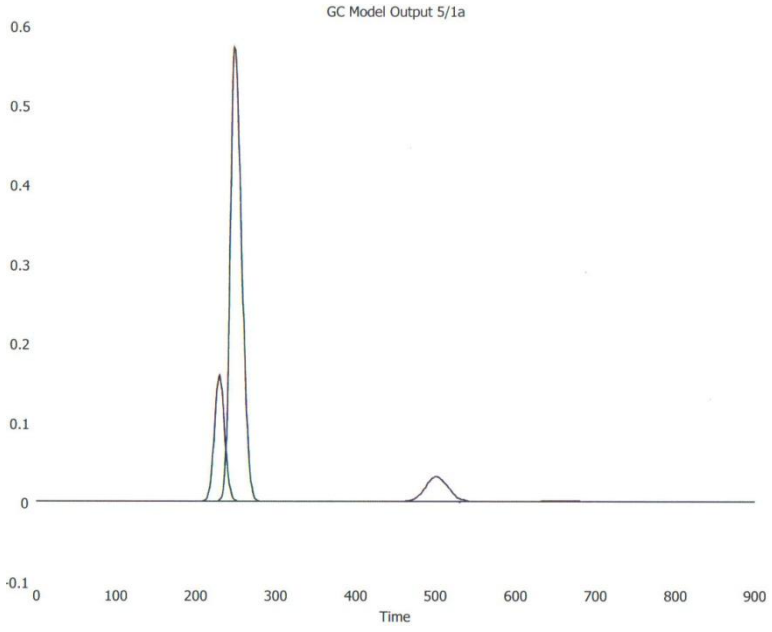
GC Model Output 5/1a
0.6
0.5
0.4
0.3
0.2
0.1
0
-0.1
0
100
200
300
400
500
600
700
800
900
Time

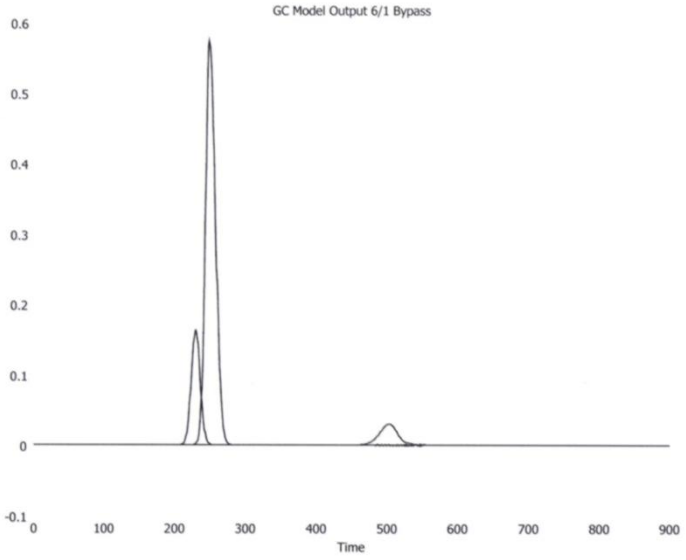
GC Model Output 6/1 Bypass
0.6
0.5
0.4
0.3
0.2
0.1
0
-0.1
0
100
200
300
400
500
600
700
800
900
Time

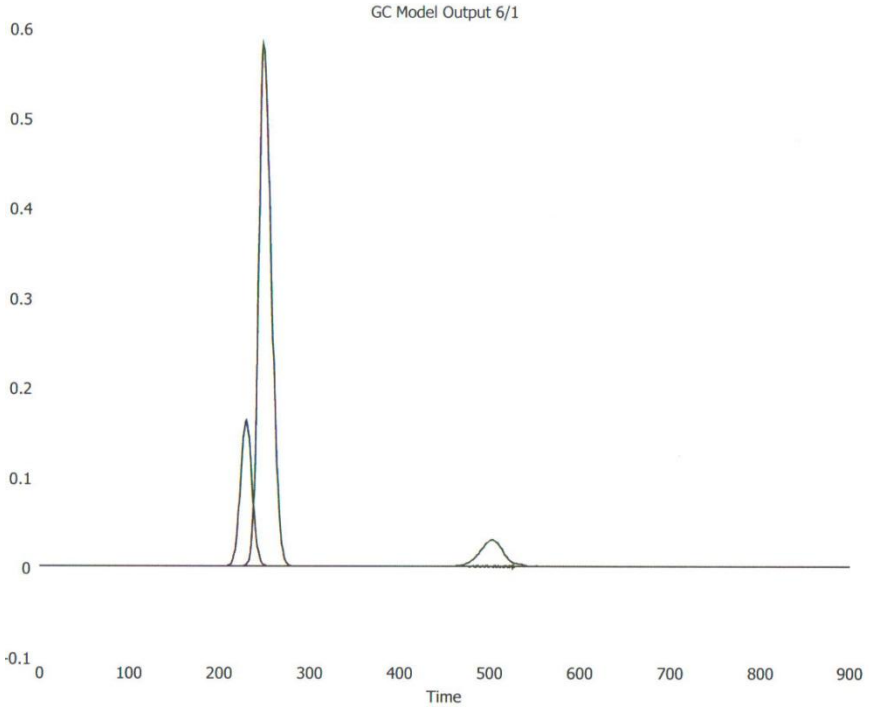
GC Model Output 6/1
0.6
0.5
0.4
0.3
0.2
0.1
0
-0.1
0
100
200
300
400
500
600
700
800
900
Time

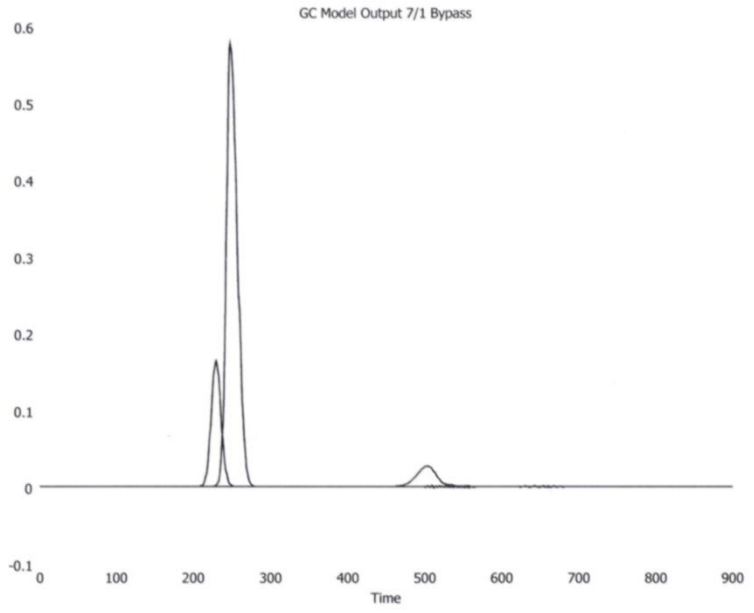
GC Model Output 7/1 Bypass
0.6
0.5
0.4
0.3
0.2
0.1
0
-0.1
0
100
200
300
400
500
600
700
800
900
Time

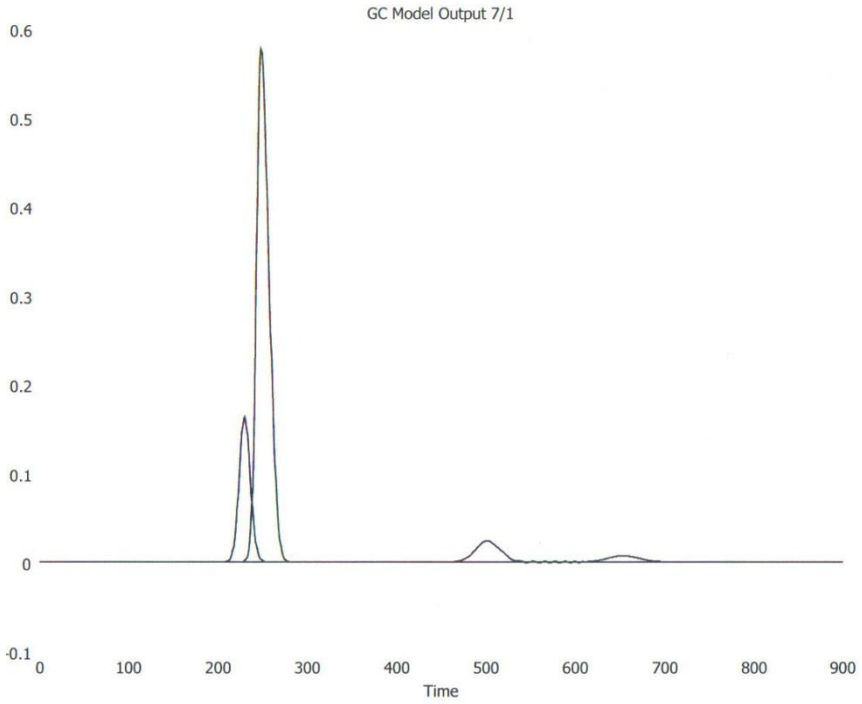
GC Model Output 7/1
0.6
0.5
0.4
0.3
0.2
0.1
0
-0.1
0
100
200
300
400
500
600
700
800
900
Time

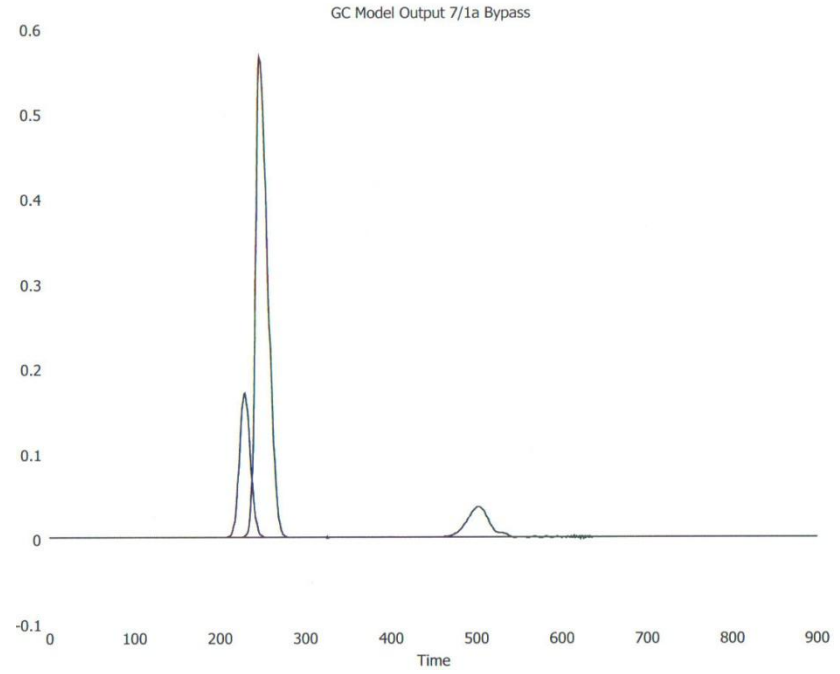
GC Model Output 7/1a Bypass
0.6
0.5
0.4
0.3
0.2
0.1
0
-0.1
0
100
200
300
400
500
600
700
800
900
Time

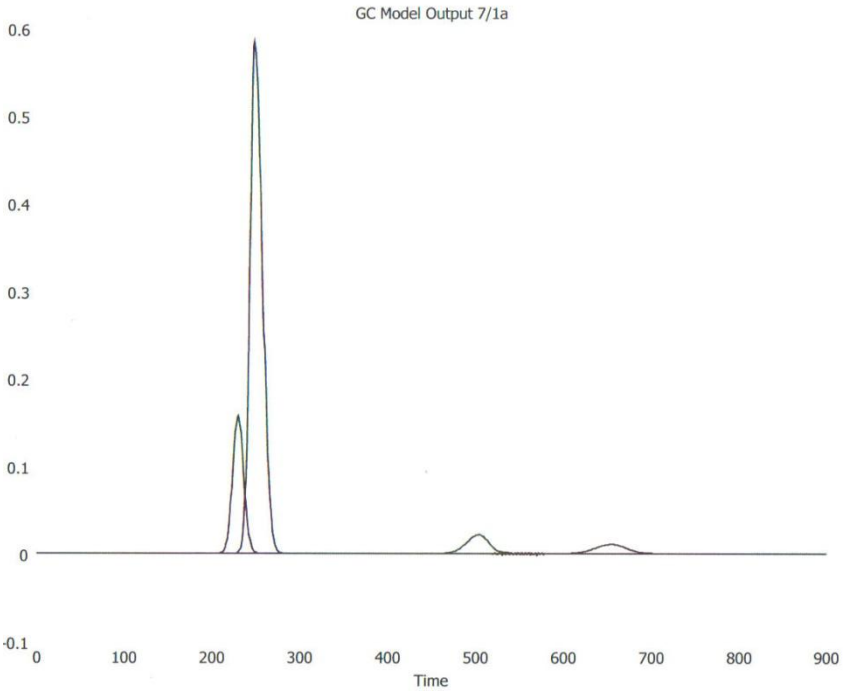
GC Model Output 7/1a
0.6
0.5
0.4
0.3
0.2
0.1
0
-0.1
0
100
200
300
400
500
600
700
800
900
Time

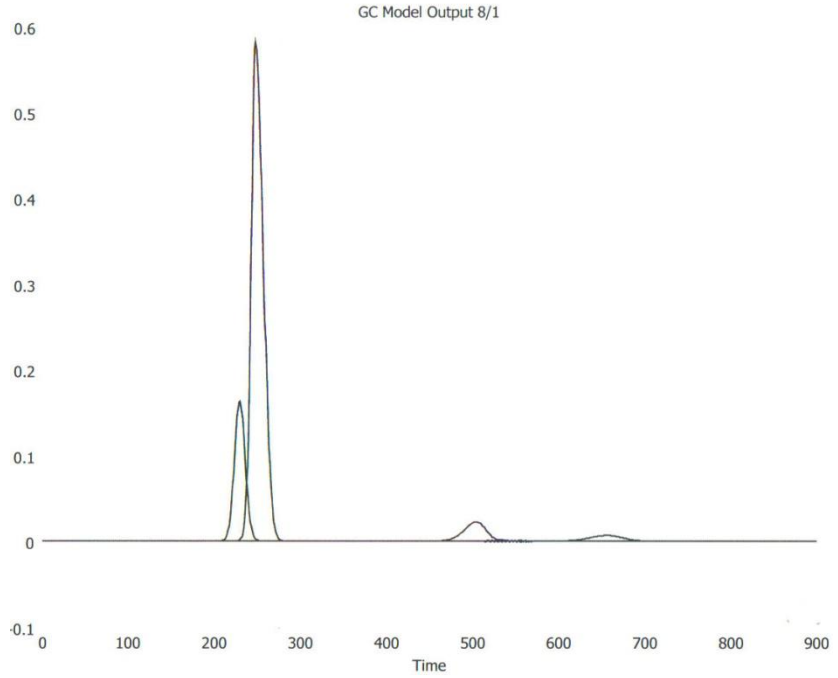
GC Model Output 8/1
0.6
0.5
0.4
0.3
0.2
0.1
0
-0.1
0
100
200
300
400
500
600
700
800
900
Time

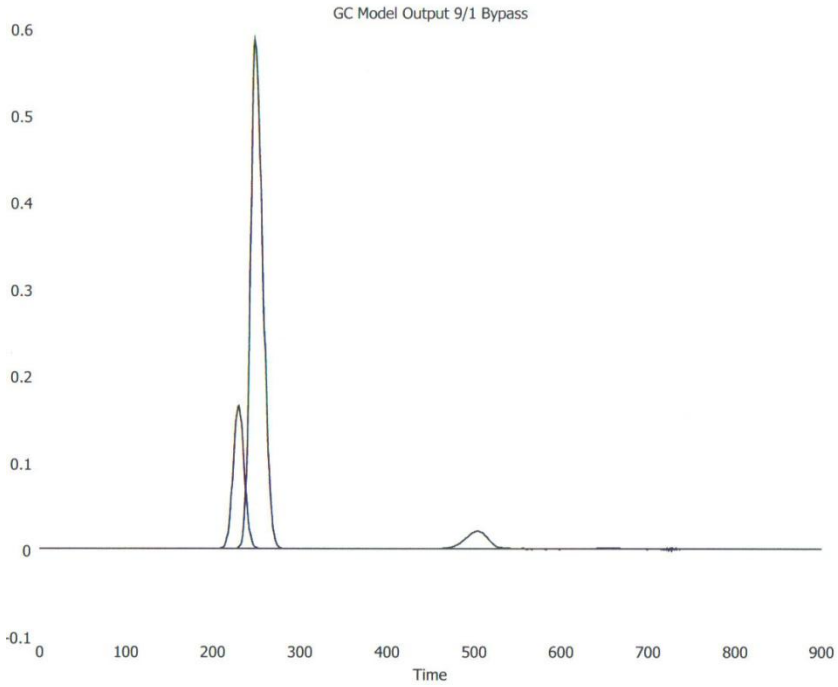
GC Model Output 9/1 Bypass
0.6
0.5
0.4
0.3
0.2
0.1
0
-0.1
0
100
200
300
400
500
600
700
800
900
Time

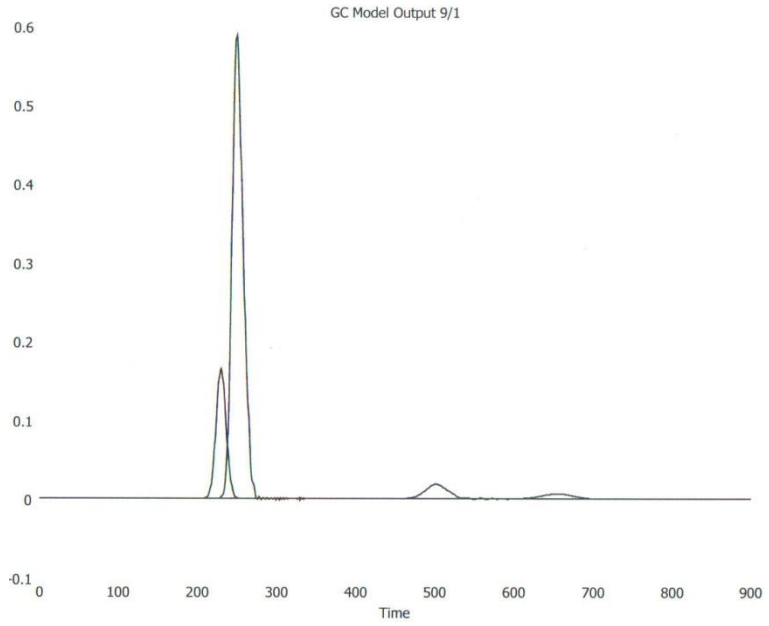
GC Model Output 9/1
0.6
0.5
0.4
0.3
0.2
0.1
0
-0.1
0
100
200
300
400
500
600
700
800
900
Time

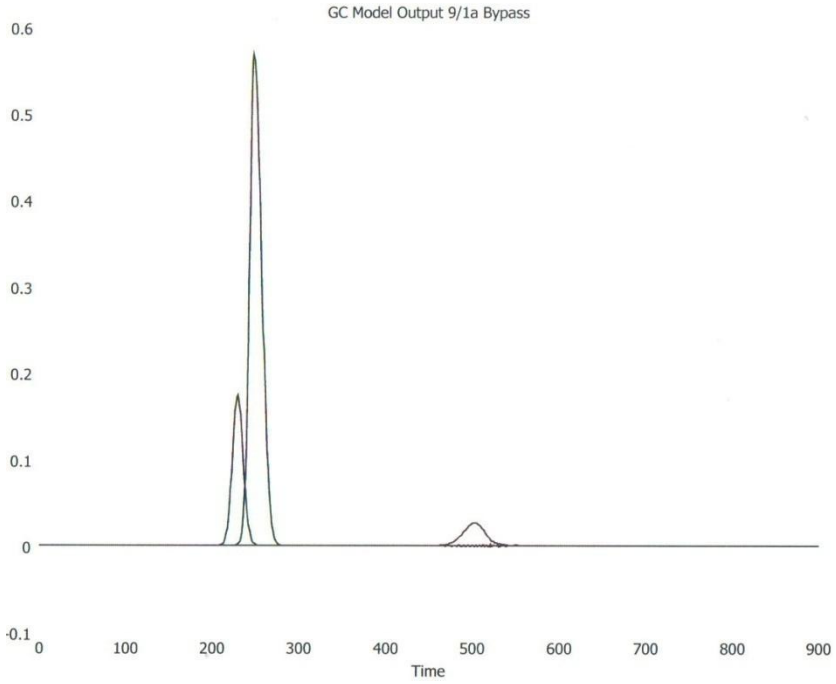
GC Model Output 9/1a Bypass
0.6
0.5
0.4
0.3
0.2
0.1
0
-0.1
0
100
200
300
400
500
600
700
800
900
Time

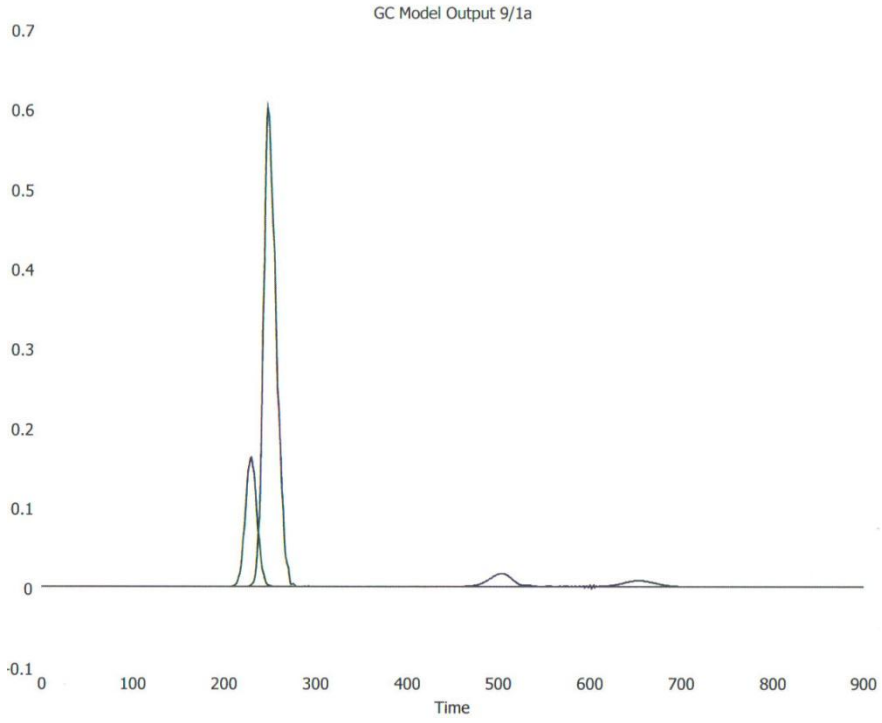
GC Model Output 9/1a
0.7
0.6
0.5
0.4
0.3
0.2
0.1
0
-0.1
0
100
200
300
400
500
600
700
800
900
Time

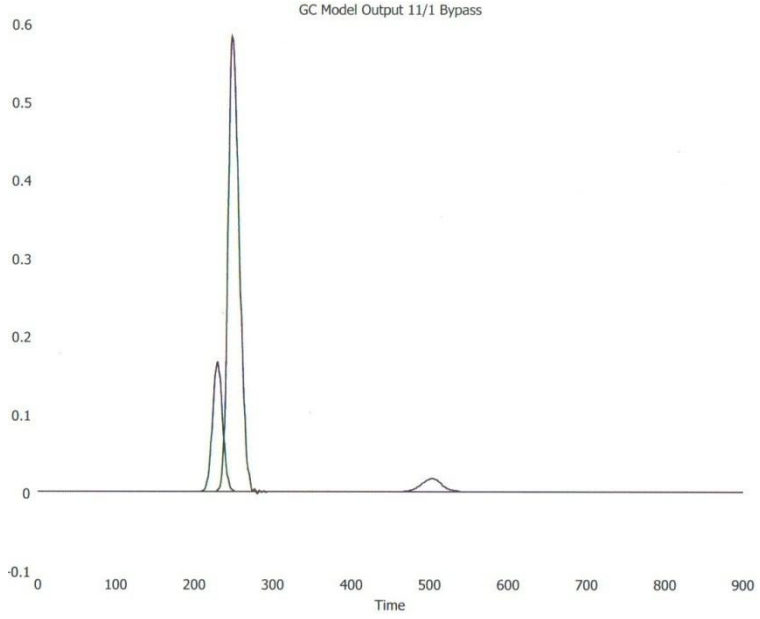
GC Model Output 11/1 Bypass
0.6
0.5
0.4
0.3
0.2
0.1
0
-0.1
0
100
200
300
400
500
600
700
800
900
Time

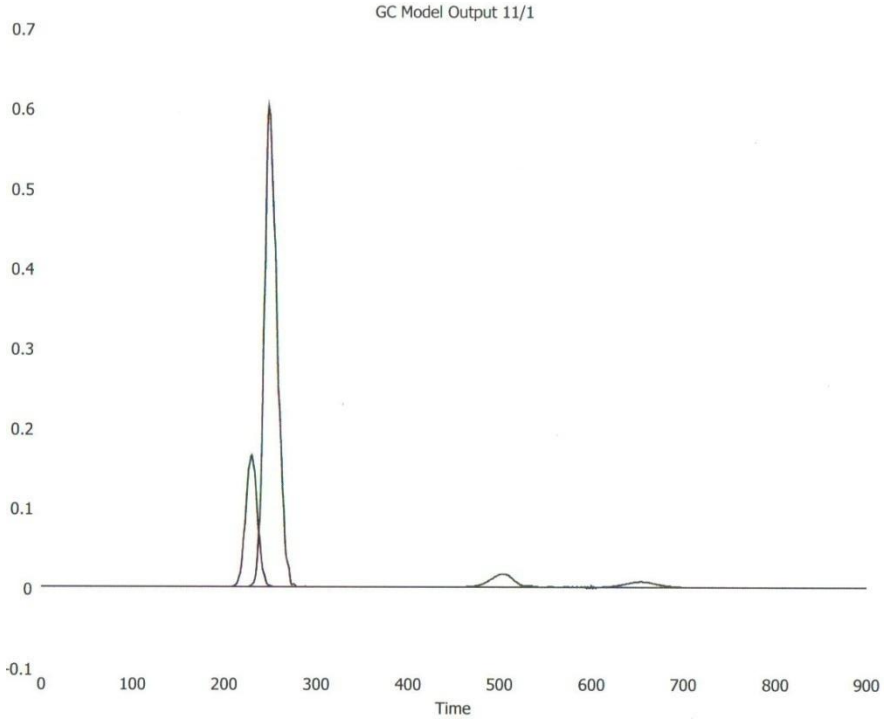
GC Model Output 11/1
0.7
0.6
0.5
0.4
0.3
0.2
0.1
0
-0.1
0
100
200
300
400
500
600
700
800
900
Time

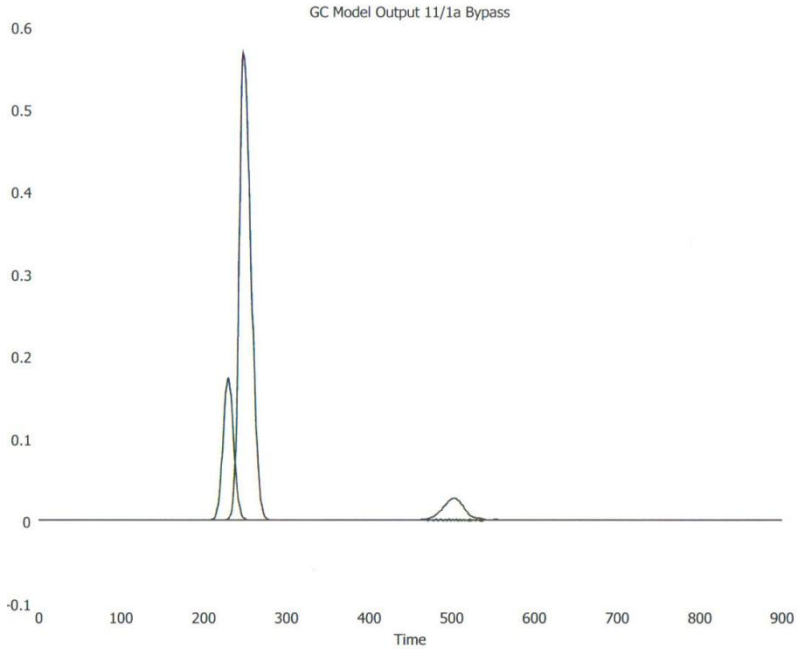
GC Model Output 11/1a Bypass
0.6
0.5
0.4
0.3
0.2
0.1
0
-0.1
0
100
200
300
400
500
600
700
800
900
Time

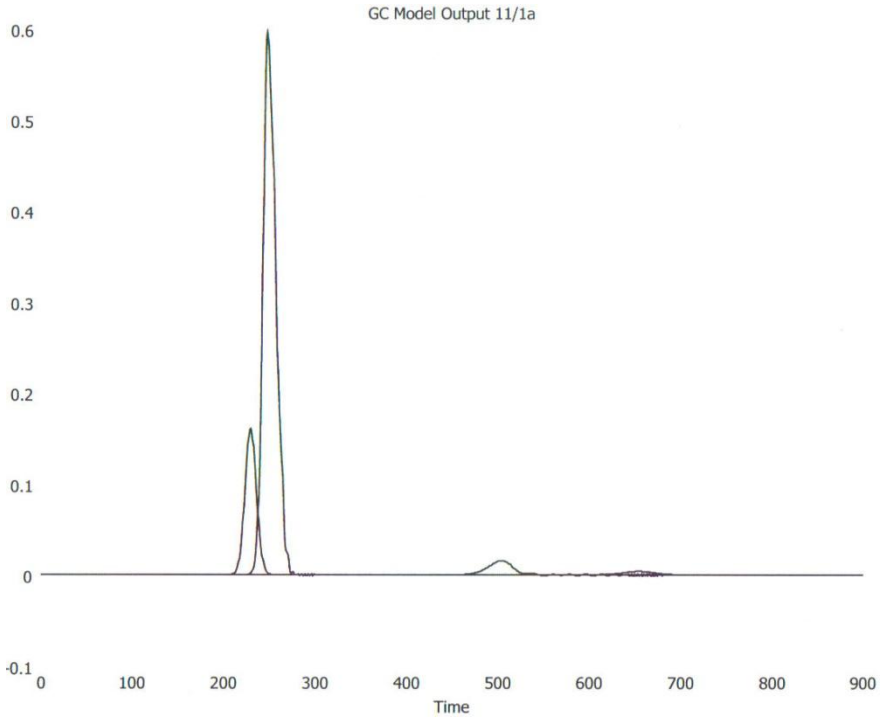
GC Model Output 11/1a
0.6
0.5
0.4
0.3
0.2
0.1
0
-0.1
0
100
200
300
400
500
600
700
800
900
Time

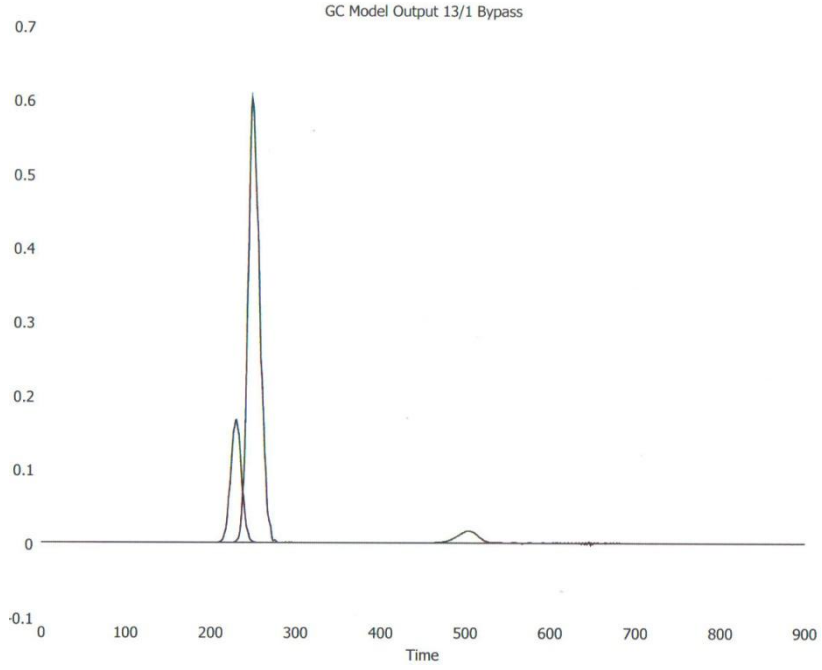
GC Model Output 13/1 Bypass
0.7
0.6
0.5
0.4
0.3
0.2
0.1
0
-0.1
0
100
200
300
400
500
600
700
800
900
Time

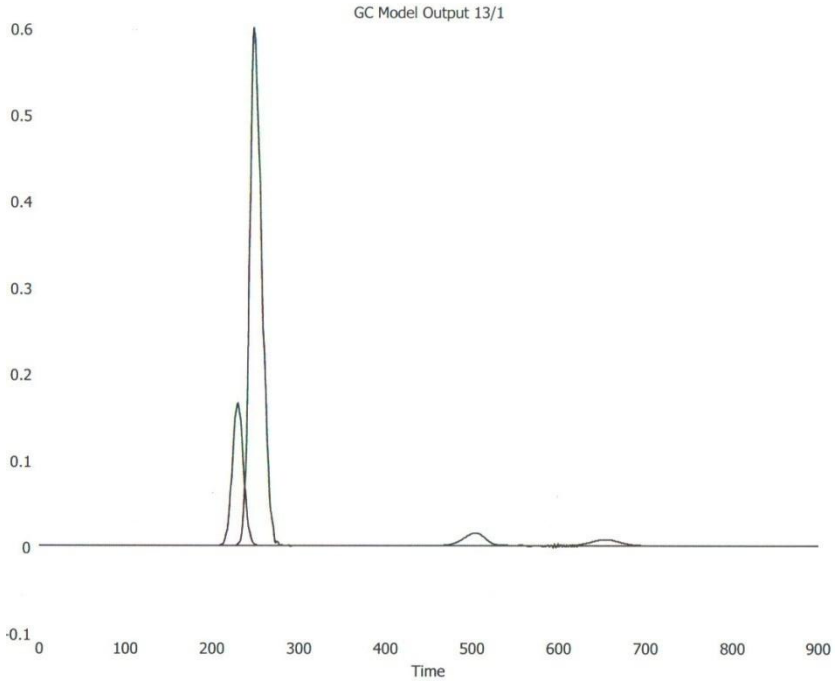
GC Model Output 13/1
0.6
0.5
0.4
0.3
0.2
0.1
0
-0.1
0
100
200
300
400
500
600
700
800
900
Time

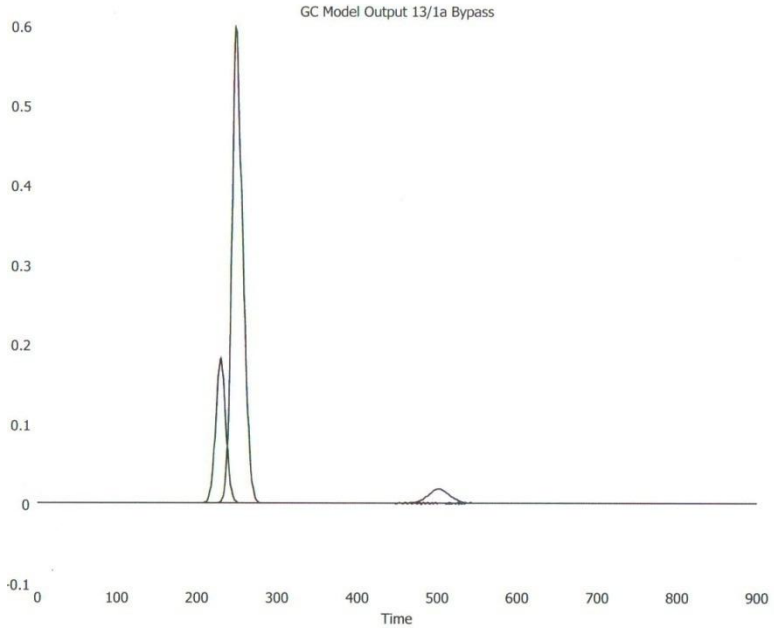
GC Model Output 13/1a Bypass
0.6
0.5
0.4
0.3
0.2
0.1
0
-0.1
0
100
200
300
400
500
600
700
800
900
Time

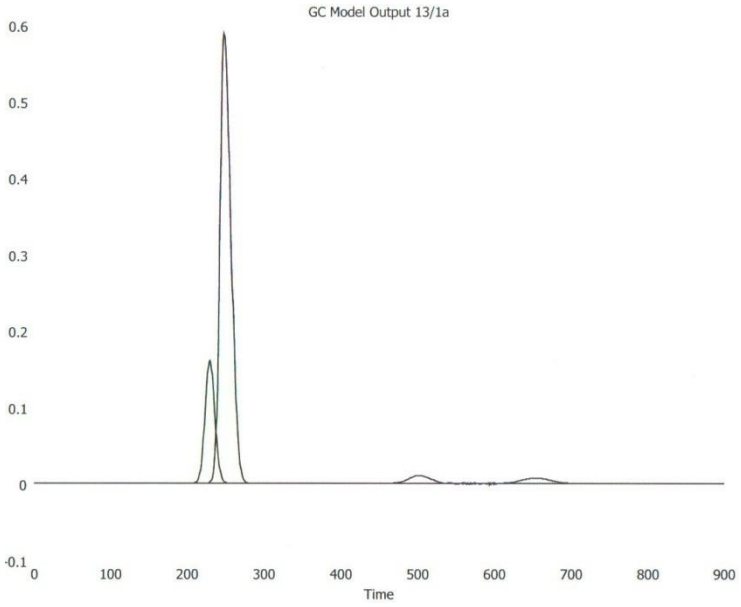
GC Model Output 13/1a
0.6
0.5
0.4
0.3
0.2
0.1
0
-0.1
0
100
200
300
400
500
600
700
800
900
Time